Aus der

Klinik und Poliklinik für Nuklearmedizin

Klinikum der Ludwig-Maximilians-Universität München

Biomarker für Amyloid, Tau, Neurodegeneration und Mikrogliaaktivierung bei Patienten mit primären und sekundären Tauopathien

Dissertation

zum Erwerb des Doktorgrades der Medizin

an der Medizinischen Fakultät

der Ludwig-Maximilians-Universität München

vorgelegt von

Anika Jacqueline Finze

aus

München

Jahr

2025

Mit Genehmigung der Medizinischen Fakultät der
Ludwig-Maximilians-Universität München

Erstes Gutachten:	Prof. Dr. Matthias Brendel
Zweites Gutachten:	Prof. Dr. Johannes Levin
Drittes Gutachten:	Prof. Dr. Dieter Edbauer
weitere Gutachten:	Prof. Dr. Michael Ewers

Dekan: Prof. Dr. med. Thomas Gudermann

Tag der mündlichen Prüfung: 06.06.2025

Affidavit

LMU LUDWIG-MAXIMILIANS-UNIVERSITÄT MÜNCHEN | Promotionsbüro Medizinische Fakultät | MMRS

Eidesstattliche Versicherung

Finze, Anika Jacqueline

Name, Vorname

Ich erkläre hiermit an Eides statt, dass ich die vorliegende Dissertation mit dem Titel:

Biomarker für Amyloid, Tau, Neurodegeneration und Mikrogliaaktivierung bei Patienten mit primären und sekundären Tauopathien

selbständig verfasst, mich außer der angegebenen keiner weiteren Hilfsmittel bedient und alle Erkenntnisse, die aus dem Schrifttum ganz oder annähernd übernommen sind, als solche kenntlich gemacht und nach ihrer Herkunft unter Bezeichnung der Fundstelle einzeln nachgewiesen habe.

Ich erkläre des Weiteren, dass die hier vorgelegte Dissertation nicht in gleicher oder in ähnlicher Form bei einer anderen Stelle zur Erlangung eines akademischen Grades eingereicht wurde.

München, 09.06.2025 — Ort, Datum

Anika Jacqueline Finze — Unterschrift Doktorandin

Inhaltsverzeichnis

1. Abkürzungsverzeichnis

Um eine Übereinstimmung mit den in den Publikationen verwendeten Abkürzungen zu gewährleisten, wurden einige davon aus dem Englischen übernommen.

Aβ	*β-Amyloid*
AD	*Alzheimer-Krankheit*
CBD	*Kortikobasale Degeneration*
CBS	*Kortikobasales Syndrom*
CSF	*Zerebrospinale Flüssigkeit*
CT	*Computer-Tomographie*
EMA	*„European Medicines Agency“*
FDA	*„Food and Drug Administration“*
FDG	*Fluordesoxyglucose*
GMV	*Volumina der grauen Substanz*
LAB	*„low-affinity-binder”*
MAPT	*Mikrotubuli-assoziierte Protein Tau*
MRT	*Magnet-Resonanz-Tomographie*
NFT	*Neurofibrilläres Knäuel*
NMDA	*N-Methyl-D-Aspartat*
PSP	*Progressive Supranukleäre Lähmung*
RT	*„Repeat“-Tauopathie, z.B. 4RT: 4-Repeat-Tauopathie*
sTREM2	*“soluble triggering receptor expressed on myeloid cells 2”*
TSPO	*Translokatorprotein*

2. Publikationsliste

Die vorliegende kumulative Dissertation umfasst zwei bereits publizierte Manuskripte:

Publikation I

Finze A*, Biechele G*****, Rauchmann BS, Franzmeier N, Palleis C, Katzdobler S, Weidinger E, Guersel S, Schuster S, Harris S, Schmitt J, Beyer L, Gnörich J, Lindner S, Albert NL, Wetzel CH, Rupprecht R, Rominger A, Danek A, Burow L, Kurz C, Tato M, Utecht J, Papazov B, Zaganjori M, Trappmann LK, Goldhardt O, Grimmer T, Haeckert J, Janowitz D, Buerger K, Keeser D, Stoecklein S, Dietrich O, Morenas-Rodriguez E, Barthel H, Sabri O, Bartenstein P, Simons M, Haass C, Höglinger GU, Levin J, Perneczky R, Brendel M. **Individual regional associations between Aβ-, tau- and neurodegeneration (ATN) with microglial activation in patients with primary and secondary tauopathies**. Molecular Psychiatry. 2023. doi: 10.1038/s41380-023-02188-8.

***** Geteilte Erstautorenschaft

IF 11.0; IF-Perzentil in der Kategorie: Psychiatrie 93.9 %, Neurowissenschaft 94.3 %, Biochemie & Molekulare Biologie 91.8 %

Publikation II

Palleis C, Brendel M, **Finze A**, Weidinger E, Bötzel K, Danek A, Beyer L, Nitschmann A, Kern M, Biechele G, Rauchmann BS, Häckert J, Höllerhage M, Stephens AW, Drzezga A, van Eimeren T, Villemagne VL, Schildan A, Barthel H, Patt M, Sabri O; German Imaging Initiative for Tauopathies (GII4T); Bartenstein P, Perneczky R, Haass C, Levin J, Höglinger GU. **Cortical [^{18}F]PI-2620 Binding Differentiates Corticobasal Syndrome Subtypes**. Movement Disorders. 2021 Sep;36(9):2104-2115. doi: 10.1002/mds.28624.

IF 9.698; IF-Perzentil in der Kategorie: Klinische Neurologie 92.69 %

3. Beschreibung des Eigenanteils

Publikation I

Erstellung eines Studienkonzeptes in Zusammenarbeit mit der Ko-Erstautorin und dem Betreuer. Datenzusammenführung (Bilddaten, klinische Daten), methodische Aufbereitung und Prozessierung der Bilddaten. Erstellung von Auswertungsskripten, Durchführung statistischer Rechnungen und Erstellung von Tabellen und Abbildungen. Interpretation und Einordnung in den Gesamtkontext, sowie Verfassen eines Manuskriptes in Zusammenarbeit mit der Ko-Erstautorin und dem Betreuer. Interdisziplinäre Überarbeitung des Manuskriptes und Finalisierung für das Peer-Review mit allen Ko-Autoren. Einreichung der Publikation bei einem geeigneten Journal und Umsetzung von Revisionsanmerkungen zusammen mit der Ko-Erstautorin und dem Betreuer.

Publikation II

Mithilfe bei der Zusammenführung und Aufbereitung von klinischen Daten. Prozessierung der Bilddaten. Erstellung von Auswertungsskripten, Durchführung statistischer Rechnungen und Erstellung von Tabellen und Abbildungen. Mithilfe beim Entwurf des Manuskriptes (Methodik, Ergebnisse). Änderungen im Review-Prozess (Statistik, Tabellen, Abbildungen).

4. Einführung in die Thematik

In den vergangenen hundert Jahren ist die Lebenserwartung der Bevölkerung, insbesondere in Industrienationen, gestiegen (1). Dies ist ein beeindruckendes Zeugnis für den Fortschritt der Medizin und stellt uns gleichzeitig vor die Herausforderung einer immer älter werdenden Bevölkerung. Mit steigendem Alter einer Bevölkerung steigt auch die Prävalenz altersbedingter Erkrankungen und somit die sozioökonomische Belastung für das Gesundheitssystem (2). Laut einer Analyse des Statistischen Bundesamtes im Jahr 2022 hat sich die Zahl der Patienten, die aufgrund einer Alzheimer-Krankheit (AD) stationär behandelt werden mussten, sowie die Gesamtzahl der AD-bedingten Todesfälle seit dem Jahr 2000 mehr als verdoppelt (3). Vor diesem Hintergrund wird im Bereich der neurodegenerativen Erkrankungen intensiv Forschung betrieben, um präventive, diagnostische und therapeutische Fortschritte auf diesem Gebiet zu erzielen.

Diese Dissertation zielt darauf ab, das Gehirn auf struktureller und molekularer Ebene bei verschiedenen neurodegenerativen Erkrankungen, speziell innerhalb des Spektrums der Tauopathien, zu analysieren und daraus potenzielle pathophysiologische sowie diagnostische Schlussfolgerungen abzuleiten. Der Fokus liegt hierbei auf der Kombination bildgebender Verfahren (PET-CT, MRT) mit klinischen Untersuchungen.

4.1. Tau und Tauopathien

Das Mikrotubuli-assoziierte Protein Tau (MAPT) spielt neurophysiologisch eine wichtige Rolle bei der Aufrechterhaltung des axonalen Transports, indem es die dynamische Mikrotubuli-Instabilität moduliert und deren Zusammenbau fördert (4, 5). Tauopathien wiederum sind eine Gruppe neurodegenerativer Erkrankungen, charakterisiert durch die Aggregation abnormaler Tau-Proteine im Gehirn (6, 7). Tauopathien weisen charakteristische Muster auf: Das Tau-Protein wird im menschlichen Gehirn

in sechs verschiedenen Isoformen durch alternatives Splicing des MAPT-Genes auf Chromosom 17q21.31 exprimiert (7). Für die verbreitete molekulare Klassifizierung der Tauopathien in 3R-, 4R-, gemischt 3/4R-Tauopathien (3RT, 4RT, 3/4RT) ist das Vorhandensein von drei oder vier sogenannter „Tandem-Repeats" in der Mikrotubuli-Bindungsdomäne des Proteins von Bedeutung, wobei physiologisch die 3R- und 4R-Tau Isoformen ungefähr gleich vertreten sind (8). Posttranslationale Modifikationen, wie Hyperphosphorylierung, sowie die Aggregation in verschiedenen morphologischen Variationen, einschließlich neurofibrillärer Knäuel (NFT), Neuropil-Fäden und neuritischer Plaques, beeinflussen die Tau-Funktion wesentlich (8, 9). Außerdem kann das Tau-Protein je nach Krankheitsentität unterschiedliche Zelltypen betreffen, darunter ausschließlich Neurone oder eine Kombination aus Neuronen und zusätzlich Gliazellen, wie Astroglia und Oligodendroglia (7, 8). Und ein weiteres Charakteristikum ist die Tau-Belastung in verschiedenen anatomischen Regionen und die spezifische Ausbreitung von frühen zu späten Krankheitsstadien (10), sowie die Ausbreitung entlang funktional vernetzter Regionen (11, 12). Der im Volksmund wohl bekannteste Vertreter der Tauopathien ist die Alzheimer-Krankheit (AD), eine sekundäre 3/4RT. AD wird als sekundäre Tauopathie bezeichnet, da hier weitere Biomarker, wie das β-Amyloid (Aβ) eine pathogenetische Rolle spielen (13, 14) und die Tau-Ablagerung beeinflusst (15). Vertreter der primären Tauopathien sind neben Weiteren die 4RT progressive supranukleäre Lähmung (PSP) und die 4RT kortikobasale Degeneration (CBD) (16), sowie die 3RT Frontotemporale Demenz („Pick´s disease") (8).

4.2. ATI(N): Aβ, Tau und Neurodegeneration – Welche Rolle spielt die Neuroinflammation?

Auf Basis der Erkenntnisse über die sekundäre Tauopathie AD wurde das ATN-System entwickelt. Das A steht für den Biomarker Aβ, welcher eine Kaskade auslöst,

und die Tau-Akkumulierung beschleunigt (T) und neurodegenerative Prozesse bedingt (N) (17-19). Da es sich hierbei um ein simplifiziertes Modell handelt und davon ausgegangen werden muss, dass weitere Mediatoren im neurodegenerativen Prozess eine Rolle spielen, wurde ATN zu ATX(N) weiterentwickelt. Das X soll hierbei weitere mögliche Biomarker repräsentieren, wie neuroimmune und synaptische Dysfunktionen oder Funktionsalterationen der Blut-Hirn-Schranke (20, 21). Insbesondere die Neuroinflammation (zellulär aktivierte Mikroglia, abgekürzt mit „I“) rückte in den Fokus als X-Parameter, dann ATI(N). Einige Studien propagierten die Neuroinflammation in Interaktion mit Aβ als Tempo-Geber der Tau-Ausbreitung über die Braak-Stadien hinweg (10, 22, 23), oder als direkter Einflussfaktor auf die fortschreitende Neurodegeneration (24). Andere Studien legten einen ähnlichen Einfluss von Aβ und Tau auf die Neuroinflammation nahe (25). Als messbares Surrogat veränderter neuronaler Aktivität (Neurodegeneration) können unter anderem der Verlust von grauer-Substanz-Volumina (GMV) in der MRT, reduzierte Perfusionseigenschaften in Frühphasen der PET (26-28) oder ein reduzierter regionaler Glucosestoffwechsel in der ^{18}F-Fluordesoxyglucose(-FDG)-PET (29) betrachtet werden. Mikroglia-Zellen gehören zur Fraktion der Gliazellen, und sind befähigt zur Differenzierung in Makrophagen zur Phagozytose und Antigen Präsentation (30). Sie bilden somit einen essenziellen Teil der zerebralen Immunantwort. Die Aktivierung der Mikroglia erfolgt bei jeglicher Art von pathologischem Insult und verändert so ihre zelluläre Morphologie in vielfältige aktivierte Phänotypen (30, 31). Mikrogliale Aktivierung kann neuroprotektive Effekte aufweisen (32-34), zum Beispiel durch Eliminierung von nicht-funktionalen Synapsen (35). Andererseits zeigt sich insbesondere bei chronisch mikroglialer Aktivierung ein neurotoxisch degenerativer Zustand, der mit der Freisetzung proinflammatorischer Zytokine einhergeht (36).

4.3. Phänotypische Vielfalt

Tauopathien manifestieren sich in einem klinisch heterogenen Spektrum. In der initialen Phase offenbart sich die AD häufig durch Störungen des episodischen Gedächtnisses, räumlich-zeitliche Desorientierung, Aufmerksamkeitsdefizite sowie durch nicht-kognitive Symptome wie eine Hyposmie oder eine depressive Verstimmung (37, 38). In fortgeschrittenen Stadien emergieren Beeinträchtigungen des deklarativen Gedächtnisses, Orientierungsverlust hinsichtlich Situation und Identität, semantische Paraphasien sowie apraktische Störungen. Ergänzend manifestieren sich motorische Dysfunktionen, beispielsweise ein Parkinsonismus, neuropsychiatrische Symptome wie Halluzinationen sowie neurovegetative Störungen, die Schlaf und Kontinenz beeinträchtigen (37, 38). Auch bei primären Tauopathien ist das klinische Spektrum vielfältig. Das kortikobasale Syndrom (CBS) ist durch asymmetrische extrapyramidale (Rigor, Dystonie, Myoklonus) und kortikale Symptome (Apraxie, sensorische Defizite, "Alien-Limb-Phänomen") charakterisiert (16, 39, 40). In circa 50 % der CBS-Fälle liegt eine CBD oder eine PSP zugrunde, während in etwa 25 % der Fälle eine AD als Ätiologie identifiziert wird („atypische AD“) (41). Das Richardson-Syndrom repräsentiert das klassische Bild einer PSP, gekennzeichnet durch eine frühe posturale Instabilität und okulomotorischen Dysfunktionen (42-47) und auch durch eine CBD verursacht werden (39). Sowohl PSP als auch CBD können sich phänotypisch als Verhaltensvariante der frontotemporalen Demenz, als nicht-flüssige agrammatische Variante der primär progressiven Aphasie, als isolierte Sprachapraxie oder als progressive Gangstörung präsentieren (16). Parkinsonismus, die primäre Lateralsklerose und spät einsetzende zerebelläre Ataxie stehen ebenfalls im Zusammenhang mit der PSP-Pathologie (16).

4.4. Diagnostische Möglichkeiten

Die klinische Diversität von Tauopathien verdeutlicht, dass eine definitive Diagnose oft erst postmortal anhand einer Autopsie erfolgen kann. Angesichts neuer, zielgerichteter therapeutischer Ansätze (siehe Kapitel 4.5.) gewinnt eine möglichst präzise

in vivo Charakterisierung der zugrundliegenden Pathologie zunehmend an Bedeutung. Eine ausführliche Anamnese und körperliche Untersuchung, ergänzt durch zielgerichtete funktionelle Tests, sind zentrale Bestandteile eines multimodalen diagnostischen Verfahrens, das zusätzlich Labor- und Liquordiagnostik sowie bildgebende Techniken umfasst.

Nuklearmedizinische Methoden zur molekularen Exploration des Gehirns haben in den vergangenen Jahrzehnten einen Stellenwert in der neurologischen Diagnostik erlangt. In der klinischen Praxis haben sich die Fluor-18 Aβ PET-Tracer Florbetapir (Amyvid®) (48), Flutemetamol (Vizamyl®) (49, 50) und Florbetaben (Neuraceq®) (51, 52) *in vivo* etabliert und bilden einen Baustein in der Differenzialdiagnostik von Demenzsyndromen. In der Entwicklung von Tau-PET Tracern ist die komplexe histopathologische Diversität des Tau-Proteins im menschlichen Gehirn, wie in Kapitel 4.1. dargelegt, für die Bindungseigenschaften der Tracer essenziell und erfordert daher eine spezifische Bewertung für jede einzelne Krankheitsentität. Im Jahr 2020 markierte die Zulassung des ersten Tau-PET Tracers, ^{18}F-AV-1451 (Flortaucipir, Tauvid®), durch die „Food and Drug Administration“ (FDA) einen signifikanten Fortschritt in der klinischen AD-Diagnostik (53). Dieser gehört zur ersten Tracer-Generation, welche eine relevante „Off-Target“-Bindung an Strukturen wie Monoaminoxidasen, Neuromelanin oder Eisen aufweist, eine bevorzugte Affinität an das bei AD dominierende 3/4R-Tau und eine verminderte Affinität zu 4R-Tau (54, 55) besitzt. Angesichts dieser Einschränkungen sind derzeit Tracer der zweiten Generation in der Entwicklung, die darauf abzielen, die Limitationen ihrer Vorgänger zu überwinden, darunter ^{18}F-PI-2620. Dieser zeichnet sich durch geringe „Off-Target“-Bindung an Monoaminoxidasen aus (56, 57) und zeigt neben einer hohen *in vivo* Affinität zu 3/4R-Tau bei AD (58) auch eine Affinität zu 4R-Tau bei PSP *in vitro* (12, 56, 59). Des Weiteren ermöglicht ^{18}F-PI-2620 in vivo eine Unterscheidung von PSP-Patienten und Kontrollpersonen (60), was ihn zu einem vielversprechenden Biomarker für die

Differenzierung verschiedener Demenzformen, einschließlich 4R-Tauopathien, macht (61, 62). Die Neuroinflammation lässt sich mittels TSPO (18 kDa Translokator Protein)-PET auf aktivierte Mikroglia regional quantifizieren (63, 64), wobei sich in den letzten Jahren der Tracer ^{18}F-GE-180 bei AD und 4RT etabliert hat (65, 66). Eine wichtige Limitation an dieser Bildgebung ist die vom genetischen Polymorphismus des TSPO-Gens abhängige Bindungsaffinität, und die dadurch geringere Tracer-Bindung bei Individuen mit sogenannten „low-affinity"-Bindungsstatus (LAB) *versus* „medium-affinity"- und „high-affinity"-Bindungsstatus (67-69). Außerdem wurde ^{18}F-GE-180 wegen einer variierenden Kinetik kritisiert, die im Sinne einer durch Neurodegeneration bedingten Störung der Blut-Hirn-Schrankenfunktion begrenzten Tracer-Aufnahme verstanden wird (70), wobei weitere Studien zeigen konnten, dass die Tracer-Bindung nicht mit der Integrität der Blut-Hirn-Schranke assoziiert ist (65). Neben den PET-Techniken können Aβ, Tau und Neuroinflammation auch mittels zerebrospinaler Flüssigkeit (CSF) erfasst werden ($Aβ_{1-42}$/$Aβ_{1-40}$-Quotient, Gesamt-Tau und Phospho-Tau, sTREM2). TREM2 („triggering receptor expressed on myeloid cells 2") ist ein membrangebundener Rezeptor, welcher von Mikroglia-Zellen exprimiert wird und die Immunantwort steuert. sTREM2 „soluble-", lässt sich im Liquor messen und wird mit einer verlangsamten kognitiven Verschlechterung bei AD in Verbindung gebracht (71).

4.5. Therapeutische Aussichten

Gemäß den aktuellen wissenschaftlichen Erkenntnissen existieren innerhalb der Europäischen Union keine etablierten kausalen Behandlungsmethoden für Patienten, die an AD, CBD oder PSP leiden. In den frühen Stadien der AD erweisen sich Acetylcholinesterase-Inhibitoren wie Donepezil, Galantamin und Rivastigmin als therapeutisch wirksam. In den fortgeschrittenen Phasen der Erkrankung wird zwar der N-Methyl-D-Aspartat (NMDA)-Antagonist Memantin eingesetzt, jedoch zeigt dieser nur eine begrenzte klinische Wirksamkeit (72, 73). Bei CBD und PSP liegt der

Schwerpunkt auf supportiven Therapieansätzen, einschließlich Ergotherapie, Logopädie und Physiotherapie. Speziell bei CBD-Patienten kann die Verabreichung von L-Dopa eine Linderung der motorischen Symptome bewirken, und lokale Injektionen von Botulinumtoxin können bei Dystonien hilfreich sein (74, 75). Über diese etablierten Therapien hinaus befinden sich zielgerichtete molekulare Behandlungsstrategien in der intensiven Forschung. Nach kontroversen Ergebnissen in klinischen Studien wurde der Aβ-Antikörper Aducanumab (Aduhelm®) im Jahr 2021 von der FDA unter der Bedingung weiterführender Studien auf dem US-Markt zugelassen (76, 77). Eine Zulassung in der Europäischen Union durch die „European Medicines Agency" (EMA) scheiterte im selben Jahr aufgrund unzureichend klarer Studienergebnisse. Weitere Aβ-Antikörper, wie Lecanemab (Leqembi®, FDA-Zulassung 2023 (78)) oder Donanemab, zeigten vielversprechende Studienergebnisse und befinden sich in der Prüfung für eine EU-Zulassung (79, 80). Die gegenwärtige Forschung zur Entwicklung von Tau-Antikörpern (zum Beispiel Tilavonemab (81, 82) oder Semorinemab (83, 84)) hat bislang noch keine eindeutigen Ergebnisse bezüglich ihrer Wirkung auf Krankheitsverläufe erbracht, zeigte jedoch, dass sich der Antikörper im zentralen Nervensystem anreichert und das freie Tau im CSF reduziert. Neben Aβ- und Tau-Antikörpern, wird auch die Neuroinflammation als Ansatzpunkt neuartiger Therapien unter die Lupe genommen (85, 86).

4.6. Wissenschaftliche Fragestellungen

Fragestellung I: Das pathophysiologische Wechselspiel zwischen ATN-Biomarkern (Aβ, Tau, Neurodegeneration) und Neuroinflammation wurde bisher hauptsächlich in Studien untersucht, die sich auf ein typisches AD-Kontinuum konzentrierten. Doch auch bei den primären Tauopathien PSP und CBD wird der Neuroinflammation eine Rolle in der Krankheitspathogenese beigemessen (87) und Aβ ist eine gängige Ko-Pathologie. Weiter identifizierte eine Studie aus dem Jahr 2021 vier verschiedene Verläufe der Tau-Ausbreitung bei AD (88) und lässt auf individuell heterogen-

anatomische Ausbreitungsmuster schließen. Eine Untersuchung der Zusammenhänge zwischen ATN-Biomarkern und Neuroinflammation in einer Kohorte bestehend aus Patienten mit typischer AD, atypischer AD, sowie mit 4R-Tauopathie könnte tiefergehende Einblicke in die zugrundeliegenden pathophysiologischen Prozesse ermöglichen. Um der Heterogenität der Biomarker-Ausbreitungswege gerecht zu werden, könnte neben einer Gruppenanalyse auch eine Analyse auf Einzelpatientenniveau von wissenschaftlichem Wert sein. In diesem Zusammenhang könnte die spezifische AT-assoziierte Neuroinflammation sowohl im klinischen Schweregrad der Erkrankungen reflektiert werden, was wesentlich zur Bewertung der Krankheitsprogression beiträgt, als auch mit sTREM2-Parametern assoziiert sein.

Fragestellung II: Eine präzise *ante-mortem* Diagnose der zugrundeliegenden Pathologie bei dementiellen Syndromen wird im Kontext molekularer Therapien zunehmend wichtiger. Der Tau-PET-Tracer ^{18}F-PI-2620 hat sich in verschiedenen Studien durch seine geringe „Off-Target"-Bindung an Monoaminooxidasen (56, 57) hervorgetan und kann sowohl 3/4R Tau (58), als auch 4R Tau (12, 56, 59, 60) abbilden. Die Anwendung von ^{18}F-PI-2620 als *in vivo* Biomarker für das CBS und dessen Fähigkeit, zugrundeliegende molekulare Entitäten zu differenzieren, könnte bedeutende therapeutische Implikationen haben und helfen, den klinischen Verlauf einer Erkrankung einzuschätzen.

5. Zusammenfassung

In Bezug auf die erste wissenschaftliche Fragestellung wurden Assoziationen von Aβ, Tau und Neurodegeneration (Perfusion, Atrophie) mit Neuroinflammation (aktivierte Mikroglia) bei 18 Patienten mit typischer AD, 11 mit AD-CBS und 26 mit 4RT analysiert und im Kontext klinischer Parameter evaluiert. Die ATI(N)-Biomarker zeigten eine heterogene Akkumulation bei den verschiedenen Studiengruppen. Genauer wurden die höchsten Aβ-PET- und Tau-PET-Signale in kortikalen Hirnregionen von Patienten mit typischer und atypischer Alzheimer-Krankheit gefunden, während Patienten mit 4RT niedrige Aβ-PET-Werte und eine überwiegend subkortikale Tau-Akkumulation aufwiesen. Ein erhöhtes Biomarker-Signal der Neuroinflammation (TSPO-PET) wurde vor allem in Tau-, nicht aber in Aβ-PET-positiven Hirnregionen beobachtet. Um der regionalen Heterogenität gerecht zu werden, wurde auf Einzelpatientenniveau eine multiple Regressionsanalyse durchgeführt. Das Regressionsmodell identifizierte Tau in allen Studiengruppen als stärksten Prädiktor für aktivierte Mikroglia. In beiden AD-Gruppen zeigte Aβ ebenfalls einen signifikanten Einfluss auf aktivierte Mikroglia, nicht jedoch 4RT, obwohl Aβ als Kopathologie bekannt ist. Die TSPO-Tracer-Spezifität von ^{18}F-GE-180 wurde durch das Aufheben einzelner Assoziationen bei einer separaten Studiengruppe mit LAB-Status (n = 7) bestätigt. Eine multiple Regression innerhalb der einzelnen Studiengruppen zeigte, dass trotz starker Tau-Aggregation ein weiterer Anstieg der aktivierten Mikroglia zu verzeichnen war, während bei bereits mäßiger Aβ-Ablagerung ein Plateau erreicht wurde. Dies deutet darauf hin, dass aktivierte Mikroglia stark mit der Tau-Aggregation bei etablierter AD und mit der Aβ-Ablagerung bei milden kognitiven Beeinträchtigungen korreliert. Abschließend korrelierte eine erhöhte individuelle Tau-assoziierte Mikrogliaaktivierung signifikant mit höherer Depressivität und mit einer schlechteren motorischen Leistung. Im Gegensatz dazu zeigte Aβ-assoziierte Mikrogliaaktivierung eine günstigere Wirkung auf klinische Parameter (signifikant positive Interaktionseffekte

zu Tau). Weiter wurde eine hohe Aβ-, aber niedrige Tau-assoziierte Mikrogliaaktivierung bei Patienten mit AD-Pathologie mit einem Anstieg von sTREM2 in Verbindung gebracht. Patienten mit 4RT zeigten einen gegenteiligen Effekt, was auf unterschiedliche Verläufe der Mikroglia-Phänotypen im Verlauf von primären und sekundären Tauopathien hinweisen könnte.

Im Rahmen der zweiten wissenschaftlichen Fragestellung wurde der klinische Nutzen des Tau-PET-Tracers ^{18}F-PI-2620 untersucht, insbesondere hinsichtlich seiner Fähigkeit, bei CBS-Patienten die zugrundeliegende Pathologie zu identifizieren und potenzielle Krankheitsverläufe abzubilden. Der Tracer zeigte eine spezifische Bindung in subkortikalen (Putamen und Globus pallidus externus) und kortikalen Zielregionen (dorsolateraler präfrontaler Kortex) bei CBS-Patienten sowohl mit Aβ- (Aβ(+)CBS, n = 11) als auch ohne Aβ-Pathologie (Aβ(-)CBS, n = 34) im Vergleich zu einer Kontrollgruppe. Die Aβ(-)CBS-Gruppe zeigte zusätzlich im Globus pallidus internus und im Nucleus subthalamicus eine subkortikale Bindung. Die Aβ(+)CBS-Gruppe wiederum zeigte eine Bindung in multiplen kortikalen Regionen, und ein Vergleich mit Patienten, die an typischer AD (n = 12) leiden, offenbarte eine zusätzliche Anreicherung im prä- und postzentralen Gyrus. Die semiquantitative Tau-PET-Positivität (91 % bei Aβ(+)CBS und 65 % bei Aβ(-)CBS) steht in Einklang mit früheren histopathologischen Daten. Das Putamen und der Globus pallidus externus zeigten die höchste Diskriminierungsrate in der gesamten CBS-Kohorte im Vergleich zu den Kontrollen, im Gegensatz zu einer früheren Studie mit PSP (Richardson-Syndrom), bei der der Globus pallidus internus, Nucleus subthalamicus und Substantia nigra die höchste Diskriminierung zeigten. Das CBS lässt hier eine Verschiebung zu Hirnarealen mit höherer Hirnfunktion erkennen. Die klinischen Skalen und subkortikalen ^{18}F-PI-2620 Signale korrelierten untereinander gut bei Aβ(-)CBS-Patienten, während bei Aβ(+)CBS-Patienten die kortikalen Signale gut untereinander korrelierten. Spezifisch korrelierte bei Aβ(-)CBS die Krankheitsdauer positiv mit dem Signal im

DLPFC und der PSP-CDS-Scores stark mit dem Signal im Gyrus postcentralis. Bei Aβ(+)CBS zeigte der PSP-CDS- und der PSPRS-Score positive Korrelationen mit subkortikalen Signalen. Eine semiquantitative Analyse zeigte, dass die Lateralisierung des subkortikalen ^{18}F-PI-2620-Signals die Asymmetrie der klinischen Symptome entsprechend der kontralateralen Hemisphäre zum klinischen Phänotyp widerspiegelte. Die ^{18}F-PI-2620 Tau-PET-Bildgebung fungiert als effektiver Biomarker zur Beurteilung von Patienten mit CBS, indem sie heterogene Neuropathologien in Aβ(+)CBS- und Aβ(-)CBS-Fällen aufdeckt und mit klinischen Parametern korreliert.

6. Abstract

In relation to the first scientific query, associations between Aβ, tau, and neurodegeneration (perfusion, atrophy) with neuroinflammation (activated microglia) were analyzed in 18 patients with typical AD, 11 with AD-CBS, and 26 with 4RT, and evaluated in the context of clinical parameters. The ATI(N) biomarkers exhibited heterogeneous accumulation across the study groups. Specifically, the highest Aβ-PET and Tau-PET signals were identified in the cortical brain regions of patients with typical and atypical Alzheimer's disease, whereas patients with 4RT exhibited low Aβ-PET values and predominantly subcortical tau accumulation. An increased biomarker signal for neuroinflammation (TSPO-PET) was predominantly observed in tau-positive, but not Aβ-PET-positive, brain regions. To account for regional heterogeneity, a multiple regression analysis was performed at the individual patient level, identifying tau as the strongest predictor of activated microglia across all study groups. In both AD groups, Aβ also significantly influenced activated microglia, unlike in 4RT, despite Aβ being known as a copathology. The specificity of the TSPO tracer ^{18}F-GE-180 was confirmed through the nullification of certain associations in a separate study group with LAB status (n = 7). A multiple regression within individual study groups revealed that despite significant tau aggregation, an increase in activated microglia was observed, whereas a plateau was reached with already moderate Aβ deposition. This suggests that activated microglia correlate strongly with tau aggregation in established AD and with Aβ deposition in mild cognitive impairments. Increased individual tau-associated microglial activation significantly correlated with higher depression and worse motor performance. Conversely, Aβ-associated microglial activation had a favorable effect on clinical parameters (significant positive interaction effects with tau). High Aβ- but low tau-associated microglial activation in patients with AD pathology was associated with an increase in sTREM2. Patients with 4RT exhibited an

opposite effect, suggesting different trajectories of microglial phenotypes in the course of primary and secondary tauopathies.

In the context of the second scientific query, the clinical utility of the Tau-PET tracer ^{18}F-PI-2620 was investigated, specifically regarding its ability to identify underlying pathology in CBS patients and to map potential disease trajectories. The tracer demonstrated specific binding in subcortical (putamen and external globus pallidus) and cortical target regions (dorsolateral prefrontal cortex) in CBS patients both with and without Aβ pathology (Aβ(+)CBS, n = 11; Aβ(-)CBS, n = 34) compared to a control group. The Aβ(-)CBS group further showed subcortical binding in the internal globus pallidus and subthalamic nucleus. Conversely, the Aβ(+)CBS group exhibited binding in multiple cortical regions, and a comparison with patients suffering from typical AD (n = 12) revealed additional enrichment in the pre- and postcentral gyrus. The semi-quantitative Tau-PET positivity (91% in Aβ(+)CBS and 65% in Aβ(-)CBS) is consistent with previous histopathological data. The putamen and external globus pallidus exhibited the highest discrimination rate across the entire CBS cohort compared to controls, contrasting with a previous study on PSP (Richardson syndrome) where the internal globus pallidus, subthalamic nucleus, and substantia nigra showed the highest discrimination. CBS indicates a shift towards brain areas associated with higher brain function. Clinical scales and subcortical ^{18}F-PI-2620 signals correlated well among Aβ(-)CBS patients, whereas in Aβ(+)CBS patients, cortical signals correlated well with each other. Specifically, in Aβ(-)CBS, disease duration positively correlated with the signal in the DLPFC, and PSP-CDS scores strongly correlated with the signal in the postcentral gyrus. In Aβ(+)CBS, both PSP-CDS and PSPRS scores showed positive correlations with subcortical signals. A semi-quantitative analysis revealed that the lateralization of the subcortical ^{18}F-PI-2620 signal reflected the asymmetry of clinical symptoms according to the contralateral hemisphere to the clinical phenotype. The ^{18}F-PI-2620 Tau-PET imaging serves as an

effective biomarker for assessing patients with CBS, unveiling heterogeneous neuropathologies in Aβ(+)CBS and Aβ(-)CBS cases and correlating with clinical parameters.

7. Literaturverzeichnis

1. United Nations - Department of Economic and Social Affairs - Population Division. World Population Prospects 2022: Summary of Results. UN DESA/POP/2022/TR/NO 3. 2022.

2. Peters E, Pritzkuleit R, Beske F, Katalinic A. Demografischer Wandel und Krankheitshäufigkeiten: Eine Projektion bis 2050. Bundesgesundheitsblatt - Gesundheitsforschung - Gesundheitsschutz. 2010;53(5):417-26.

3. Statistisches Bundesamt [Internet]. Diagnose Alzheimer: Zahl der Klinikbehandlungen und Todesfälle binnen 20 Jahren mehr als verdoppelt. 2022 [cited 2023 Okt 24]. Available from: https://www.destatis.de/DE/Presse/Pressemitteilungen/Zahl-der-Woche/2022/PD22_38_p002.html.

4. Drechsel DN, Hyman AA, Cobb MH, Kirschner MW. Modulation of the dynamic instability of tubulin assembly by the microtubule-associated protein tau. Mol Biol Cell. 1992;3(10):1141-54.

5. Trinczek B, Biernat J, Baumann K, Mandelkow EM, Mandelkow E. Domains of tau protein, differential phosphorylation, and dynamic instability of microtubules. Mol Biol Cell. 1995;6(12):1887-902.

6. Lee G, Leugers CJ. Tau and tauopathies. Prog Mol Biol Transl Sci. 2012;107:263-93.

7. Arendt T, Stieler JT, Holzer M. Tau and tauopathies. Brain Res Bull. 2016;126(Pt 3):238-92.

8. Kovacs GG. Invited review: Neuropathology of tauopathies: principles and practice. Neuropathol Appl Neurobiol. 2015;41(1):3-23.

9. Iqbal K, Liu F, Gong CX, Alonso Adel C, Grundke-Iqbal I. Mechanisms of tau-induced neurodegeneration. Acta Neuropathol. 2009;118(1):53-69.

10. Braak H, Braak E. Neuropathological stageing of Alzheimer-related changes. Acta Neuropathol. 1991;82(4):239-59.

11. Franzmeier N, Neitzel J, Rubinski A, Smith R, Strandberg O, Ossenkoppele R, et al. Functional brain architecture is associated with the rate of tau accumulation in Alzheimer's disease. Nat Commun. 2020;11(1):347.

12. Franzmeier N, Brendel M, Beyer L, Slemann L, Kovacs GG, Arzberger T, et al. Tau deposition patterns are associated with functional connectivity in primary tauopathies. Nat Commun. 2022;13(1):1362.

13. Hardy JA, Higgins GA. Alzheimer's disease: the amyloid cascade hypothesis. Science. 1992;256(5054):184-5.

14. Selkoe DJ, Hardy J. The amyloid hypothesis of Alzheimer's disease at 25 years. EMBO Mol Med. 2016;8(6):595-608.

15. Gotz J, Halliday G, Nisbet RM. Molecular Pathogenesis of the Tauopathies. Annu Rev Pathol. 2019;14:239-61.

16. Rosler TW, Tayaranian Marvian A, Brendel M, Nykanen NP, Hollerhage M, Schwarz SC, et al. Four-repeat tauopathies. Prog Neurobiol. 2019;180:101644.

17. Jack CR, Jr., Holtzman DM. Biomarker modeling of Alzheimer's disease. Neuron. 2013;80(6):1347-58.

18. Jack CR, Jr., Knopman DS, Jagust WJ, Petersen RC, Weiner MW, Aisen PS, et al. Tracking pathophysiological processes in Alzheimer's disease: an updated hypothetical model of dynamic biomarkers. Lancet Neurol. 2013;12(2):207-16.

19. Tan MS, Ji X, Li JQ, Xu W, Wang HF, Tan CC, et al. Longitudinal trajectories of Alzheimer's ATN biomarkers in elderly persons without dementia. Alzheimers Res Ther. 2020;12(1):55.

20. Hampel H, Cummings J, Blennow K, Gao P, Jack CR, Jr., Vergallo A. Developing the ATX(N) classification for use across the Alzheimer disease continuum. Nat Rev Neurol. 2021;17(9):580-9.

21. Jack CR, Jr., Bennett DA, Blennow K, Carrillo MC, Dunn B, Haeberlein SB, et al. NIA-AA Research Framework: Toward a biological definition of Alzheimer's disease. Alzheimers Dement. 2018;14(4):535-62.

22. Pascoal TA, Benedet AL, Ashton NJ, Kang MS, Therriault J, Chamoun M, et al. Microglial activation and tau propagate jointly across Braak stages. Nat Med. 2021;27(9):1592-9.

23. Pascoal TA, Benedet AL, Ashton NJ, Kang MS, Therriault J, Chamoun M, et al. Publisher Correction: Microglial activation and tau propagate jointly across Braak stages. Nat Med. 2021;27(11):2048-9.

24. Serrano-Pozo A, Mielke ML, Gomez-Isla T, Betensky RA, Growdon JH, Frosch MP, et al. Reactive glia not only associates with plaques but also parallels tangles in Alzheimer's disease. Am J Pathol. 2011;179(3):1373-84.

25. Dani M, Wood M, Mizoguchi R, Fan Z, Walker Z, Morgan R, et al. Microglial activation correlates in vivo with both tau and amyloid in Alzheimer's disease. Brain. 2018;141(9):2740-54.

26. Hammes J, Leuwer I, Bischof GN, Drzezga A, van Eimeren T. Multimodal correlation of dynamic [(18)F]-AV-1451 perfusion PET and neuronal hypometabolism in [(18)F]-FDG PET. Eur J Nucl Med Mol Imaging. 2017;44(13):2249-56.

27. Volter F, Beyer L, Eckenweber F, Scheifele M, Bui N, Patt M, et al. Assessment of perfusion deficit with early phases of [(18)F]PI-2620 tau-PET versus [(18)F]flutemetamol-amyloid-PET recordings. Eur J Nucl Med Mol Imaging. 2023;50(5):1384-94.

28. Beyer L, Nitschmann A, Barthel H, van Eimeren T, Unterrainer M, Sauerbeck J, et al. Early-phase [(18)F]PI-2620 tau-PET imaging as a surrogate marker of neuronal injury. Eur J Nucl Med Mol Imaging. 2020;47(12):2911-22.

29. Minoshima S, Cross D, Thientunyakit T, Foster NL, Drzezga A. (18)F-FDG PET Imaging in Neurodegenerative Dementing Disorders: Insights into Subtype Classification, Emerging Disease Categories, and Mixed Dementia with Copathologies. J Nucl Med. 2022;63(Suppl 1):2S-12S.

30. Wolf SA, Boddeke HW, Kettenmann H. Microglia in Physiology and Disease. Annu Rev Physiol. 2017;79:619-43.

31. Ransohoff RM, Perry VH. Microglial physiology: unique stimuli, specialized responses. Annu Rev Immunol. 2009;27:119-45.

32. Biber K, Owens T, Boddeke E. What is microglia neurotoxicity (Not)? Glia. 2014;62(6):841-54.

33. Chen Z, Trapp BD. Microglia and neuroprotection. J Neurochem. 2016;136 Suppl 1:10-7.

34. Wang WY, Tan MS, Yu JT, Tan L. Role of pro-inflammatory cytokines released from microglia in Alzheimer's disease. Ann Transl Med. 2015;3(10):136.

35. Blinzinger K, Kreutzberg G. Displacement of synaptic terminals from regenerating motoneurons by microglial cells. Z Zellforsch Mikrosk Anat. 1968;85(2):145-57.

36. Heneka MT, Carson MJ, El Khoury J, Landreth GE, Brosseron F, Feinstein DL, et al. Neuroinflammation in Alzheimer's disease. Lancet Neurol. 2015;14(4):388-405.

37. Bature F, Guinn BA, Pang D, Pappas Y. Signs and symptoms preceding the diagnosis of Alzheimer's disease: a systematic scoping review of literature from 1937 to 2016. BMJ Open. 2017;7(8):e015746.

38. Breijyeh Z, Karaman R. Comprehensive Review on Alzheimer's Disease: Causes and Treatment. Molecules. 2020;25(24).

39. Armstrong MJ, Litvan I, Lang AE, Bak TH, Bhatia KP, Borroni B, et al. Criteria for the diagnosis of corticobasal degeneration. Neurology. 2013;80(5):496-503.

40. Constantinides VC, Paraskevas GP, Paraskevas PG, Stefanis L, Kapaki E. Corticobasal degeneration and corticobasal syndrome: A review. Clin Park Relat Disord. 2019;1:66-71.

41. Ling H, O'Sullivan SS, Holton JL, Revesz T, Massey LA, Williams DR, et al. Does corticobasal degeneration exist? A clinicopathological re-evaluation. Brain. 2010;133(Pt 7):2045-57.

42. Hoglinger GU, Respondek G, Stamelou M, Kurz C, Josephs KA, Lang AE, et al. Clinical diagnosis of progressive supranuclear palsy: The movement disorder society criteria. Mov Disord. 2017;32(6):853-64.

43. Grimm MJ, Respondek G, Stamelou M, Arzberger T, Ferguson L, Gelpi E, et al. How to apply the movement disorder society criteria for diagnosis of progressive supranuclear palsy. Mov Disord. 2019;34(8):1228-32.

44. Voglein J, Kostova I, Arzberger T, Roeber S, Schmitz P, Simons M, et al. First symptom guides diagnosis and prognosis in neurodegenerative diseases-a retrospective study of autopsy proven cases. Eur J Neurol. 2021;28(6):1801-11.

45. Williams DR, de Silva R, Paviour DC, Pittman A, Watt HC, Kilford L, et al. Characteristics of two distinct clinical phenotypes in pathologically proven progressive supranuclear palsy: Richardson's syndrome and PSP-parkinsonism. Brain. 2005;128(Pt 6):1247-58.

46. Litvan I, Agid Y, Jankovic J, Goetz C, Brandel JP, Lai EC, et al. Accuracy of clinical criteria for the diagnosis of progressive supranuclear palsy (Steele-Richardson-Olszewski syndrome). Neurology. 1996;46(4):922-30.

47. Respondek G, Kurz C, Arzberger T, Compta Y, Englund E, Ferguson LW, et al. Which ante mortem clinical features predict progressive supranuclear palsy pathology? Mov Disord. 2017;32(7):995-1005.

48. Clark CM, Schneider JA, Bedell BJ, Beach TG, Bilker WB, Mintun MA, et al. Use of florbetapir-PET for imaging β-amyloid pathology. JAMA. 2011;305(3):275-83.

49. Curtis C, Gamez JE, Singh U, Sadowsky CH, Villena T, Sabbagh MN, et al. Phase 3 trial of flutemetamol labeled with radioactive fluorine 18 imaging and neuritic plaque density. JAMA Neurology. 2015;72(3):287-94.

50. Snellman A, Rokka J, Lopez-Picon FR, Eskola O, Wilson I, Farrar G, et al. Pharmacokinetics of [(1)(8)F]flutemetamol in wild-type rodents and its binding to beta amyloid deposits in a mouse model of Alzheimer's disease. Eur J Nucl Med Mol Imaging. 2012;39(11):1784-95.

51. Sabri O, Sabbagh MN, Seibyl J, Barthel H, Akatsu H, Ouchi Y, et al. Florbetaben PET imaging to detect amyloid beta plaques in Alzheimer's disease: Phase 3 study. Alzheimer's and Dementia. 2015;11(8):964-74.

52. Martinez G, Vernooij RW, Fuentes Padilla P, Zamora J, Flicker L, Bonfill Cosp X. 18F PET with florbetaben for the early diagnosis of Alzheimer's disease dementia and other dementias in people with mild cognitive impairment (MCI). Cochrane Database Syst Rev. 2017;11(11):CD012883.

53. Hunt A. FDA Approves First Drug to Image Tau Pathology in Patients Being Evaluated for Alzheimer's Disease: U.S. Food and Drug Administration [Internet]; 2020 [cited 2023 Dez 1]. Available from: https://www.fda.gov/news-events/press-announcements/fda-approves-first-drug-image-tau-pathology-patients-being-evaluated-alzheimers-disease.

54. Passamonti L, Vazquez Rodriguez P, Hong YT, Allinson KS, Williamson D, Borchert RJ, et al. 18F-AV-1451 positron emission tomography in Alzheimer's disease and progressive supranuclear palsy. Brain. 2017;140(3):781-91.

55. Wang YT, Edison P. Tau Imaging in Neurodegenerative Diseases Using Positron Emission Tomography. Curr Neurol Neurosci Rep. 2019;19(7):45.

56. Kroth H, Oden F, Molette J, Schieferstein H, Capotosti F, Mueller A, et al. Discovery and preclinical characterization of [(18)F]PI-2620, a next-generation tau PET tracer for the assessment of tau pathology in Alzheimer's disease and other tauopathies. Eur J Nucl Med Mol Imaging. 2019;46(10):2178-89.

57. Murugan NA, Chiotis K, Rodriguez-Vieitez E, Lemoine L, Agren H, Nordberg A. Cross-interaction of tau PET tracers with monoamine oxidase B: evidence from in silico modelling and in vivo imaging. Eur J Nucl Med Mol Imaging. 2019;46(6):1369-82.

58. Mueller A, Bullich S, Barret O, Madonia J, Berndt M, Papin C, et al. Tau PET imaging with (18)F-PI-2620 in Patients with Alzheimer Disease and Healthy Controls: A First-in-Humans Study. J Nucl Med. 2020;61(6):911-9.

59. Willroider M, Roeber S, Horn AKE, Arzberger T, Scheifele M, Respondek G, et al. Superiority of Formalin-Fixed Paraffin-Embedded Brain Tissue for in vitro Assessment of Progressive Supranuclear Palsy Tau Pathology With [(18) F]PI-2620. Front Neurol. 2021;12:684523.

60. Brendel M, Barthel H, van Eimeren T, Marek K, Beyer L, Song M, et al. Assessment of 18F-PI-2620 as a Biomarker in Progressive Supranuclear Palsy. JAMA Neurol. 2020;77(11):1408-19.

61. Malarte ML, Gillberg PG, Kumar A, Bogdanovic N, Lemoine L, Nordberg A. Correction: Discriminative binding of tau PET tracers PI2620, MK6240 and RO948 in Alzheimer's disease, corticobasal degeneration and progressive supranuclear palsy brains. Mol Psychiatry. 2023.

62. Malarte ML, Gillberg PG, Kumar A, Bogdanovic N, Lemoine L, Nordberg A. Discriminative binding of tau PET tracers PI2620, MK6240 and RO948 in Alzheimer's disease, corticobasal degeneration and progressive supranuclear palsy brains. Mol Psychiatry. 2023;28(3):1272-83.

63. Cumming P, Burgher B, Patkar O, Breakspear M, Vasdev N, Thomas P, et al. Sifting through the surfeit of neuroinflammation tracers. J Cereb Blood Flow Metab. 2018;38(2):204-24.

64. Stefaniak J, O'Brien J. Imaging of neuroinflammation in dementia: a review. J Neurol Neurosurg Psychiatry. 2016;87(1):21-8.

65. Palleis C, Sauerbeck J, Beyer L, Harris S, Schmitt J, Morenas-Rodriguez E, et al. In Vivo Assessment of Neuroinflammation in 4-Repeat Tauopathies. Mov Disord. 2021;36(4):883-94.

66. Rauchmann BS, Brendel M, Franzmeier N, Trappmann L, Zaganjori M, Ersoezlue E, et al. Microglial Activation and Connectivity in Alzheimer Disease and Aging. Ann Neurol. 2022;92(5):768-81.

67. Vettermann FJ, Harris S, Schmitt J, Unterrainer M, Lindner S, Rauchmann BS, et al. Impact of TSPO Receptor Polymorphism on [(18)F]GE-180 Binding in Healthy Brain and Pseudo-Reference Regions of Neurooncological and Neurodegenerative Disorders. Life (Basel). 2021;11(6).

68. Owen DR, Gunn RN, Rabiner EA, Bennacef I, Fujita M, Kreisl WC, et al. Mixed-affinity binding in humans with 18-kDa translocator protein ligands. J Nucl Med. 2011;52(1):24-32.

69. Owen DR, Yeo AJ, Gunn RN, Song K, Wadsworth G, Lewis A, et al. An 18-kDa translocator protein (TSPO) polymorphism explains differences in binding affinity of the PET radioligand PBR28. J Cereb Blood Flow Metab. 2012;32(1):1-5.

70. Zanotti-Fregonara P, Pascual B, Rostomily RC, Rizzo G, Veronese M, Masdeu JC, et al. Anatomy of (18)F-GE180, a failed radioligand for the TSPO protein. Eur J Nucl Med Mol Imaging. 2020;47(10):2233-6.

71. Ewers M, Franzmeier N, Suarez-Calvet M, Morenas-Rodriguez E, Caballero MAA, Kleinberger G, et al. Increased soluble TREM2 in cerebrospinal fluid is associated with reduced cognitive and clinical decline in Alzheimer's disease. Sci Transl Med. 2019;11(507).

72. DGN e. V. & DGPPN e. V. (Hrsg.). S3-Leitlinie Demenzen, Version 4.0. 2023 Nov 28 [cited 2023 Dez 23]. Available from: https://register.awmf.org/de/leitlinien/detail/038-013.

73. McShane R, Westby MJ, Roberts E, Minakaran N, Schneider L, Farrimond LE, et al. Memantine for dementia. Cochrane Database of Systematic Reviews. 2019(3).

74. Vanek Z, Jankovic J. Dystonia in corticobasal degeneration. Mov Disord. 2001;16(2):252-7.

75. Levin J, Kurz A, Arzberger T, Giese A, Hoglinger GU. The Differential Diagnosis and Treatment of Atypical Parkinsonism. Dtsch Arztebl Int. 2016;113(5):61-9.

76. Budd Haeberlein S, Aisen PS, Barkhof F, Chalkias S, Chen T, Cohen S, et al. Two Randomized Phase 3 Studies of Aducanumab in Early Alzheimer's Disease. J Prev Alzheimers Dis. 2022;9(2):197-210.

77. Cavazzoni P. FDA's Decision to Approve New Treatment for Alzheimer's Disease: U.S. Food and Drug Administration [Internet]; 2021 [cited 2023 Dez 3]. Available from: https://www.fda.gov/drugs/our-perspective/fdas-decision-approve-new-treatment-alzheimers-disease.

78. Grant A. FDA Grants Accelerated Approval for Alzheimer's Disease Treatment: U.S. Food and Drug Administration [Internet]; 2023 [cited 2023 Dez 3]. Available from: https://www.fda.gov/news-events/press-announcements/fda-grants-accelerated-approval-alzheimers-disease-treatment.

79. van Dyck CH, Swanson CJ, Aisen P, Bateman RJ, Chen C, Gee M, et al. Lecanemab in Early Alzheimer's Disease. N Engl J Med. 2023;388(1):9-21.

80. Sims JR, Zimmer JA, Evans CD, Lu M, Ardayfio P, Sparks J, et al. Donanemab in Early Symptomatic Alzheimer Disease: The TRAILBLAZER-ALZ 2 Randomized Clinical Trial. JAMA. 2023;330(6):512-27.

81. Florian H, Wang D, Arnold SE, Boada M, Guo Q, Jin Z, et al. Tilavonemab in early Alzheimer's disease: results from a phase 2, randomized, double-blind study. Brain. 2023;146(6):2275-84.

82. Hoglinger GU, Litvan I, Mendonca N, Wang D, Zheng H, Rendenbach-Mueller B, et al. Safety and efficacy of tilavonemab in progressive supranuclear palsy: a phase 2, randomised, placebo-controlled trial. Lancet Neurol. 2021;20(3):182-92.

83. Edland SD, Llibre-Guerra JJ. Semorinemab in Mild-to-Moderate Alzheimer Disease: A Glimmer of Hope Though Cautions Remain. Neurology. 2023;101(14):593-4.

84. Monteiro C, Toth B, Brunstein F, Bobbala A, Datta S, Ceniceros R, et al. Randomized Phase II Study of the Safety and Efficacy of Semorinemab in Participants With Mild-to-Moderate Alzheimer Disease: Lauriet. Neurology. 2023;101(14):e1391-e401.

85. Reading CL, Ahlem CN, Murphy MF. NM101 Phase III study of NE3107 in Alzheimer's disease: rationale, design and therapeutic modulation of neuroinflammation and insulin resistance. Neurodegener Dis Manag. 2021;11(4):289-98.

86. Howard R, Zubko O, Bradley R, Harper E, Pank L, O'Brien J, et al. Minocycline at 2 Different Dosages vs Placebo for Patients With Mild Alzheimer Disease: A Randomized Clinical Trial. JAMA Neurol. 2020;77(2):164-74.

87. Ishizawa K, Dickson DW. Microglial activation parallels system degeneration in progressive supranuclear palsy and corticobasal degeneration. J Neuropathol Exp Neurol. 2001;60(6):647-57.

88. Vogel JW, Young AL, Oxtoby NP, Smith R, Ossenkoppele R, Strandberg OT, et al. Four distinct trajectories of tau deposition identified in Alzheimer's disease. Nat Med. 2021;27(5):871-81.

8. Danksagung

Ein besonderer Dank geht an meinen Doktorvater, Betreuer und Problemlöser Matthias Brendel. Von der Bereitstellung der Forschungsarbeiten, über die methodische Heranführung und Einarbeitung bis zur Publikation der Arbeiten fühlte ich mich immer gut betreut und unterstützt. Dank seiner offenen Tür und seiner rekordverdächtigen Mail-Antwortgeschwindigkeit blieb ich an keinem Tag ratlos. So macht Wissenschaft Spaß!

Vielen Dank an meine Koautorinnen Gloria Biechele und Carla Palleis, mit denen die Zusammenarbeit an den Publikationen immer viel Spaß gemacht hat und die mir bei Fragen schnell weiterhelfen konnten.

Ich danke meinen Eltern (Annette und Claus) und meinen Geschwistern (Nikola, Tabea und Adrian), die mir den Rücken stärken und immer ein offenes Ohr für mich haben.

Danke Micha, dass du immer für mich da bist!

9. Publikation I

Molecular Psychiatry www.nature.com/mp

ARTICLE OPEN

Check for updates

Individual regional associations between Aβ-, tau- and neurodegeneration (ATN) with microglial activation in patients with primary and secondary tauopathies

Anika Finze[1,20], Gloria Biechele[1,2,20], Boris-Stephan Rauchmann[2,3], Nicolai Franzmeier[4,5,6], Carla Palleis[5,7,8], Sabrina Katzdobler[5,7,8], Endy Weidinger[7,8], Selim Guersel[9], Sebastian Schuster[1], Stefanie Harris[1], Julia Schmitt[1], Leonie Beyer[1], Johannes Gnörich[1], Simon Lindner[1], Nathalie L. Albert[1], Christian H. Wetzel[10], Rainer Rupprecht[10], Axel Rominger[1,11], Adrian Danek[7,8], Lena Burow[9], Carolin Kurz[9], Maia Tato[9], Julia Utecht[9], Boris Papazov[2,3], Mirlind Zaganjori[1,9], Lena-Katharina Trappmann[9], Oliver Goldhardt[12], Timo Grimmer[12], Jan Haeckert[13], Daniel Janowitz[4], Katharina Buerger[4], Daniel Keeser[3,9], Sophia Stoecklein[2], Olaf Dietrich[2], Estrella Morenas-Rodriguez[7], Henryk Barthel[14], Osama Sabri[14], Peter Bartenstein[1,5], Mikael Simons[5,7,15], Christian Haass[5,7,16], Günter U. Höglinger[7,8,17], Johannes Levin[5,7,8], Robert Perneczky[5,7,9,18,19] and Matthias Brendel[1,5,7]✉

β-amyloid (Aβ) and tau aggregation as well as neuronal injury and atrophy (ATN) are the major hallmarks of Alzheimer's disease (AD), and biomarkers for these hallmarks have been linked to neuroinflammation. However, the detailed regional associations of these biomarkers with microglial activation in individual patients remain to be elucidated. We investigated a cohort of 55 patients with AD and primary tauopathies and 10 healthy controls that underwent TSPO-, Aβ-, tau-, and perfusion-surrogate-PET, as well as structural MRI. *Z*-score deviations for 246 brain regions were calculated and biomarker contributions of Aβ (A), tau (T), perfusion (N1), and gray matter atrophy (N2) to microglial activation (TSPO, I) were calculated for each individual subject. Individual ATN-related microglial activation was correlated with clinical performance and CSF soluble TREM2 (sTREM2) concentrations. In typical and atypical AD, regional tau was stronger and more frequently associated with microglial activation when compared to regional Aβ (AD: $\beta_T = 0.412 \pm 0.196$ vs. $\beta_A = 0.142 \pm 0.123$, $p < 0.001$; AD-CBS: $\beta_T = 0.385 \pm 0.176$ vs. $\beta_A = 0.131 \pm 0.186$, $p = 0.031$). The strong association between regional tau and microglia reproduced well in primary tauopathies ($\beta_T = 0.418 \pm 0.154$). Stronger individual associations between tau and microglial activation were associated with poorer clinical performance. In patients with 4RT, sTREM2 levels showed a positive association with tau-related microglial activation. Tau pathology has strong regional associations with microglial activation in primary and secondary tauopathies. Tau and Aβ related microglial response indices may serve as a two-dimensional in vivo assessment of neuroinflammation in neurodegenerative diseases.

Molecular Psychiatry; https://doi.org/10.1038/s41380-023-02188-8

INTRODUCTION

Tauopathies account for the majority of neurodegenerative disorders. These include the secondary 3/4-repeat tauopathy Alzheimer's disease (AD) as the most prevalent form of dementia in societies with aging populations [1]. Primary tauopathies, such as Pick's disease, progressive supranuclear palsy (PSP), or corticobasal degeneration (CBD) are characterized by abnormal tau protein aggregation with three or four microtubule-binding-domains [2, 3]. However, regardless of the distinct neuropathology, there is also overlap in clinical phenotypes, for example, in corticobasal syndrome (CBS), which can be characterized by 3/4-repeat AD-like tau or 4-repeat tau (4RT) aggregation [4].

The neuropathological cascade of AD is characterized by the triad of accumulation of extracellular β-amyloid (Aβ) plaques,

[1]Department of Nuclear Medicine, LMU University Hospital, LMU Munich, Munich, Germany. [2]Department of Radiology, LMU University Hospital, LMU Munich, Munich, Germany. [3]NeuroImaging Core Unit Munich (NICUM), LMU University Hospital, LMU Munich, Munich, Germany. [4]Institute for Stroke and Dementia Research, Munich, Germany. [5]Munich Cluster for Systems Neurology (SyNergy), Munich, Germany. [6]Department of Psychiatry and Neurochemistry, Sahlgrenska Academy at the University of Gothenburg, Gothenburg, Sweden. [7]German Center for Neurodegenerative Diseases (DZNE), Munich, Germany. [8]Department of Neurology, LMU University Hospital, LMU Munich, Munich, Germany. [9]Department of Psychiatry and Psychotherapy, LMU University Hospital, LMU Munich, Munich, Germany. [10]Department of Psychiatry and Psychotherapy, University Regensburg, Regensburg, Germany. [11]Department of Nuclear Medicine, University Hospital, Inselspital Bern, Bern, Switzerland. [12]Department of Psychiatry and Psychotherapy, Klinikum Rechts der Isar, Technical University of Munich, School of Medicine, Munich, Germany. [13]Department of Psychiatry, Psychotherapy and Psychosomatics, Medical Faculty, University of Augsburg, Augsburg, Germany. [14]Department of Nuclear Medicine, University of Leipzig, Leipzig, Germany. [15]Institute of Neuronal Cell Biology, Technical University of Munich, Munich, Germany. [16]Chair of Metabolic Biochemistry, Biomedical Center (BMC), Faculty of Medicine, LMU Munich, Munich, Germany. [17]Department of Neurology, Hannover Medical School, Hannover, Germany. [18]Ageing Epidemiology (AGE) Research Unit, School of Public Health, Imperial College London, London, UK. [19]Sheffield Institute for Translational Neurosciences (SITraN), University of Sheffield, Sheffield, UK. [20]These authors contributed equally: Anika Finze, Gloria Biechele. ✉email: matthias.brendel@med.uni-muenchen.de

Received: 22 November 2022 Revised: 27 June 2023 Accepted: 10 July 2023
Published online: 26 July 2023

fibrillary tau aggregates in neurons, and microgliosis and astrogliosis [5–9]. In AD, this is conceptualized as the ATN sequence, where β-amyloidosis [A] is thought to precede and accelerate tau pathology [T] that leads to neurodegeneration [N] [10], now expanding towards an ATX(N) system, where X represents novel candidate biomarkers for additional pathophysiological mechanisms such as neuroimmune dysregulation, synaptic dysfunction or blood-brain-barrier alterations [11].

In AD and primary tauopathies, neuroinflammation represents an important mediator of protein aggregation and spread as well as disease progression, creating a positive feedback-loop in the disease cascade [12–15] and could serve as a valuable "X" parameter of ATX(N), then termed ATI(N). In this context, molecular imaging with 18 kDa translocator protein (TSPO) positron-emission-tomography (TSPO-PET) for stratification and monitoring of neuroinflammation could become crucial for targeting and assessing response to immunomodulatory therapies and has spurned the development of a wide range of tracers for human studies [16–19]. However, despite several studies with tau and TSPO tracers [20–22], ATI(N)-like schemes and interactions have only rarely been investigated in atypical AD or primary tauopathies, although Aβ copathology is common in 4RTs [23].

A detailed understanding of the pathophysiological interplay between the accumulation of misfolded proteins (i.e. Aβ and tau) and their contribution to neuroinflammation may provide deeper insight into mechanistic pathways [24]. In recent years, several multi-tracer studies in cohorts composed mainly of patients along the typical AD continuum revealed discrepant findings. Some investigations attributed the equal influence of Aβ and tau to microglial activation [25], while others supported the interaction of Aβ and microglia activation to set the pace for subsequent tau spread [12, 26]. The effects of microglial activation on cognition are thought to be strongly mediated by gray matter atrophy [27], and activated microglia have been correlated with parietal atrophy post mortem [28]. Thus, we aimed to investigate the interplay between ATI(N) biomarkers and microglial activation in a cohort composed of primary and secondary tauopathies, including atypical and typical AD. We analyzed the regional heterogeneity of ATI(N) biomarker alterations in tauopathies and we computed the partial contributions of ATN biomarkers to microglial activation at the individual patient level. Furthermore, we questioned the shape and magnitude of expurgated regional associations between aggregation of Aβ and tau with microglial activation. Finally, we correlated the individual Aβ- and tau-related microglial responses with clinical performance and cerebrospinal sTREM2 (soluble triggering receptor expressed on myeloid cells 2) levels.

MATERIAL AND METHODS

Study design

We enrolled patients with typical AD, AD-CBS, and 4RTs as well as healthy controls from ActiGliA, a prospective cohort study at Ludwig-Maximilians-University (LMU), approved by the local ethics committee (project-number 17-755; human PET analyses project-numbers 17-569, 19-022). Written informed consent was obtained from all participants in accordance with the Declaration of Helsinki. Requirements for inclusion were tau- and TSPO-PET, and T1w-MRI if available, within a time period of 18 months (mean time difference: 2.9 ± 4.4 months). Aβ-PET was tolerated up to 24 months prior to the remaining examinations (mean time difference: 6.7 ± 8.3 months). Tau-PET had to be conducted with dynamic emission recording to ensure the availability of the early-phase as an "N" biomarker. Patients with a low affinity TSPO binding status were assigned to a separate "LAB" study group regardless of their clinical diagnosis.

Patients with dementia, mild cognitive impairment (MCI), or subjective memory decline (SCD) due to AD were diagnosed according to the diagnostic criteria of the National Institute on Aging [29]. All patients with AD had a positive Aβ-PET scan and were allocated to the "typical AD" group. Clinical diagnosis of CBS was made as defined in the MDS-PSP criteria [30]. All enrolled CBS patients also fulfilled the Armstrong criteria of probable or possible CBD-CBS [31]. Only CBS patients with negative family history of Parkinson's disease and AD were included. The positivity or negativity of the Aβ-PET scan defined the allocation into "AD-CBS" or "4RT" study groups.

Group level TSPO-PET data of this cohort was previously published for patients with AD, 4RTs, and controls [32, 33]. Group level tau-PET data of this cohort was partially published for patients with AD, AD-CBS, 4RTs, and controls [21]. Group level data of early-phase imaging ([^{18}F]flutemetamol and [^{18}F]PI-2620) of parts of the cohort were previously published for AD-CBS and 4RTs [34, 35]. All reported data are unpublished.

PET imaging

PET data acquisition, reconstruction, and post-processing. For all PET procedures, including radiochemistry, acquisition, and pre-processing, we used an established and standardized protocol [21, 32, 35, 36]. Patients were scanned at the Department of Nuclear Medicine, LMU, using a Biograph 64 PET/CT scanner or a harmonized Biograph mCT (Siemens, Erlangen, Germany). In brief, [^{18}F]GE-180 TSPO-PET recordings (average dose: 179 ± 13 MBq) with an emission window of 60-80 min after injection were obtained to measure microglial activation [32]. [^{18}F]flutemetamol Aβ-PET recordings (average dose: 185 ± 16 MBq) with an emission window of 90-110 min after injection were performed for assessment of fibrillar Aβ accumulation [36]. Dynamic [^{18}F]PI-2620 tau-PET (average dose: 188 ± 15 MBq) with emission recording 0–60 min after injection was performed to quantify tau aggregation. Static frames of the perfusion phase (0.5–2.5 min) [35] and the late phase (20-40 min) [37] were reconstructed.

PET image analysis. Several established processing pipelines [21, 32, 34, 35, 37] were executed to ensure reproducibility by different analysis methodology. We performed all PET data analyses using PMOD (V3.9; PMOD Technologies LLC; Zurich; Switzerland). The primary analysis used static emission recordings which were coregistered to the Montreal Neurology Institute (MNI) space using non-linear warping (16 iterations, frequency cutoff 25, transient input smoothing 8 x 8 x 8 mm^3) to tracer-specific templates acquired in previous in-house studies [21, 32, 35, 36]. Given the strong binding differences between positive and negative Aβ-PET images, we used positive (number of subjects in the template: $n_t = 15$) and negative ($n_t = 27$) Aβ-PET templates after classification of the Aβ-status by a visual read by a single rater. A unified template was used for TSPO-PET ($n_t = 11$). Tau-PET images were coregistered to early (mixed [^{18}F]PI-2620 and [^{18}F]Flutemetamol; $n_t = 15$) [38] and late phase ($n_t = 28$) templates without distinction of tau-positivity.

Intensity normalization of all PET images was performed by calculation of standardized uptake value ratios (SUVr) using the cerebellum as an established pseudo-reference tissue for TSPO-PET [39]. The cerebellum was selected as the best compromise of a unified pseudo-reference tissue since it was also validated for [^{18}F]flutemetamol [40] and [^{18}F]PI-2620. To account for tau-positive areas in the cerebellum and to avoid spill-over of adjacent extracerebral structures, the dentate nucleus as well as superior and posterior layers of the cerebellum were excluded. Using the Brainnetome atlas [41], the brain was parcellated into 210 cortical and 36 subcortical volume-of-interests (VOIs), and standardized-uptake-value-ratios (SUVr) were calculated for all four PET read-outs. Per subject, the standardized regional deviation of SUVr (z-score) was calculated versus previously established age- and sex- matched normal cohorts for [^{18}F]flutemetamol (number of controls: $n_c = 13$, [34]), [^{18}F]GE-180 ($n_c = 13$, [42]), early [^{18}F]PI-2620 ($n_c = 14$, [43]) and late [^{18}F]PI-2620 ($n_c = 14$, [4]).

Structural MR imaging

Three-dimensional T1-weighted (T1w) MRI data were collected for the majority (60/72) of the cohort as reported previously [33]. The data were coregistered into the MNI standard space using the PNEURO tool (V3.9; PMOD Technologies LLC) and segmented into all 246 Brainnetome atlas VOIs. In this step, regional gray-matter-volumes (GMV), for analysis of possible brain atrophy, were collected. As described above, we used age- and sex- matched controls for the calculation of standardized *z*-scores ($n_c = 13$).

DNA extraction and SNP genotyping

Since the binding properties of second-generation TSPO ligands have been found to depend on genetic polymorphism of the TSPO gene [44, 45], all individuals underwent rs6971 single nucleotide polymorphism (SNP)

genotyping and were classified as low, medium, or high affinity binder (LAB, MAB or HAB). For this purpose, whole-blood samples were sent to the Department of Psychiatry of the University Hospital Regensburg for genotyping. Genomic DNA was extracted from 4 ml of whole blood using a QIAamp DNA Blood Maxi kit (Qiagen, Hilden, Germany) according to the manufacturer's protocol. DNA quality was assessed by optical absorbance and gel electrophoresis. Exon 4 of the TSPO gene and exon/intron junctions were amplified by PCR and sequenced using the Sanger method with the following primers: ex4-FAGTTGGGCAGTGGGACAG and ex4-R-CAGATCCTGCAGAGACGA. Sequencing data were analyzed using SnapGene software (GSL Biotech; http://snapgene.com).

sTREM2

sTREM2 concentrations were measured in all available CSF samples (4RT 14/26, AD-CBS 7/11, AD 10/18) by a modified assay based on the previously described sTREM2 ELISA using the MSD platform [46–48]. This assay was designed to selectively detect sTREM2 coming from the cleavage of the full-length protein. Prior to data analysis, the sTREM2 data were log-transformed.

Clinical assessments

As a part of the ActiGliA protocol, patients underwent comprehensive clinical examinations. Some of these data were used to compare ATN-related microglial activation with clinical performance. In this work, the PSP-rating scale (PSPRS: 0–100) [49], the motor-examination of the Movement Disorder Society revised form of the Unified Parkinson's Disease Rating Scale (UPDRS: 0 – 100) [50] and the Geriatric Depression Scale (GDS: 0–15) [51] were analyzed. In addition, the Montreal Cognitive Assessment scale (MoCA: 0–30) [52] and the Mini-Mental State examination (MMSE: 0–30) [53] were evaluated. For patients without MoCA but MMSE, the MMSE was converted to a comparable MoCA score [54]. For simplicity, other clinical performance data collected by ActiGliA are not further mentioned.

Statistics

For statistical calculations, SPSS (V25; IBM; Ehningen; Germany) and R (V4.1.2; R Core Team; 2021; Vienna; Austria) were used. Unless declared otherwise, the significance level was set to 0.05. The day of Tau-PET examination was used to define the age of the patients. Due to the lack of significant [^{18}F]GE-180 binding differences between individuals with MAB and HAB status [55], the rs6971-SNP status was not used as a covariate after the exclusion of individuals with LAB status.

Biomarker positivity classification. To assign patients to specific study groups, PET images were visually rated for Aβ-PET-positivity (single expert reader). In addition, an optimal cutoff based on a sensitivity / specificity tradeoff was defined for each of the 246 Brainnetome VOIs for each biomarker (excluding GMV) using single-region-ROC-analysis (cutoff: criterion of the point on the ROC curve closest to the point 0,1 [56, 57]). For semi-quantitative Aβ-PET we defined the threshold to best discriminate the AD groups (AD-CBS and typical AD) from 4RT and CTRL. For TSPO-PET, tau-PET, and perfusion, the optimal cutoff was determined to discriminate 4RT, AD-CBS, and AD against CTRL. For every patient and biomarker, we summed up the positivity of the five regions with the highest area-under-curve (AUC) values and calculated another optimal cutoff via roc analysis to finally declare a patient as biomarker positive or negative.

Demographics, clinical performance, and sTREM2. To test for group differences in demographic data, a 1-way analysis of variance (ANOVA) was used for age, sTREM2, and MoCA. Sex and rs6971-SNP were subject to a chi-square (χ^2) test. With significant ANOVA or χ^2-test, multiple posthoc unpaired two-tailed Student's *t*-tests were subsequently performed between all groups (unadjusted for multiple testing).

Multiregion analyses. A descriptive heatmap was created by calculating arithmetic means ($\bar{x}$) within 24 composed Brainnetome regions [58] from the acquired *z*-scores and displayed in color scale per patient group and biomarker. Thereby, all $\bar{x} > 2$ were set equal to 2, and all $\bar{x} < -2$ were set equal to −2. For each of the 24 composite regions, the frequency of patients with peak *z*-scores (highest *z*-score along all 24 regions) was determined and visualized relative to the total amount of patients per group. These arithmetic means and biomarker peak distributions of the 24 brain regions were then tested for intercorrelations between those biomarkers (4RT, AD-CBS, and AD pooled) using linear Pearson's correlation (r).

Regression models. For each subject, a multiple linear regression model was defined to analyze the influence of the independent ATN variables (Aβ A, Tau T, Perfusion N1, GMV N2) on microglial activity (I), taking all 246 Brainnetome VOIs into account. The obtained standardized β-coefficients of ATN were visualized by a combined violin-box-plot. Within each diagnosis group, the β-coefficients of the four independent variables were tested for group differences using ANOVA with age and sex as covariates. Multiple post-hoc tests (dichotomous ANOVA, age, and sex corrected) were performed if there was a significant group difference. False discovery rate (FDR, six tests) correction to decrease the risk of α-error-accumulation was applied. Furthermore, each *p*-value was Bonferroni adjusted for a total of five diagnostic groups.

As a supplementary analysis, similar to the methodology explained before, we ordered all β-values from the single-patient regression per biomarker and tested for group differences between the five diagnostic groups. Post-hoc analysis and correction for multiple testing were performed using FDR (ten tests) and Bonferroni (four biomarkers). To analyze the influence of ATN on microglial activity at the group level, multivariate linear regression models (covariates: age, sex, subject-ID, and all other ATN biomarkers) were applied (including all 246 Brainnetome VOI *z*-scores of all patients per group). Partial regressions were analyzed and fitted values were used to classify a VOI as biomarker positive or negative. For ATN, the z-score cutoff for the classification of positivity was determined at >2 (AT) and <−2 (N). The *z*-score cutoff of I was set >0, to ensure inclusion of regions with low-level inflammation above the average of controls. Proportions of I+ A+ / I+ T+ / I+ N+ to the total amount of A+ / T+ / N+ VOIs were calculated.

Correlation and interaction analyses. Spearman's rank correlation (r_s) was used to analyze the relationship of clinical parameters and sTREM2 with AT-related microglial activation, in a cohort of composed 4RT, AD-CBS, and AD patients. Correlation analyses were adjusted for sex, age, global-patient-TSPO-load (mean *z*-scores of 246 VOIs), and global-patient-AT-load (mean *z*-scores of 246 VOIs of the respective biomarker). When significant correlations were observed, individual correlation sub-analyses were conducted within 4RT and AD (AD, AD-CBS). For sTREM2, we primarily separated the cohort into a group with AD-pathology (AD-CBS, AD) and a group with 4R-tauopathies. No correction for multiple testing due to the exploratory character was applied in these analyses. Subsequently, A and T were tested for interaction effects.

RESULTS

Demographics

The analyzed cohort consisted of 26 patients with 4RTs, 11 patients with AD-CBS, 18 patients with typical AD, 7 mixed LABs, and 10 controls who received examinations with all ATN imaging biomarkers (Table 1). Age, sex, and sTREM2 did not differ between subgroups of the cohort. A significant group difference for rs6971 SNP status was identified (4RT: MAB/HAB = 7/18, AD-CBS: MAB/HAB = 5/6, AD: MAB/HAB = 8/8, CTRL: MAB/HAB = 7/2, $\chi^2 = 8.575$, $p = 0.036$). The MoCA scores of the controls were found to be significantly higher than those of 4RT, AD-CBS, and AD. AD-CBS showed significantly lower MoCA scores than 4RT and AD (4RT: 22.8 ± 4.6, AD-CBS: 17.6 ± 6.6, AD: 22.4 ± 6.2, LAB: 22.0 ± 7.5, CTRL: 28.6 ± 1.6, F = 5.175, $p = 0.001$). Further demographic statistics are displayed in Table 1. Demographics of larger tracer specific control cohorts that were used for the calculation of individual *z*-scores are reported in Supplemental Table 1.

Strong regional heterogeneity of ATN biomarker alterations in primary and secondary tauopathies

First, we investigated regional alterations of microglial activity, Aβ, tau, perfusion, and GMV in our cohort of primary (4RT) and secondary (typical AD, AD-CBS) tauopathies at the group level. Frequencies of overall biomarker positivity across subgroups are illustrated in Fig. 1A. As expected from previous studies [4, 21] we found the highest levels of Aβ-PET and tau-PET signals in cortical brain regions of patients with typical and atypical AD, whereas

Table 1. Demographics.

Table 1	Neurodegenerative disease				Controls	ANOVA / χ^2
	4RT	AD-CBS	AD	LAB	CTRL	F (*p*-value)
n	26	11	18	7	10	
Age (years)	70.8 ± 6.3	75.7 ± 5.5	70.7 ± 7.4	75.0 ± 6.5	69.5 ± 8.9	1.781 (0.143)
Sex	♀ 13 / ♂ 13	♀ 7 / ♂ 4	♀ 9 / ♂ 9	♀ 2 / ♂ 5	♀ 7 / ♂ 3	3.492 (0.479)
rs6971 SNP	MAB: 7	MAB: 5	MAB: 9		MAB: 8	8.575 (0.036)
	HAB: 19	HAB: 6	HAB: 9		HAB: 2	
	(*n* = 26)	(*n* = 11)	(*n* = 18)		(*n* = 10)	
sTREM2	0.969 ± 0.138	1.012 ± 0.108	0.955 ± 0.088	0.981 ± NA	1.009 ± 0.094	0.388 (0.816)
	(*n* = 14)	(*n* = 7)	(*n* = 10)	(*n* = 1)	(*n* = 6)	
MoCA	22.8 ± 4.6	17.6 ± 6.6	22.4 ± 6.2	22.0 ± 7.5	28.6 ± 1.6	5.175 (0.001)
	(*n* = 24)	(*n* = 10)	(*n* = 14)	(*n* = 3)	(*n* = 9)	

Posthoc *p*-value MoCA	4RT	AD-CBS	AD	LAB
AD-CBS	0.011			
AD	0.838	0.0315		
LAB	0.807	0.209	0.898	
CTRL	0.007	< 0.001	0.008	0.067

Data are presented as mean ± standard deviation and number of frequency (*n*). Demographics were statistically tested by ANOVA or chi-square (χ^2) test. With significant ANOVA group difference, multiple unpaired two-tailed Student's *t*-tests were performed.
AD Alzheimer's disease, *AD-CBS* corticobasal syndrome with AD-pathology, *4RT* four-repeat tauopathies, *LAB* low affinity binder, *MAB* medium affinity binder, *HAB* high affinity binder, *CTRL* healthy controls, *ANOVA* analysis of variance, χ^2 chi-square, *MoCA* Montreal-Cognitive-Assessment-Scale, *MMSE* Mini-Mental State Examination, *sTREM2* soluble triggering receptor expressed on myeloid cells 2.

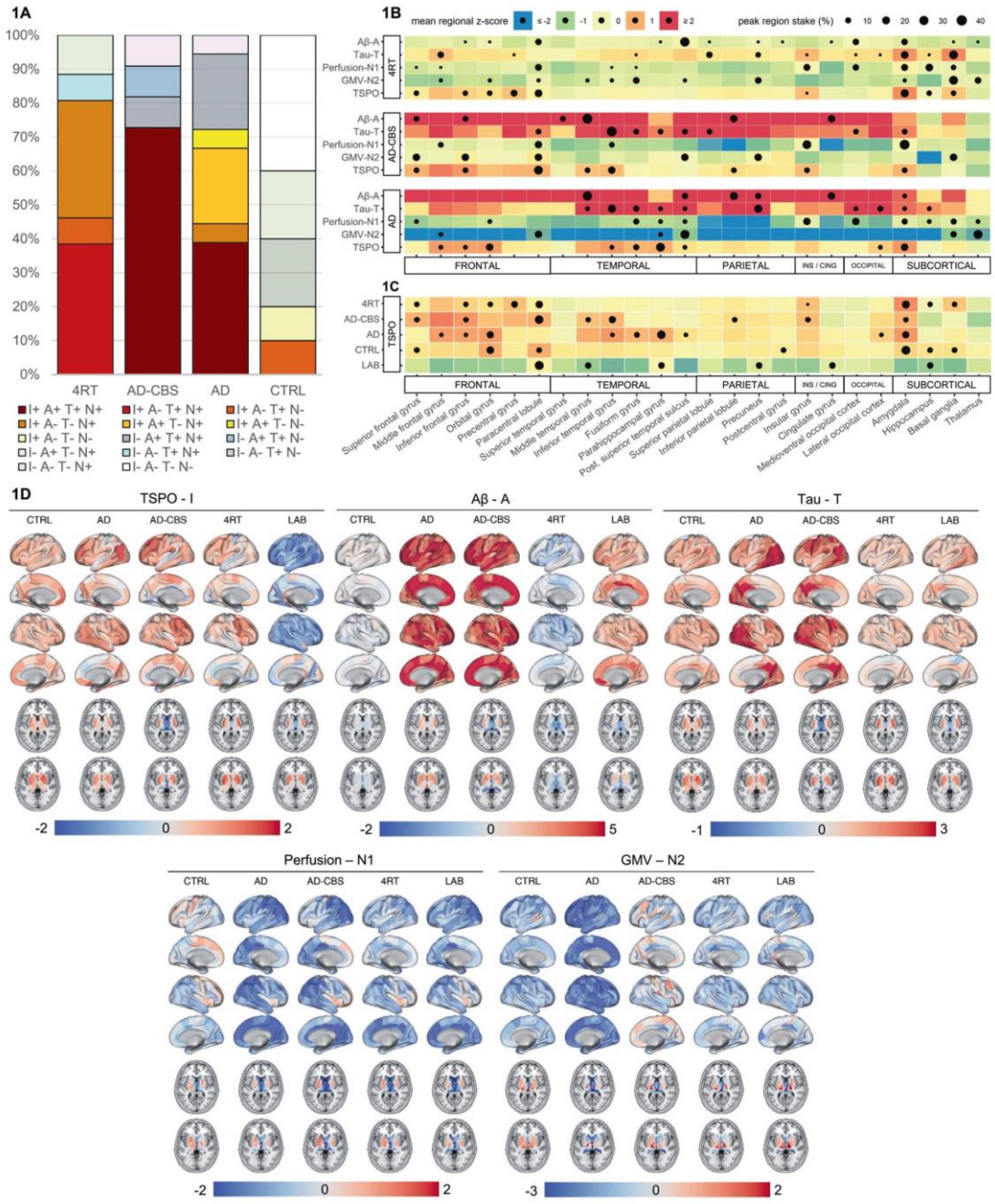

patients with 4RTs showed low Aβ-PET levels and subcortical predominance of tau accumulation (Fig. 1B). TSPO-PET signal increases were abundantly observed in tau-, but not Aβ-PET positive brain regions (tau-TSPO: $r = 0.312$, $p = 0.008$ / Aβ-TSPO: $r = 0.071$, $p = 0.552$). Regional peak distribution of "N" biomarkers followed the individual patterns of tau- (tau-perfusion: $r = 0.246$, $p = 0.037$ / tau-atrophy: $r = 0.270$, $p = 0.022$), but not Aβ-PET (Aβ-perfusion: $r = -0.023$, $p = 0.851$ / Aβ-atrophy: $r = 0.035$, $p = 0.771$). TSPO-PET levels were distinctly higher in primary and secondary tauopathies with MAB and HAB status when compared to a mixed cohort ($n = 2$ AD, $n = 4$ 4RT, $n = 1$ healthy control) of low-affinity binders (Fig. 1C).

Importantly, we found a scattered distribution of individual ATN peak regions within subgroups of primary and secondary

Fig. 1 Determination of ATI(N) biomarker positivity and ATI(N) biomarker heterogeneity using a multiregional analysis. A Overall ATI(N) biomarker positivity of all included subjects for I(TSPO)-, A(Aβ)-, T(tau)- and N(perfusion, early tau)-PET at the group level. Single-region-ROC-analyses were applied to identify regions ($n = 5$) that discriminate best among the study groups (maximum area-under-curve) for each biomarker. For each region an individual cutoff was set based on a sensitivity/specificity tradeoff and patients were classified as biomarker-positive or –negative based on the averaged regions that allowed the most optimal discrimination. Please note that AD also includes AD pathological change according to NIA-AA. **B** Heterogeneity of regional ATI(N) biomarker peak distribution. The heatmap was determined by calculating arithmetic means ($\bar{x}$) within 24 composed brain regions (from *z*-scores) and displayed in color scale. All $\bar{x} > 2$ were set equal to 2 and all $\bar{x} < -2$ were set equal to -2. The brain region with the highest *z*-score was determined for each study participant and the peak region frequency was plotted proportionally (%) to the number of patients in one group. **C** Comparison of TSPO-PET levels in patients with primary and secondary tauopathies and medium- and high-affinity TSPO binding status when compared to a mixed cohort ($n = 2$ AD, $n = 4$ 4RT, $n = 1$ healthy control) of individuals with low-affinity TSPO binding status using the same methodological approach as in (**B**). **D** Regional ATI(N) biomarker PET signal alterations at the group level. Within each study group, the mean *z*-score of each Brainnetome region was calculated and plotted as surface projections (lateral and medial view) and axial slices of the basal ganglia. AD Alzheimer's disease, AD-CBS corticobasal syndrome with AD-pathology, 4RT four-repeat tauopathies, LAB low affinity binder, CTRL healthy controls, TSPO 18-kDa translocator protein, Aβ β-amyloid, GMV gray-matter-volume, PET positron-emissions-tomography, ROC receiver-operating-characteristic.

tauopathy subgroups (Fig. 1D). Highest Aβ-PET *z*-scores in individual patients with typical AD were observed in temporal (44.4%) and parietal lobe (33.3%), as well as cingulate gyrus (16.7%) and amygdala (5.6%), whereas individual patients with AD-CBS had highest Aβ-PET *z*-scores in the middle and superior temporal gyrus (45.5%), parietal lobe (18.2%), cingulate (18.2%) and frontal cortices (18.2%). As expected from previous work [4], the highest individual tau-PET alterations in patients with 4RTs were observed in the basal ganglia (26.9%), but heterogeneity of peak signal alterations was observed with involvement of limbic regions (23.1%), parietal (19.2%), frontal (15.4%) and temporal (3.8%) cortices. In line with previous pattern classification [59], we found various peak regions of individual tau-PET not only in AD-CBS but also in typical AD, with a predominance of temporal regions (50.0%) but peaks in the precuneus (22.2%), occipital cortices (16.7%) as well as limbic regions (11.1%).

Regional Tau-PET is closely associated with the individual microglia response in primary and secondary tauopathies

Given the strong regional heterogeneity of Aβ and tau accumulation in primary and secondary tauopathies, we applied a multi-regional regression model to investigate the detailed associations of ATN biomarker alterations with microglia activation at the individual patient level (Fig. 2A). In 4RTs, Tau-PET contributed significantly to the regional explanation of TSPO-PET ($\beta_T = 0.418 \pm 0.154$ / $p < 0.001$ in 88% of individuals), whereas Aβ-PET did not ($\beta_A = -0.030 \pm 0.124$ / $p < 0.001$ in 15% of individuals; Fig. 2B/C). Perfusion ($\beta_{N1} = 0.218 \pm 0.176$ / $p < 0.001$ in 54% of individuals) and GMVs ($\beta_{N2} = 0.026 \pm 0.108$ / $p < 0.001$ in 12% of individuals) were associated with regional TSPO-PET in individuals with 4RTs but did not exceed controls at the group level (Supplemental Fig. 1). The positive character of these regional associations suggested an unspecific coupling of regional tracer signals by perfusion and atrophy. Within the 4RT subgroup, the explanation of TSPO-PET alterations by tau-PET distinctly exceeded the explanation by "A" and "N" biomarkers (Fig. 2B).

In patients with AD-CBS and typical AD, we observed a significant explanation of regional TSPO-PET by Aβ-PET (AD-CBS: $\beta_A = 0.131 \pm 0.186$ / $p < 0.001$ in 64% of individuals; AD: $\beta_A = 0.142 \pm 0.123$ / $p < 0.001$ in 33% of individuals) and tau-PET (AD-CBS: $\beta_T = 0.385 \pm 0.176$ / $p < 0.001$ in 82% of individuals; AD: $\beta_T = 0.412 \pm 0.196$ / $p < 0.001$ in 83% individuals; Fig. 2B/C), but explanation by perfusion and GMVs did again not exceed the level of controls (Supplemental Fig. 1). Tau-PET indicated the strongest regional relations with TSPO-PET in both AD groups among all ATN biomarkers (Fig. 2B).

In the subgroup of mixed LABs, we did not observe a significant explanation of the TSPO-PET signal by ATN biomarkers ($p = 0.420$). Associations between tau-PET and Aβ-PET with TSPO-PET were obliterated in individual cases with LAB status (Supplemental Fig. 2). Noteworthy, the individual positive associations between perfusion and TSPO-PET were still present for cases with LAB status, pinpointing the unspecific regional association between perfusion and TSPO uptake patterns when the tracer cannot bind the target.

Incremental tau aggregation is associated with high regional activation of microglia

To test for regional associations between ATN biomarkers and microglia activation at the disease level, we applied a partial regression model to study the specific association of single ATN parameters with TSPO-PET, controlled for all other ATN biomarkers, age, sex, and subject-ID.

When pooling VOI-specific data across 4RT subjects (26 patients with 246 Brainnetome VOIs), 6396 analyzed brain regions revealed high proportions of TSPO-positive (I+) regions among T+ (82%) but a low proportion of TSPO-positive regions among A+ (48%) and N+ (27%) regions (Fig. 3A). There was a weak partial association between regional Aβ ($\beta = 0.030$, $p = 0.011$) with TSPO but a strong partial association between regional Tau and TSPO ($\beta = 0.381$, $p < 0.001$; Fig. 3A). The partial association between perfusion and TSPO ($\beta = 0.270$, $p < 0.001$) was driven by lower TSPO-PET signals in regions with strong decreases in perfusion (Fig. 3A).

Both AD cohorts (2706 analyzed regions of AD-CBS and 4428 analyzed regions of typical AD) revealed similar partial associations between regional ATN biomarker alterations and TSPO-PET. There was a weak but significant regional association between Aβ and TSPO in patients with AD-CBS ($\beta = 0.117$, $p < 0.001$) and typical AD ($\beta = 0.117$, $p < 0.001$; Fig. 3B/C). Regional tau again appeared as the strongest driver of TSPO-PET signals in AD-CBS ($\beta = 0.357$, $p < 0.001$) and typical AD ($\beta = 0.412$, $p < 0.001$) with high proportions of regional TSPO-PET positivity in regions with significant tau accumulation (AD-CBS: 81%, typical AD: 79%; Fig. 3B/C). Perfusion indicated a significant association with TSPO-PET signals for both AD subgroups (Fig. 3B/C). Controls validated the applied thresholds of ATN positivity and indicated only a few A+, T+, and N+ regions (Fig. 3D).

Associations of Aβ- and tau-associated microglial response with clinical performance and sTREM2

Finally, we tested if individual associations between Aβ and tau with microglial activation were correlated with indices of clinical severity and sTREM2. The rationale was to investigate if specific "A" or "T" associated microglial activation can be linked to improved or deteriorated clinical performance. Tau associated microglial activation revealed a general association with worse clinical performance (Fig. 4). Patients indicated more depressive symptoms ($r_s = 0.460$, $p = 0.011$) and worse results on the UPDRS scale ($r_s = 0.503$, $p = 0.006$), when patients had high associations between regional tau and microglial activation. We observed a significant interaction effect between Aβ and tau associated

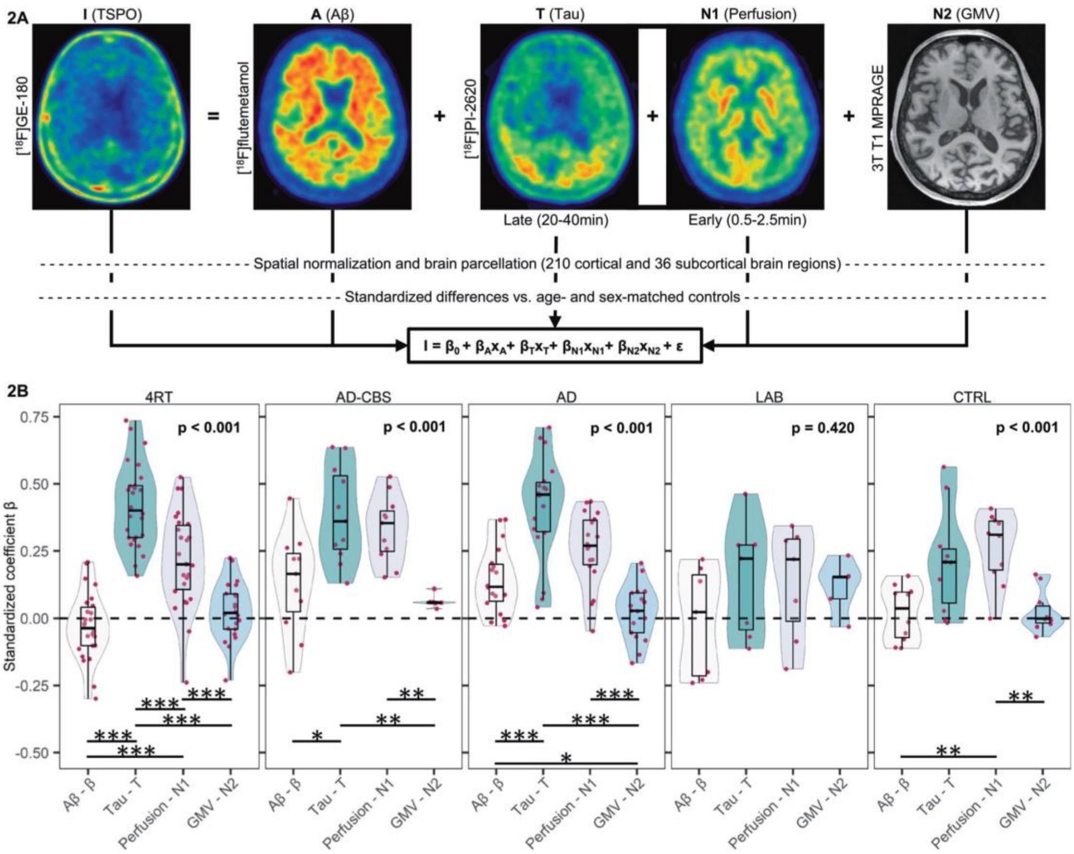

2C

4RT																											
A	+	-	-	-	+	-	-	-	-	+	+	-	+	-	+	-	+	-	+	-	+	-	-	-	-	-	15%
T	+	+	+	+	+	+	+	+	+	+	+	+	+	+	+	+	+	+	+	+	+	+	+	+	+	+	88%
N1	+	+	+	-	+	+	+	+	+	+	+	+	+	+	+	+	+	+	+	+	+	-	+	+	+	+	54%
N2	-	+	-	-		+	+		+	+	-	+	+	+		-	-	+	-		+	+	+	-	+	-	12%

AD-CBS												
A	+	-	+	-	+	+	+	+	-	+	+	64%
T	+	+	+	+	+	+	+	+	+	+	+	82%
N1	+	+	+	+	+	+	+	+	+	+	+	82%
N2	+	+	+		+		+			+		0%

AD																			
A	+	+	+	+	+	+	+	-	+	-	+	-	+	+	+	+	+	+	33%
T	+	+	+	+	+	+	+	+	+	+	+	+	+	+	+	+	+	+	83%
N1	+	+	+	+	+	+	+	+	+	-	+	+	+	+	+	+	+	+	78%
N2	+	+	+	+	+	-	+	-	+	-	+	+	-		-	+	-	+	6%

LAB								
A	+	-	-	+	+	-	+	57%
T	-	-	+	+	+	-	+	43%
N1	+	-	+	-	+	+	+	57%
N2	+	+	+		-		+	14%

CTRL											
A	+	-	-	+	+	-	+	-	-	+	0%
T	-	+	+	+	+	+	+	+	+	-	30%
N1	+	+	+	+	+	+	+	-	+	+	60%
N2	+	-	+	-	-	-	-	+	+	+	0%

Fig. 2 Multiregional regression analysis to determine the association of ATN biomarkers with microglial activation at the individual patient level. A Methodological workflow: PET and MRI data were spatial normalized to tracer specific templates acquired in previous in house studies (Montreal Neurology Institute (MNI) space) and parcellated into 210 cortical and 36 subcortical brain regions. PET-tracer uptake and gray-matter-volumes (GMV, from MRI) were transformed into *z*-scores with age- and sex-matched controls. **A** multiple linear regression model was performed ($I = \beta_0 + \beta_A x_A + \beta_T x_T + \beta_{N1} x_{N1} + \beta_{N2} x_{N2} + \varepsilon$) at the single-patient-level and standardized coefficients (β) were derived for each ATN biomarker. **B** β-coefficients were visualized as a combined violin-box-plot and show the association of ATN biomarkers with microglia activation, each dot representing a single subject. Within each diagnosis group, the β-coefficients of the four independent variables were tested for group differences using ANOVA with age and sex as covariates. Multiple posthoc tests (dichotomous ANOVA, age, and sex corrected) were performed if there was a significant group difference. Combined false discovery rate (FDR, six *p*-values) and Bonferroni (five p-values) correction were applied to decrease the risk of α-error-accumulation. *$p < 0.05$, **$p < 0.01$, ***$p < 0.001$. **C** Heatmap indicates the significance of ATN biomarker contribution to microglia activation resulting from the regression analysis in different diagnostic subgroups. Orange: $p < 0.001$. Gray: $p \geq 0.001$. The percentage was calculated as the proportion of significant regression models of patients, relative to the total number of patients in the diagnostic group. Plus and minus signs were used to indicate the positivity or negativity of the associated β-coefficients. AD Alzheimer's disease, AD-CBS corticobasal syndrome with AD-pathology, 4RT four-repeat tauopathies, LAB low affinity binder, CTRL healthy controls, TSPO 18-kDa translocator protein, Aβ β-amyloid, GMV gray-matter-volume, PET positron-emissions-tomography, MRI magnetic-resonance-imaging, MNI Montreal Neurology Institute, ANOVA analysis of variance, FDR false discovery rate.

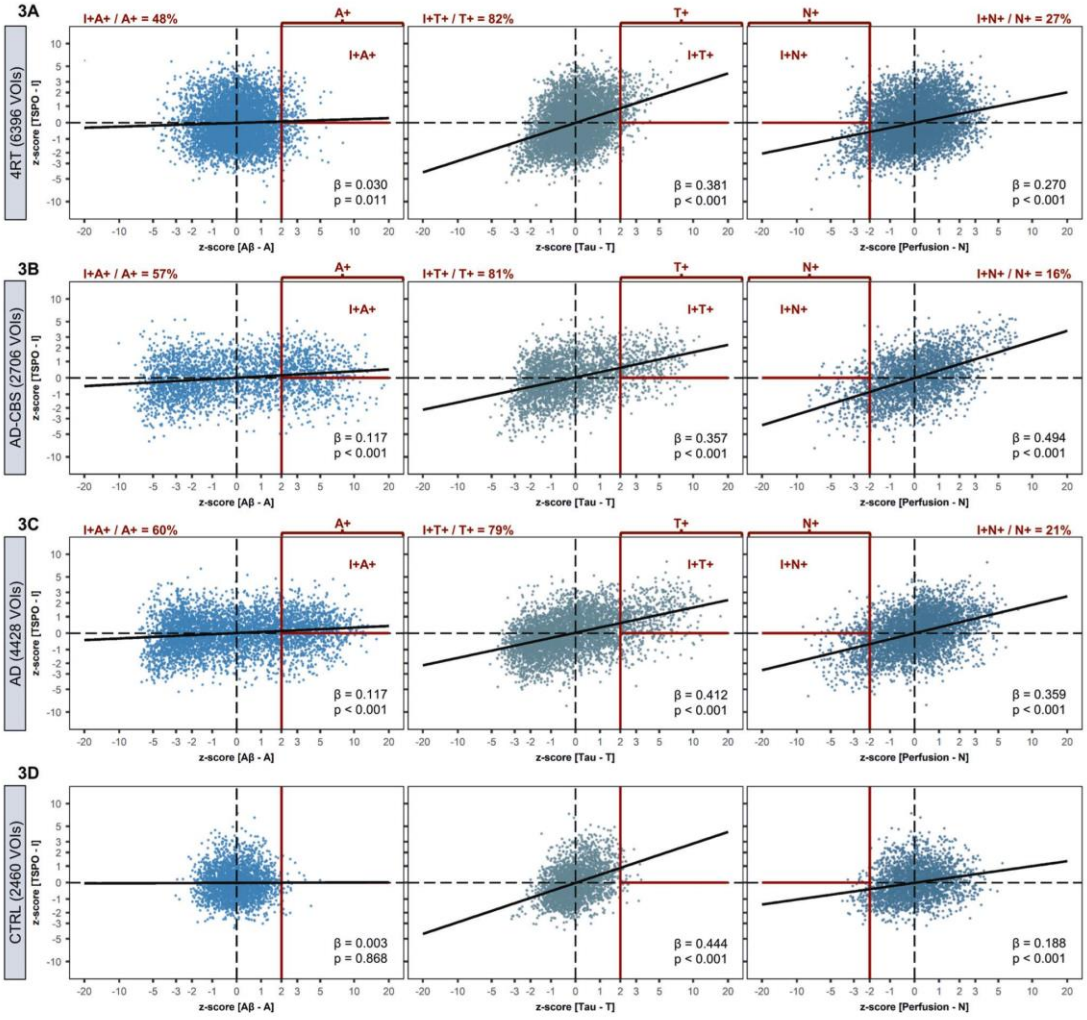

Fig. 3 Multiregional regression analysis to determine the association of ATN biomarkers with microglial activation at the group level. A multiple linear regression model was performed ($I = \beta_0 + \beta_A x_A + \beta_T x_T + \beta_N x_N + \text{age} + \text{sex} + \text{subject-ID} + \varepsilon$) at group-level for (**A**) 4RT, (**B**) AD-CBS, (**C**) AD, and (**D**) CTRL using z-scores of all single regions of all individuals combined. The standardized coefficient (β) and the associated *p*-value were calculated. Fitted values of the partial regressions were used to classify a VOI as biomarker positive or negative. For ATN, the *z*-score cutoff for the classification of positivity was determined at >2 (AT) and <−2 (N). The *z*-score cutoff of I was set >0. Proportions of I+ A+ / I+ T+ / I+ N+ to the total amount of A+ / T+ / N+ VOIs were calculated. AD Alzheimer's disease, AD-CBS corticobasal syndrome with AD-pathology, 4RT four-repeat tauopathies, CTRL healthy controls, TSPO 18-kDa translocator protein, Aβ β-amyloid.

microglial activation for UPDRS ($T = 2.401$, $p = 0.019$) and GDS ($T = 3.581$, $p < 0.001$), suggesting that microglial response to different protein aggregation may have opposite effects on brain function and clinical severity. Significant correlations were further examined to determine whether they were driven by a specific patient subgroup. The correlation of tau-associated microglial activation with GDS appeared to be driven by the AD cohort (4RT: $r_s = 0.354$, $p = 0.150$; AD + AD-CBS: $r_s = 0.758$, $p = 0.029$), whereas the correlation between tau-associated microglial activation and UPDRS appeared to be driven by the 4RT cohort (4RT: $r_s = 0.593$, $p = 0.007$; AD + AD-CBS: $r_s = -0.698$, $p = 0.190$). There were no correlations, nor interaction effects for MoCA or PSPRS. The AD-group showed a significant interaction effect when Aβ-associated TSPO-PET signals and tau-associated TSPO-PET signals were correlated with sTREM2 ($T = 2.732$, $p = 0.011$; Fig. 5). This indicated that high Aβ-TSPO associations but low tau-TSPO associations are linked with sTREM2 increases at the individual patient level. Contrary, patients with 4RT showed high sTREM2 levels when regional TSPO-PET was associated with tau-PET ($r_s = 0.705$, $p = 0.034$), which may indicate different trajectories of microglia phenotypes in the course of primary and secondary tauopathies.

DISCUSSION

We provide the first study that uses a regional resolution of ATI(N) PET and grey matter volumes in a combined cohort of primary and secondary tauopathies to investigate the detailed associations between the accumulation of misfolded proteins, perfusion, and

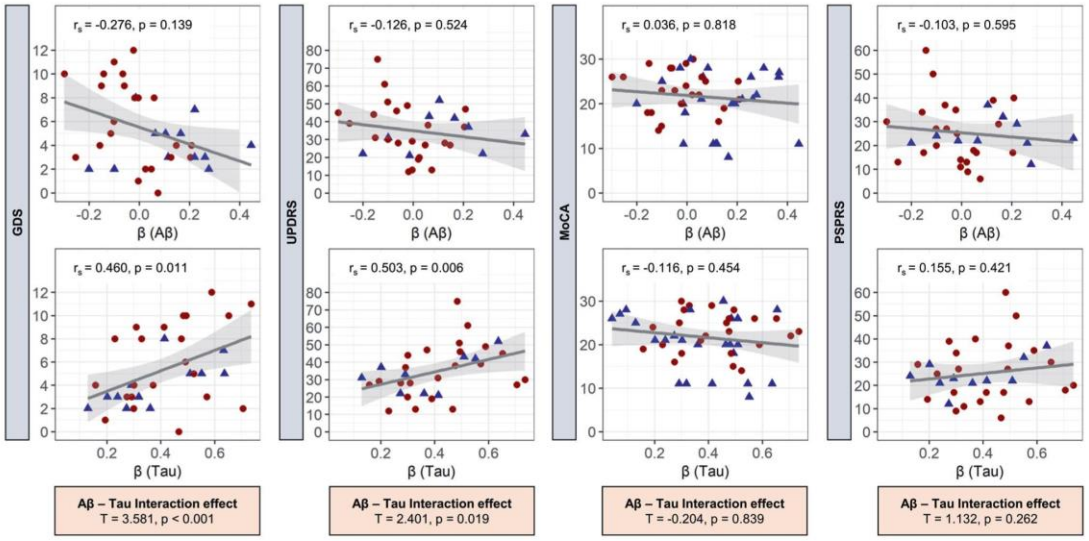

Fig. 4 Correlation of AT associated microglial activation with clinical performance. Standardized coefficients β (single patient regression), to detect Aβ (A)- and tau (T)- associated microglial activation, were correlated with clinical performance scores (Spearman's correlation coefficient, r_s). For statistical calculations, 4RT, AD-CBS, and AD were pooled. ● = 4RT, ▲ = AD-CBS + AD. Correlation analyses were adjusted for sex, age, global-patient-TSPO-load (mean z-scores of 246 VOIs), and global-patient-AT-load (mean z-scores of 246 VOIs of the respective biomarker). No correction for multiple testing was applied. Subsequently, A and T were tested for interaction effects. AD Alzheimer's disease, AD-CBS corticobasal syndrome with AD-pathology, 4RT four-repeat tauopathies, LAB low affinity binder, CTRL healthy controls, TSPO 18-kDa translocator protein, Aβ β-amyloid, GMV gray-matter-volume, MoCA Montreal-Cognitive-Assessment-Scale, MMSE Mini-Mental State Examination, UPDRS Unified-Parkinson's-Disease-Rating-Scale (motor part), PSPRS Progressive-Supranuclear-Palsy-Rating-Scale, GDS Geriatric-Depression-Scale.

volume changes with microglial activation. We find distinct heterogeneity of regional distribution patterns of ATI(N) biomarkers among patients with tauopathies. Regional accumulation of tau was the strongest predictor of microglial activation in individual patients with primary and secondary tauopathies, whereas Aβ, perfusion, and gray matter volumes indicated only weaker associations with regional TSPO-PET. Individual associations between ATN biomarkers and microglial activation were abrogated in low-affinity binders, demonstrating in vivo specificity of [^{18}F]GE-180 to TSPO. Finally, we obtained preliminary evidence of worse clinical performance when microglial activation was associated with tau at the individual patient level.

The major finding of our study revealed that, among all ATN biomarkers, aggregated tau has the closest link with colocalized microglia activation in primary tauopathies and AD. Thus, our study confirmed joint accumulation of tau and microglial activation in typical AD [12] and adds evidence of similar regional trajectories in 4RTs and atypical AD. Several clinical and preclinical investigations indicated that both Aβ and tau are closely related to PET and histological measurements of increased microglial activity [12, 15, 25, 60–62]. However, the detailed interplay between ATN biomarkers and neuroinflammation was discussed controversially. Even at the stage of single ATN biomarkers, distinct subtypes of microglia activation have been shown to occur in response to Aβ accumulation, depending on disease stage [63]: a protective neuroinflammatory response that could be beneficial due to phagocytosis of neurotoxic Aβ species, and a detrimental one with negative effects that leads to inhibition of synaptic functioning and increased cell death [63, 64]. Furthermore, atrophy was found to mediate the effects of both tau pathology and neuroinflammation on cognition in AD [27]. We hypothesized that regression models of multiple biomarkers in different brain regions could deepen the understanding of the ATI(N) biomarker interplay with I as an index of microglial activation. The application of this approach at the individual patient level enabled us to directly compare the partial influence of ATN biomarkers and we clearly observed a stronger association between regional aggregation of tau with microglial activation than did Aβ deposits. This finding could be related to exhausted microglia at advanced stages of Aβ accumulation [65]. Patients with typical and atypical AD showed a significant influence of regional Aβ on microglial activation but this association was not found in 4RTs. This is of particular interest since subthreshold levels of Aβ occur in 4RTs [66] but do not have a major impact on neuroinflammation according to our data.

With regard to therapy monitoring, it is of tremendous interest to understand associations between ATN biomarkers and neuroinflammation during the progressive aggregation of misfolded proteins in the brain. Thus, we also applied a model comprising all individual regional ATN biomarker data within groups of patients with 4RTs, typical AD, and atypical AD, again exploring the associations of the individual ATN biomarker adjusted for the remaining indices. Importantly, we found that, in a cross-sectional design, microglial activation still continuous to rise coupled with increasing tau pathology at stages with very high tau accumulation in primary and secondary tauopathies (Fig. 3). Contrary, TSPO-PET associations with regional Aβ aggregation tended to peak or plateau at stages of moderate Aβ abundance. This observation fits a recent study, suggesting that microglial activation correlates strongly with tau aggregation in established AD and with Aβ deposition in MCI [25]. Furthermore, two other studies indicated specific associations between Aβ and neuroinflammation at early stages of Aβ pathology [67, 68]. Thus, targeting tau associated microglial activation could still be beneficial at later stages of the disease, whereas modifying Aβ associated microglial activation may be only beneficial at early disease stages [48]. Understanding differences in microglia phenotypes associated either with Aβ or

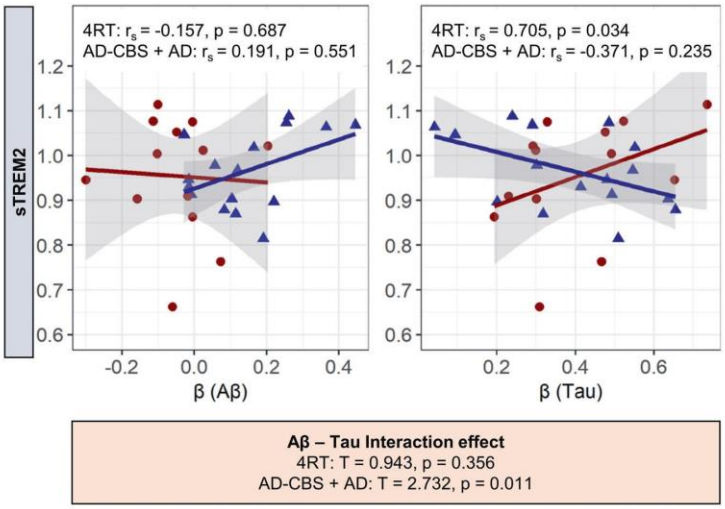

Fig. 5 Correlation of ATN associated microglial activation with sTREM2. Standardized coefficients β (single patient regression), to detect Aβ (A)- and tau (T)-associated microglial activation, were correlated with sTREM2 data (Spearman's correlation coefficient, r_s). The statistical analysis was calculated for the combined AD group (AD-CBS + AD), and the 4RT group. ● = 4RT, ▲ = AD-CBS + AD. Correlation analyses were adjusted for sex, age, global-patient-TSPO-load (mean z-scores of 246 VOIs), and global-patient-AT-load (mean z-scores of 246 VOIs of the respective biomarker). No correction for multiple testing was applied. Subsequently, A and T were tested for interaction effects. AD Alzheimer's disease, AD-CBS corticobasal syndrome with AD-pathology, 4RT four-repeat tauopathies, LAB low affinity binder, CTRL healthy controls, TSPO 18-kDa translocator protein, Aβ β-amyloid, GMV gray-matter-volume, sTREM2 soluble triggering receptor expressed on myeloid cells 2, PSPRS Progressive-Supranuclear-Palsy-Rating-Scale, MMSE Mini-Mental State Examination.

tau aggregation will likely have a major impact on selection of appropriate immunomodulatory strategies.

The relevance of regression models at the individual patient level was pinpointed by the observation of distinct heterogeneity of regional ATN biomarker alterations in patients with 4RTs and AD. In line, four distinct trajectories of tau deposition were recently identified in typical AD, which implies that pathology originates and spreads through distinct networks in the different subtypes [59, 66]. Distinct regional patterns of neurodegeneration were similarly reported for 4RTs [69]. This heterogeneity implies that conservative regional assessments at the group level limit the possibility to capture the full picture of ATN biomarker alterations because effects in single regions are diminished by differing regional peaks of pathology.

An exploratory analysis of our study suggested that strong regional associations between tau and microglial activation indicated worse clinical performance at a cross-sectional level of analysis in patients with primary and secondary tauopathies. This finding is in line with improved cognition in tauopathy models with NLRP3 inflammasome knock-out [70]. In contrast, the individual regional association of microglial activation with Aβ showed a more beneficial effect on clinical performance indices in patients with AD. Supporting this claim, levels of sTREM2 were specifically associated with Aβ related but not tau related microglial activation in our cohort, while sTREM2 was reported to be associated with reduced cognitive decline in AD [71]. In this regard, TREM2 may slow AD progression and reduce tau-driven neurodegeneration by restricting the degree to which β-amyloid facilitates the spreading of pathogenic tau [72]. Our observations also had similarities to serial preclinical studies in mouse models, where microglial activation was correlated with worse outcome parameters in the P301S tau model [61], but with improved spatial learning performance in PS2APP [73, 74] and $App^{NL\text{-}G\text{-}F}$ [17] Aβ models. A clinical study in patients with AD also suggested that anterior temporal [^{11}C]PK11195 binding, a region with abundant tau but low Aβ deposition is associated with progressive cognitive decline [75]. In this regard, our individual index of tau- and Aβ-associated microglia activation could serve to account for regional heterogeneity and standardized quantification of the multidimensional neuroinflammatory response. This may enable stratification for immunomodulatory therapies by identification of patients with a high risk of future clinical deterioration [75].

The characteristics of the used molecular imaging biomarkers for the assessment of ATI(N) need to be considered for the interpretation of our results. A strength of this study is given by the use of the novel tau-PET tracer [^{18}F]PI-2620 which proved absent of off-target binding to monoamine oxidases [76], high affinity to 3/4R-tau in AD [77] and also high affinity to recombinant 4R tau fibrils and PSP brain homogenate [76]. Colocalization of [^{18}F]PI-2620 binding with 4R tau in micro-autoradiography [76] and quantitative agreement of autoradiography and immunohistochemistry [66, 78] as well as in vivo discrimination of PSP [21] and CBS [4] from controls highlight the potential of this radioligand. Since currently available tau-PET tracers were optimized to detect AD-related tau tangles, the used tau-PET tracer shows differential binding characteristics to different tau isoforms, which is relevant in the described patient cohorts. Predominant 3/4R tau isoforms of patients with AD patients comprise favorable energetic and kinetic properties with regard to [^{18}F]PI-2620 binding, compared to predominant 4 R tau isoforms of primary tauopathies [79]. In this regard, [^{18}F]PI-2620 showed higher specificity to 4R tau in comparison to other second-generation tau-PET tracers in vitro [80]. In consideration of stronger binding to AD-related tau tangles compared to 4R-tau aggregates in primary tauopathies, the availability of a tau tracer with higher affinity to non-AD tau could even lead to stronger tau-related effects in the group of patients with 4R-tauopathies. Furthermore, early-phase [^{18}F]PI-2620 PET indicated feasibility for perfusion surrogate imaging in patients with AD and 4RTs [35, 43], which was applied as an "N" biomarker in the current study. [^{18}F] flutemetamol is an FDA and EMA approved Aβ-PET tracer and is characterized by fast brain uptake, fast clearance, and excellent

binding properties to Aβ deposits in vitro and in vivo [81]. TSPO-PET represents a sensitive biomarker for monitoring immunomodulation and can act as a surrogate for activated microglia. Several TSPO radioligands allow monitoring neuroinflammation in AD and 4R-tauopathies [18] and we were able to show that [^{18}F]GE-180 recapitulates the expected topology of microglial activation in 4RTs [22] and AD [33]. However, [^{18}F]GE-180 has recently been criticized for limited uptake across the blood-brain-barrier [22, 82] since blood-brain integrity can be disturbed in neurodegenerative disorders with a potential impact on tracer kinetics [83, 84]. We circumvented blood-brain-barrier related perfusion alterations and interrogated them as a potential cofounder by the inclusion of a perfusion surrogate as an "N" biomarker into our regression model. With this approach, we were able to show that perfusion has a substantial impact on [^{18}F]GE-180 binding, but our model also allowed us to determine the specific perfusion-adjusted impact of tau and Aβ pathology on TSPO-PET signal alterations. More importantly, we were able to show that associations between regional tau and Aβ accumulation with microglial activity were lost in low-affinity-binders. Furthermore, regional TSPO-PET signals were distinctly lower in participants with low-affinity binding status when compared to medium and high affinity binders. Thus, our data provide evidence of the specificity of the [^{18}F]GE-180 TSPO-PET signal in patients with neurodegenerative diseases.

Limitations of the study include that we cannot draw detailed conclusions about the cell type specificity of the TSPO-PET signal to activated microglia, since we did not measure associations with reactive astrocytosis by glial fibrillary acidic protein or a PET radioligand targeting reactive astrocytes. Furthermore, our study enrolled patients based on state-of-the-art clinical diagnosis but was not enriched by neuropathological confirmation. Thus, although the characterization of our patients was based on several biomarkers and detailed clinical work-up, misdiagnosed patients need to be considered as potential confounders in this study population.

CONCLUSION

A multi-regional regression model of PET and grey matter volume can serve for a personalized assessment of specific "A (Amyloid) T (Tau) and N (Neurodegeneration)" related microglial response rates. Tau pathology dominates the regional associations of these ATN biomarkers with microglial activation in primary and secondary tauopathies, while strong regional heterogeneity of ATN biomarker alterations needs to be considered at the individual patient level. Tau and Aβ related microglial response indices showed differential associations with cognitive performance and sTrem2-levels and may serve as a two-dimensional index for in vivo assessment of neuroinflammation in neurodegenerative diseases.

AVAILABILITY OF DATA AND MATERIALS

The datasets used and/or analyzed during the current study are available from the corresponding author upon reasonable request. Supplementary information is available on MP's website.

REFERENCES

1. Ziegler-Graham K, Brookmeyer R, Johnson E, Arrighi HM. Worldwide variation in the doubling time of Alzheimer's disease incidence rates. Alzheimers Dement. 2008;4:316–23.
2. Selkoe DJ, Hardy J. The amyloid hypothesis of Alzheimer's disease at 25 years. EMBO Mol Med. 2016;8:595–608.
3. Kovacs GG. Invited review: neuropathology of tauopathies: principles and practice. Neuropathol Appl Neurobiol. 2015;41:3–23.
4. Palleis C, Brendel M, Finze A, Weidinger E, Botzel K, Danek A, et al. Cortical [(18) F] PI-2620 binding differentiates corticobasal syndrome subtypes. Mov Disord. 2021;36:2104–15.
5. Braak H, Braak E. Demonstration of amyloid deposits and neurofibrillary changes in whole brain sections. Brain Pathol. 1991;1:213–6.
6. Hyman BT, Phelps CH, Beach TG, Bigio EH, Cairns NJ, Carrillo MC, et al. National Institute on Aging-Alzheimer's Association guidelines for the neuropathologic assessment of Alzheimer's disease. Alzheimers Dement. 2012;8:1–13.
7. Serrano-Pozo A, Frosch MP, Masliah E, Hyman BT. Neuropathological alterations in Alzheimer disease. Cold Spring Harb Perspect Med. 2011;1:a006189.
8. Querfurth HW, LaFerla FM. Alzheimer's disease. N Engl J Med. 2010;362:329–44.
9. Heneka MT, Carson MJ, Khoury JE, Landreth GE, Brosseron F, Feinstein DL, et al. Neuroinflammation in Alzheimer's disease. The Lancet Neurology. 2015;14:388–405.
10. Tan MS, Ji X, Li JQ, Xu W, Wang HF, Tan CC, et al. Longitudinal trajectories of Alzheimer's ATN biomarkers in elderly persons without dementia. Alzheimers Res Ther. 2020;12:55.
11. Hampel H, Cummings J, Blennow K, Gao P, Jack CR Jr., Vergallo A. Developing the ATX(N) classification for use across the Alzheimer disease continuum. Nat Rev Neurol. 2021;17:580–9.
12. Pascoal TA, Benedet AL, Ashton NJ, Kang MS, Therriault J, Chamoun M, et al. Microglial activation and tau propagate jointly across Braak stages. Nat Med. 2021;27:1592–9.
13. Ishizawa K, Dickson DW. Microglial activation parallels system degeneration in progressive supranuclear palsy and corticobasal degeneration. J Neuropathol Exp Neurol. 2001;60:647–57.
14. Villemagne VL, Burnham S, Bourgeat P, Brown B, Ellis KA, Salvado O, et al. Amyloid beta deposition, neurodegeneration, and cognitive decline in sporadic Alzheimer's disease: a prospective cohort study. Lancet Neurol. 2013;12:357–67.
15. Serrano-Pozo A, Mielke ML, Gomez-Isla T, Betensky RA, Growdon JH, Frosch MP, et al. Reactive glia not only associates with plaques but also parallels tangles in Alzheimer's disease. Am J Pathol. 2011;179:1373–84.
16. Werry EL, Bright FM, Piguet O, Ittner LM, Halliday GM, Hodges JR, et al. Recent developments in TSPO PET imaging as a biomarker of neuroinflammation in neurodegenerative disorders. Int J Mol Sci. 2019;20.
17. Biechele G, Blume T, Deussing M, Zott B, Shi Y, Xiang X, et al. Pre-therapeutic microglia activation and sex determine therapy effects of chronic immunomodulation. Theranostics. 2021;11:8964–76.
18. Cumming P, Burgher B, Patkar O, Breakspear M, Vasdev N, Thomas P, et al. Sifting through the surfeit of neuroinflammation tracers. J Cereb Blood Flow Metab. 2018;38:204–24.
19. Stefaniak J, O'Brien J. Imaging of neuroinflammation in dementia: a review. J Neurol Neurosurg Psychiatry. 2016;87:21–8.
20. Malpetti M, Passamonti L, Jones PS, Street D, Rittman T, Fryer TD, et al. Neuroinflammation predicts disease progression in progressive supranuclear palsy. J Neurol Neurosurg Psychiatry. 2021;92:769–75.
21. Brendel M, Barthel H, van Eimeren T, Marek K, Beyer L, Song M, et al. Assessment of 18F-PI-2620 as a biomarker in progressive supranuclear palsy. JAMA Neurol. 2020;77:1408–19.
22. Palleis C, Sauerbeck J, Beyer L, Harris S, Schmitt J, Morenas-Rodriguez E, et al. In Vivo assessment of neuroinflammation in 4-repeat tauopathies. Mov Disord. 2021;36:883–94.
23. Jecmenica Lukic M, Kurz C, Respondek G, Grau-Rivera O, Compta Y, Gelpi E, et al. Copathology in progressive supranuclear palsy: does it matter? Mov Disord. 2020;35:984–93.
24. Heneka MT, Kummer MP, Latz E. Innate immune activation in neurodegenerative disease. Nat Rev Immunol. 2014;14:463–77.
25. Dani M, Wood M, Mizoguchi R, Fan Z, Walker Z, Morgan R, et al. Microglial activation correlates in vivo with both tau and amyloid in Alzheimer's disease. Brain. 2018;141:2740–54.
26. Biel D, Suárez-Calvet M, Hager P, Rubinski A, Dewenter A, Steward A, et al. sTREM2 is associated with amyloidrelated p-tau increases and glucose hypermetabolism in Alzheimer's disease. EMBO Mol Med. 2023;15:e16987.
27. Su L, Surendranathan A, Huang Y, Bevan-Jones WR, Passamonti L, Hong YT, et al. Relationship between tau, neuroinflammation and atrophy in Alzheimer's disease: The NIMROD study. Inf Fusion. 2021;67:116–24.
28. Frigerio I, Boon BDC, Lin CP, Galis-de Graaf Y, Bol J, Preziosa P, et al. Amyloid-beta, p-tau and reactive microglia are pathological correlates of MRI cortical atrophy in Alzheimer's disease. Brain Commun. 2021;3:fcab281.
29. Jack CR Jr., Bennett DA, Blennow K, Carrillo MC, Dunn B, Haeberlein SB, et al. NIA-AA research framework: toward a biological definition of Alzheimer's disease. Alzheimers Dement. 2018;14:535–62.
30. Hoglinger GU, Respondek G, Stamelou M, Kurz C, Josephs KA, Lang AE, et al. Clinical diagnosis of progressive supranuclear palsy: the movement disorder society criteria. Mov Disord. 2017;32:853–64.
31. Armstrong MJ, Litvan I, Lang AE, Bak TH, Bhatia KP, Borroni B, et al. Criteria for the diagnosis of corticobasal degeneration. Neurology. 2013;80:496–503.

32. Palleis C, Sauerbeck J, Beyer L, Harris S, Schmitt J, Morenas-Rodriguez E, et al. In Vivo Assessment of Neuroinflammation in 4-Repeat Tauopathies. Mov Disord. 2021;36:883–94.
33. Rauchmann BS, Brendel M, Franzmeier N, Trappmann L, Zaganjori M, Ersoezlue E, et al. Microglial Activation and Connectivity in Alzheimer Disease and Aging. Ann Neurol. 2022;92:768–81.
34. Schmitt J, Palleis C, Sauerbeck J, Unterrainer M, Harris S, Prix C, et al. Dual-Phase beta-Amyloid PET Captures Neuronal Injury and Amyloidosis in Corticobasal Syndrome. Front Aging Neurosci. 2021;13:661284.
35. Beyer L, Nitschmann A, Barthel H, van Eimeren T, Unterrainer M, Sauerbeck J, et al. Early-phase [(18)F]PI-2620 tau-PET imaging as a surrogate marker of neuronal injury. Eur J Nucl Med Mol Imaging. 2020;47:2911–22.
36. Wollenweber FA, Darr S, Muller C, Duering M, Buerger K, Zietemann V, et al. Prevalence of amyloid positron emission tomographic positivity in poststroke mild cognitive impairment. Stroke. 2016;47:2645–8.
37. Song M, Scheifele M, Barthel H, van Eimeren T, Beyer L, Marek K, et al. Feasibility of short imaging protocols for [(18)F]PI-2620 tau-PET in progressive supranuclear palsy. Eur J Nucl Med Mol Imaging. 2021;48:3872–85.
38. Volter F, Beyer L, Eckenweber F, Scheifele M, Bui N, Patt M, et al. Assessment of perfusion deficit with early phases of [(18)F]PI-2620 tau-PET versus [(18)F]flutemetamol-amyloid-PET recordings. Eur J Nucl Med Mol Imaging. 2023;50:1384–94.
39. Lyoo CH, Ikawa M, Liow JS, Zoghbi SS, Morse CL, Pike VW, et al. Cerebellum can serve as a pseudo-reference region in alzheimer disease to detect neuroinflammation measured with PET radioligand binding to translocator protein. J Nucl Med. 2015;56:701–6.
40. Cho SH, Choe YS, Park S, Kim YJ, Kim HJ, Jang H, et al. Appropriate reference region selection of (18)F-florbetaben and (18)F-flutemetamol beta-amyloid PET expressed in Centiloid. Sci Rep. 2020;10:14950.
41. Fan L, Li H, Zhuo J, Zhang Y, Wang J, Chen L, et al. The human brainnetome atlas: a new brain atlas based on connectional architecture. Cereb Cortex. 2016;26:3508–26.
42. Kolabas ZI, Kuemmerle LB, Perneczky R, Förstera B, Büttner M, Caliskan OS, et al. Multi-omics and 3D-imaging reveal bone heterogeneity and unique calvaria cells in neuroinflammation. Cell. 2023. In press.
43. Katzdobler S, Nitschmann A, Barthel H, Bischof G, Beyer L, Marek K, et al. Additive value of [(18)F]PI-2620 perfusion imaging in progressive supranuclear palsy and corticobasal syndrome. Eur J Nucl Med Mol Imaging. 2023;50:423–34.
44. Owen DR, Gunn RN, Rabiner EA, Bennacef I, Fujita M, Kreisl WC, et al. Mixed-affinity binding in humans with 18-kDa translocator protein ligands. J Nucl Med. 2011;52:24–32.
45. Owen DR, Yeo AJ, Gunn RN, Song K, Wadsworth G, Lewis A, et al. An 18-kDa translocator protein (TSPO) polymorphism explains differences in binding affinity of the PET radioligand PBR28. J Cereb Blood Flow Metab. 2012;32:1–5.
46. Kleinberger G, Yamanishi Y, Suarez-Calvet M, Czirr E, Lohmann E, Cuyvers E, et al. TREM2 mutations implicated in neurodegeneration impair cell surface transport and phagocytosis. Sci Transl Med. 2014;6:243ra86.
47. Suarez-Calvet M, Morenas-Rodriguez E, Kleinberger G, Schlepckow K, Araque Caballero MA, Franzmeier N, et al. Early increase of CSF sTREM2 in Alzheimer's disease is associated with tau related-neurodegeneration but not with amyloid-beta pathology. Mol Neurodegener. 2019;14:1.
48. Morenas-Rodriguez E, Li Y, Nuscher B, Franzmeier N, Xiong C, Suarez-Calvet M, et al. Soluble TREM2 in CSF and its association with other biomarkers and cognition in autosomal-dominant Alzheimer's disease: a longitudinal observational study. Lancet Neurol. 2022;21:329–41.
49. Golbe LI, Ohman-Strickland PA. A clinical rating scale for progressive supranuclear palsy. Brain. 2007;130:1552–65.
50. Goetz CG, Tilley BC, Shaftman SR, Stebbins GT, Fahn S, Martinez-Martin P, et al. Movement disorder society-sponsored revision of the unified parkinson's disease rating scale (MDS-UPDRS): scale presentation and clinimetric testing results. Mov Disord. 2008;23:2129–70.
51. Sheikh J, Yesavage JA. Geriatric depression scale (GDS): recent evidence and development of a shorter version. Clin Gerontol. 1986;5:165–73.
52. Nasreddine ZS, Phillips NA, Bédirian V, Charbonneau S, Whitehead V, Collin I, et al. The Montreal cognitive assessment, MoCA: a brief screening tool for mild cognitive impairment. J Am Geriatr Soc. 2005;53:695–9.
53. Folstein MF, Folstein SE, McHugh PR. "Mini-mental state". A practical method for grading the cognitive state of patients for the clinician. J Psychiatr Res. 1975;12:189–98.
54. Bergeron D, Flynn K, Verret L, Poulin S, Bouchard RW, Bocti C, et al. Multicenter validation of an MMSE-MoCA conversion table. J Am Geriatr Soc. 2017;65:1067–72.
55. Vettermann FJ, Harris S, Schmitt J, Unterrainer M, Lindner S, Rauchmann BS, et al. Impact of TSPO Receptor Polymorphism on [(18)F]GE-180 Binding in Healthy Brain and Pseudo-Reference Regions of Neurooncological and Neurodegenerative Disorders. Life (Basel). 2021;11:484.
56. Metz CE. Basic principles of ROC analysis. Semin Nucl Med. 1978;8:283–98.
57. Vermont J, Bosson J-L, François P, Robert C, Rueff A, Demongeot J. Strategies for graphical threshold determination. Comput Methods Programs Biomed. 1991;35:141–50.
58. Brainnetome parcellation (http://atlas.brainnetome.org/bnatlas.html).
59. Vogel JW, Young AL, Oxtoby NP, Smith R, Ossenkoppele R, Strandberg OT, et al. Four distinct trajectories of tau deposition identified in Alzheimer's disease. Nat Med. 2021;27:871–81.
60. Kreisl WC. Discerning the relationship between microglial activation and Alzheimer's disease. Brain. 2017;140:1825–8.
61. Eckenweber F, Medina-Luque J, Blume T, Sacher C, Biechele G, Wind K, et al. Longitudinal TSPO expression in tau transgenic P301S mice predicts increased tau accumulation and deteriorated spatial learning. J Neuroinflammation. 2020;17:208.
62. Zou J, Tao S, Johnson A, Tomljanovic Z, Polly K, Klein J, et al. Microglial activation, but not tau pathology, is independently associated with amyloid positivity and memory impairment. Neurobiol Aging. 2020;85:11–21.
63. Wang WY, Tan MS, Yu JT, Tan L. Role of pro-inflammatory cytokines released from microglia in Alzheimer's disease. Ann Transl Med. 2015;3:136.
64. Bamberger ME, Harris ME, McDonald DR, Husemann J, Landreth GE. A cell surface receptor complex for fibrillar beta-amyloid mediates microglial activation. J Neurosci. 2003;23:2665–74.
65. Blume T, Focke C, Peters F, Deussing M, Albert NL, Lindner S, et al. Microglial response to increasing amyloid load saturates with aging: a longitudinal dual tracer in vivo muPET-study. J Neuroinflammation. 2018;15:307.
66. Franzmeier N, Brendel M, Beyer L, Slemann L, Kovacs GG, Arzberger T, et al. Tau deposition patterns are associated with functional connectivity in primary tauopathies. Nat Commun. 2022;13:1362.
67. Ismail R, Parbo P, Madsen LS, Hansen AK, Hansen KV, Schaldemose JL, et al. The relationships between neuroinflammation, beta-amyloid and tau deposition in Alzheimer's disease: a longitudinal PET study. J Neuroinflammation. 2020;17:151.
68. Toppala S, Ekblad LL, Tuisku J, Helin S, Johansson JJ, Laine H, et al. Association of early beta-amyloid accumulation and neuroinflammation measured with [(11)C]PBR28 in elderly individuals without dementia. Neurology. 2021;96:e1608–e19.
69. Beyer L, Meyer-Wilmes J, Schonecker S, Schnabel J, Brendel E, Prix C, et al. Clinical routine FDG-PET imaging of suspected progressive supranuclear palsy and corticobasal degeneration: a gatekeeper for subsequent Tau-PET imaging? Front Neurol. 2018;9:483.
70. Ising C, Venegas C, Zhang S, Scheiblich H, Schmidt SV, Vieira-Saecker A, et al. NLRP3 inflammasome activation drives tau pathology. Nature. 2019;575:669–73.
71. Ewers M, Franzmeier N, Suárez-Calvet M, Morenas-Rodriguez E, Caballero MAA, Kleinberger G, et al. Increased soluble TREM2 in cerebrospinal fluid is associated with reduced cognitive and clinical decline in Alzheimer's disease. Sci Transl Med. 2019;11:eaav6221.
72. Lee SH, Meilandt WJ, Xie L, Gandham VD, Ngu H, Barck KH, et al. Trem2 restrains the enhancement of tau accumulation and neurodegeneration by β-amyloid pathology. Neuron. 2021;109:1283–301.e6.
73. Focke C, Blume T, Zott B, Shi Y, Deussing M, Peters F, et al. Early and longitudinal microglial activation but not amyloid accumulation predicts cognitive outcome in PS2APP mice. J Nucl Med. 2019;60:548–54.
74. Blume T, Deussing M, Biechele G, Peters F, Zott B, Schmidt C, et al. Chronic PPARgamma stimulation shifts amyloidosis to higher fibrillarity but improves cognition. Front Aging Neurosci. 2022;14:854031.
75. Malpetti M, Kievit RA, Passamonti L, Jones PS, Tsvetanov KA, Rittman T, et al. Microglial activation and tau burden predict cognitive decline in Alzheimer's disease. Brain. 2020;143:1588–602.
76. Kroth H, Oden F, Molette J, Schieferstein H, Capotosti F, Mueller A, et al. Discovery and preclinical characterization of [(18)F]PI-2620, a next-generation tau PET tracer for the assessment of tau pathology in Alzheimer's disease and other tauopathies. Eur J Nucl Med Mol Imaging. 2019;46:2178–89.
77. Mueller A, Bullich S, Barret O, Madonia J, Berndt M, Papin C, et al. Tau PET imaging with (18)F-PI-2620 in patients with Alzheimer disease and healthy controls: a first-in-humans study. J Nucl Med. 2020;61:911–9.
78. Willroider M, Roeber S, Horn AKE, Arzberger T, Scheifele M, Respondek G, et al. Superiority of formalin-fixed paraffin-embedded brain tissue for in vitro assessment of progressive supranuclear palsy tau pathology with [(18) F]PI-2620. Front Neurol. 2021;12:684523.
79. Kunze G, Kumpfel R, Rullmann M, Barthel H, Brendel M, Patt M, et al. Molecular simulations reveal distinct energetic and kinetic binding properties of [(18)F]PI-2620 on Tau filaments from 3R/4R and 4R Tauopathies. ACS Chem Neurosci. 2022;13:2222–34.
80. Malarte ML, Gillberg PG, Kumar A, Bogdanovic N, Lemoine L, Nordberg A. Discriminative binding of tau PET tracers PI2620, MK6240 and RO948 in Alzheimer's disease, corticobasal degeneration and progressive supranuclear palsy brains. Mol Psychiatry. 2023;28:1272–83.

81. Snellman A, Rokka J, Lopez-Picon FR, Eskola O, Wilson I, Farrar G, et al. Pharmacokinetics of [(1)(8)F]flutemetamol in wild-type rodents and its binding to beta amyloid deposits in a mouse model of Alzheimer's disease. Eur J Nucl Med Mol Imaging. 2012;39:1784–95.
82. Zanotti-Fregonara P, Pascual B, Rostomily RC, Rizzo G, Veronese M, Masdeu JC, et al. Anatomy of (18)F-GE180, a failed radioligand for the TSPO protein. Eur J Nucl Med Mol Imaging. 2020;47:2233–6.
83. van Assema DM, Lubberink M, Bauer M, van der Flier WM, Schuit RC, Windhorst AD, et al. Blood-brain barrier P-glycoprotein function in Alzheimer's disease. Brain. 2012;135:181–9.
84. de Vries HE, Kuiper J, de Boer AG, Van Berkel TJ, Breimer DD. The blood-brain barrier in neuroinflammatory diseases. Pharmacol Rev. 1997;49:143–55.

AUTHOR CONTRIBUTIONS

(1) Research project: (A) Conception: AF, GB, AR, PB, RP, CH, JL, GUH, and MB. (B) Organization: AF, GB, AR, PB, RP, CH, JL, GUH, and MB. (C) Execution: BR, SSc, SH, JS, LB, JG, SL, NLA, DK, SSt, and OD performed human PET and MRI scans and their analysis. CP, SK, EW, SG, KB, AD, LB, CK, MT, JU, BP, MZ, LT, OG, TG, JH, DJ, BR, RP, MS, PB, JL and GH recruited patients, examined patients and controls. SL, PB, HB, and OS contributed to tracer synthesis and delivery. (2) Statistical Analysis: (A) Design: AF, GB, NF, EW, CP, KB, AD, BR, RP, JL, GUH and MB designed analysis of clinical data. (B) Execution: NF, EW, CP, KB, AD, BR, RP, JL, GH and MB analyzed clinical data. EM and CH performed sTREM2 analysis. NLA, CW and RR performed TSPO polymorphism analysis. AF, GB, LB, PB and MB interpreted human PET data. (C) Review and Critique: all authors. (3) Manuscript Preparation: (A) Writing of the first draft: AF, GB and MB. (B) Review and Critique: all authors.

FUNDING

This work was supported by grants from the Deutsche Forschungsgemeinschaft (DFG, German Research Foundation) under Germany's Excellence Strategy within the framework of the Munich Cluster for Systems Neurology (EXC 2145 SyNergy – ID 390857198) and within research units (FOR-2858 project numbers 403161218, 421887978, 422188432, 422182557 and 422179811). GUH was funded by the Hannover Cluster RESIST (EXC 2155 – project number 39087428), the German Federal Ministry of Education and Research (BMBF, 01KU1403A EpiPD; 01EK1605A HitTau; 01DH18025 TauTherapy); European Joint Programme on Rare Diseases (Improve-PSP); Deutsche Forschungsgemeinschaft (DFG, HO2402/18-1 MSAomics), VolkswagenStiftung (Niedersächsisches Vorab); Petermax-Müller Foundation (Etiology and Therapy of Synucleinopathies and Tauopathies). The Lüneburg Heritage and Friedrich-Baur-Stiftung have supported the work of CP. SK was supported by Ehrmann Foundation and Lüneburg Heritage. The Alzheimer Forschung Initiative e.V. provided grant no. 19063p to MB. The Hirnliga e.V. supported recruitment and imaging of the ActiGliA cohort (Manfred-Strohscheer-Stiftung) by a grant to BSR and MB. RP was supported by the Davos Alzheimer's Collaborative, the VERUM Foundation, the Robert-Vogel-Foundation, the National Institute for Health and Care Research (NIHR) Sheffield Biomedical Research Centre (NIHR203321), the University of Cambridge - Ludwig-Maximilians-University Munich Strategic Partnership within the framework of the German Excellence Initiative and Excellence Strategy and the European Commission under the Innovative Health Initiative program (project 101132356). Open Access funding enabled and organized by Projekt DEAL.

COMPETING INTERESTS

CH collaborates with Denali Therapeutics. CH is chief advisor of ISAR Bioscience and a member of the advisory board of AviadoBio. TG received consulting fees from AbbVie, Alector, Anavex, Biogen, Eli Lilly, Functional Neuromodulation, Grifols, Iqvia, Noselab, Novo Nordisk, NuiCare, Orphanzyme, Roche Diagnostics, Roche Pharma, UCB, and Vivoryon; lecture fees from Grifols, Medical Tribune, Novo Nordisk, Roche Pharma, and Schwabe; and has received grants to his institution from Roche Diagnostics. GUH participated in industry-sponsored research projects from Abbvie, Biogen, Biohaven, Novartis, Roche, Sanofi, UCB; serves as a consultant for Abbvie, Alzprotect, Aprineua, Asceneuron, Bial, Biogen, Biohaven, Kyowa Kirin, Lundbeck, Novartis, Retrotope, Roche, Sanofi, UCB; received honoraria for scientific presentations from Abbvie, Bayer Vital, Bial, Biogen, Bristol Myers Squibb, Kyowa Kirin, Roche, Teva, UCB, Zambon; holds a patent on Treatment of Synucleinopathies. United States Patent No.: US 10,918,628 B2: EP 17 787 904.6-1109 / 3 525 788; received publication royalties from Academic Press, Kohlhammer, and Thieme. MB received speaker honoraria from GE healthcare, Roche and LMI and is an advisor of LMI. LB is a Novartis Radiopharmaceuticals GmbH employee since 10/2022, unrelated to this work.

ADDITIONAL INFORMATION

Supplementary information The online version contains supplementary material available at https://doi.org/10.1038/s41380-023-02188-8.

Correspondence and requests for materials should be addressed to Matthias Brendel.

Reprints and permission information is available at http://www.nature.com/reprints

Publisher's note Springer Nature remains neutral with regard to jurisdictional claims in published maps and institutional affiliations.

10. Publikation II

RESEARCH ARTICLE

Cortical [^{18}F]PI-2620 Binding Differentiates Corticobasal Syndrome Subtypes

Carla Palleis, MD,[1,2†] Matthias Brendel, MD,[3,4†] Anika Finze,[3] Endy Weidinger, MD,[1,2] Kai Bötzel, MD,[1] Adrian Danek, MD,[1] Leonie Beyer, MD,[3] Alexander Nitschmann,[3] Maike Kern,[3] Gloria Biechele,[3] Boris-Stephan Rauchmann, MD,[5,6] Jan Häckert, MD,[6] Matthias Höllerhage, MD,[7] Andrew W. Stephens, MD, PhD,[8] Alexander Drzezga, MD,[9,10,11] Thilo van Eimeren, MD,[9,10,12] Victor L. Villemagne, MD,[13] Andreas Schildan, PhD,[14] Henryk Barthel, MD,[14] Marianne Patt, PhD,[14] Osama Sabri, MD,[14] German Imaging Initiative for Tauopathies (GII4T), Peter Bartenstein, MD,[3,4] Robert Perneczky, MD,[2,4,6,15] Christian Haass, PhD,[2,4,16] Johannes Levin, MD,[1,2,4†*] and Günter U. Höglinger, MD[2,4,7†*]

[1]*Department of Neurology, Ludwig-Maximilians-University, Munich, Germany*
[2]*German Center for Neurodegenerative Diseases (DZNE), Munich, Germany*
[3]*Department of Nuclear Medicine, Ludwig-Maximilians-University, Munich, Germany*
[4]*Munich Cluster for Systems Neurology (SyNergy), Munich, Germany*
[5]*Department of Radiology, Ludwig-Maximilians-University, Munich, Germany*
[6]*Department of Psychiatry and Psychotherapy, Ludwig-Maximilians-University, Munich, Germany*
[7]*Department of Neurology, Hannover Medical School, Hannover, Germany*
[8]*Life Molecular Imaging GmbH, Berlin, Germany*
[9]*Department of Nuclear Medicine, Faculty of Medicine and University Hospital Cologne, University of Cologne, Cologne, Germany*
[10]*German Center for Neurodegenerative Diseases (DZNE), Bonn-Cologne, Germany*
[11]*Institute of Neuroscience and Medicine (INM-2), Molecular Organization of the Brain, Forschungszentrum Jülich, Julich, Germany*
[12]*Department of Neurology, University Hospital Cologne, Cologne, Germany*
[13]*Department of Psychiatry, The University of Pittsburgh, Pittsburgh, Pennsylvania, USA*
[14]*Department of Nuclear Medicine, University of Leipzig, Leipzig, Germany*
[15]*Ageing Epidemiology (AGE) Research Unit, School of Public Health, Imperial College, London, United Kingdom*
[16]*Chair of Metabolic Biochemistry, Biomedical Center (BMC), Faculty of Medicine, Ludwig-Maximilians-University, Munich, Germany*

***Correspondence to:** Prof. Dr. med. J. Levin, Department of Neurology University of Munich and German Center of Neurodegenerative Diseases (DZNE) e.V., Marchioninistraße 15, 81377 Munich, Germany; E-mail: johannes.levin@med.uni-muenchen.de; or Prof. Dr. med. G.U. Höglinger, Department of Neurology, Medizinische Hochschule Hannover; Carl-Neuberg-Str. 1, 30625 Hannover, Germany; E-mail: guenter.hoeglinger@dzne.de

†Contributed equally.

Members of the German Imaging Initiative for Tauopathies (GII4T) Study Group are listed in the Appendix.

Relevant conflicts of interest/financial disclosures: M.B. received speaker honoraria from GE Healthcare and LMI and is an adviser of LMI. G.U.H. has ongoing research collaborations with Prothena; serves as a consultant for AbbVie, AlzProtect, Asceneuron, Biogen, Biohaven, Lundbeck, Novartis, Roche, Sanofi, UCB; received honoraria for scientific presentations from AbbVie, Bial, Biogen, Bristol Myers Squibb, Roche, Teva, UCB, and Zambon; and holds a patent on PERK Activation for the Treatment of Neurodegenerative Diseases (PCT/EP2015/068734). C.H. is chief scientific adviser of ISAR Biosciences and collaborates with DENALI Therapeutics. R.P. is on the advisory board for Biogen, has consulted for Eli Lilly, is a grant recipient from Janssen Pharmaceutica and Boehringer Ingelheim, and has received speaker honoraria from Janssen-Cilag, Pfizer, and Biogen. J.L. reports speaker fees from Bayer Vital, consulting fees from Axon Neuroscience, author fees from Thieme medical publishers and W. Kohlhammer GmbH medical publishers, nonfinancial support from AbbVie and compensation for duty as part-time CMO from MODAG GmbH, all outside the submitted work. O.S. receives research funding from LMI. A.W.S. is an employee of LMI. All other authors report no conflicts of interest.

Funding agencies: This work was funded by the Deutsche Forschungsgemeinschaft (DFG, German Research Foundation) to P.B. and N.A. — project number 421887978, to C.W. — project number DFG WE2298/10-1, 422182557, and to A.R. and M.B. — project numbers BR4580/1-1/ RO5194/1-1. The recruitment of the ActiGliA cohort was supported by the presidential fund of the Helmholtz Society (to C.H.). This project was also supported by the German Center for Neurodegenerative Diseases (DZNE, DescribePSP Study), the German Parkinson's Association (DPG, ProPSP Study), and the Hirnliga e.V. (Manfred-Strohscheer-Stiftung). Tau PET imaging was funded by the Alzheimer Forschung Initiative e.V. (grant 19063p). C.P., P.B., G.U.H., C.H., J.L., and R.P. were supported by the Deutsche Forschungsgemeinschaft (DFG, German Research Foundation) under Germany's Excellence Strategy within the framework of the Munich Cluster for Systems Neurology (EXC 2145 SyNergy – ID 390857198). G.U.H. and C.H. were also funded by the NOMIS Foundation (FTLD project), Volkswagen Stiftung/Lower Saxony Ministry for Science/ Petermax-Müller Foundation (Etiology and Therapy of Synucleinopathies and Tauopathies). The Lüneburg Heritage has supported the work of C.P. and J.L. L.B. was funded by the Munich-Clinician-Scientist Program.

Received: 30 January 2021; **Revised:** 23 March 2021; **Accepted:** 5 April 2021

Published online in Wiley Online Library (wileyonlinelibrary.com). DOI: 10.1002/mds.28624

ABSTRACT: Background: Corticobasal syndrome is associated with cerebral protein aggregates composed of 4-repeat (~50% of cases) or mixed 3-repeat/4-repeat tau isoforms (~25% of cases) or nontauopathies (~25% of cases).

Objectives: The aim of this single-center study was to investigate the diagnostic value of the tau PET-ligand [^{18}F]PI-2620 in patients with corticobasal syndrome.

Methods: Forty-five patients (71.5 ± 7.6 years) with corticobasal syndrome and 14 age-matched healthy controls underwent [^{18}F]PI-2620-PET. Beta-amyloid status was determined by cerebral β-amyloid PET and/or CSF analysis. Subcortical and cortical [^{18}F]PI-2620 binding was quantitatively and visually compared between β-amyloid-positive and -negative patients and controls. Regional [^{18}F]PI-2620 binding was correlated with clinical and demographic data.

Results: Twenty-four percent (11 of 45) were β-amyloid-positive. Significantly elevated [^{18}F]PI-2620 distribution volume ratios were observed in both β-amyloid-positive and β-amyloid-negative patients versus controls in the dorsolateral prefrontal cortex and basal ganglia. Cortical [^{18}F]PI-2620 PET positivity was distinctly higher in β-amyloid-positive compared with β-amyloid-negative patients with pronounced involvement of the dorsolateral prefrontal cortex. Semiquantitative analysis of [^{18}F]PI-2620 PET revealed a sensitivity of 91% for β-amyloid-positive and of 65% for β-amyloid-negative cases, which is in excellent agreement with prior clinicopathological data. Regardless of β-amyloid status, hemispheric lateralization of [^{18}F]PI-2620 signal reflected contralateral predominance of clinical disease severity.

Conclusions: Our data indicate a value of [^{18}F]PI-2620 for evaluating corticobasal syndrome, providing quantitatively and regionally distinct signals in β-amyloid-positive as well as β-amyloid-negative corticobasal syndrome. In corticobasal syndrome, [^{18}F]PI-2620 may potentially serve for a differential diagnosis and for monitoring disease progression. © 2021 The Authors. *Movement Disorders* published by Wiley Periodicals LLC on behalf of International Parkinson and Movement Disorder Society

Key Words: tau; PET; corticobasal syndrome; four-repeat tauopathies; Alzheimer's disease

Corticobasal syndrome (CBS) is a rare adult-onset disorder characterized by a combination of cortical signs and movement disorder signs. Clinically, CBS can be diagnosed using the Movement Disorder Society (MDS) criteria for progressive supranuclear palsy (PSP)[1] or the corticobasal degeneration (CBD) criteria.[2] The pathology of CBS is characterized by 4-repeat (4R) tau aggregation in CBD and PSP (approximately 50% of patients) or by mixed 3-repeat/4-repeat (3R/4R) tau aggregation in Alzheimer's disease (AD) pathology (about 25%).[1-4] The 4R tauopathies are characterized by intracellular aggregates of tau isoforms with 4 repeats in the microtubule-binding domain in neurons, astrocytes, and oligodendrocytes. There are proposals to classify CBD and PSP as closely related variants within a coherent disease spectrum, that is, 4R tauopathies.[1,5] In rare cases, CBS with rapid decline and early death after diagnosis can occur in prion disease[6] or *C9orf72* mutation carriers.[7] Antemortem misdiagnosis of CBS and the underlying pathologies is very common[8,9] because of a lack of reliable biomarkers and overlapping phenotypes of the different neuropathologies.[4,10] Diagnostic biomarkers are only available for CBS with underlying AD pathology, including β-amyloid (Aβ) PET and quantification of Aβ, total, and phosphorylated tau concentrations in cerebrospinal fluid (CSF).[11-13] The definite diagnosis of the different neuropathological entities underlying CBS relies on postmortem examination. The precise antemortem diagnosis of the molecular pathologies in individual CBS patients, however, becomes more important, as molecularly targeted therapies for the underlying proteinopathies are being developed.[4,10]

Multiple radioligands for PET are currently investigated for their potential to detect tau deposits in vivo. In the first generation of tau-targeting tracers, off-target binding, for example, to monoamine-oxidase B,[14,15] limited the specific visualization of tau burden in vivo.[16-19] The newer tau PET ligand [^{18}F]PI-2620[20] showed less off-target binding to monoamine oxidases, high affinity to 3R/4R tau in AD and recently also revealed binding in the 4R tauopathy PSP.[21]

Therefore, we investigated the utility of [^{18}F]PI-2620 as an in vivo biomarker for CBS and its heterogeneous underlying molecular entities.

Material and Methods

Participants and Clinical Evaluation

The study cohort is embedded in Activity of Cerebral Networks, Amyloid and Microglia in Aging and Alzheimer's Disease (ActiGliA), a prospective cohort study at Ludwig-Maximilians-University (LMU), approved by the local ethics committee (project number 17-755; see File S1 for details; human PET analyses project numbers 17-569 and 19-022). Written informed consent was obtained from all participants in accordance with the Declaration of Helsinki.

Clinical diagnosis of CBS was made as defined in the MDS-PSP criteria.[1] All enrolled patients also fulfilled the Armstrong criteria of probable or possible CBD-CBS.[2] Only patients with negative family history for Parkinson's disease and AD were included.

Disease duration was defined as the time between symptom onset and clinical assessment. For clinical rating, we used the PSP rating scale (PSPRS)[22] and the PSP clinical deficits scale (PSP-CDS).[23] Functional independence was measured using the Schwab and England Activities of Daily Living (SEADL) scale.[24] Cognitive state was assessed with the Montreal Cognitive Assessment (MoCA) scale.[25] The Dementia Apraxia Test (DATE)[26] was used for assessment of buccofacial and upper limb apraxia. Verbal fluency was tested using the lexical fluency task from the Frontal Assessment Battery.[27]

Aβ concentration and Aβ ratio in CSF and [18F] flutemetamol PET served for assessment of the Aβ status (see Methods section, below). In healthy controls, [18F]florbetaben PET within 12 months prior to study inclusion was also accepted. In case of β-amyloid positivity in CSF or PET, patients were classified as CBS with underlying AD pathology (Aβ-positive CBS; Aβ[+] CBS).[12] In case of β-amyloid negativity (Aβ-negative CBS; Aβ[−]CBS), patients were subclassified as CBS with either "suggestive" or "probable" underlying 4R tauopathy.[28,29]

The [18F]PI-2620 PET was performed in 45 CBS patients (see Methods section, below). Distribution of [18F]PI-2620 tracer binding of 8 patients included in the current report has already been reported previously.[21]

Results were compared with 14 age-matched cognitively healthy individuals without motor or cognitive signs or symptoms (CTRL). Four were scanned in Munich, and 10 were scanned in New Haven or Melbourne.[21] There were no statistically significant differences in binding characteristics of [18F]PI-2620 between external and inhouse controls (Table S1 in File S1).

The regional [18F]PI-2620 distribution of Aβ(+)CBS and Aβ(−)CBS patients in the central region for pattern analysis was compared with 12 patients with typical AD dementia or mild cognitive impairment (MCI) according to the diagnostic criteria of the National Institute on Aging and Alzheimer's Association[12] from the ActiGliA cohort. The AD cohort has partially been published previously.[21]

PET Imaging

Tau-PET Acquisition and Analysis

The [18F]PI-2620 acquisition, reconstruction, and harmonization across scanners at the Department of Nuclear Medicine at LMU were performed as described previously[21] (see File S1 for details). The subcortical target regions (putamen, globus pallidus externus, globus pallidus internus, subthalamic nucleus, substantia nigra, dentate nucleus, midbrain), the dorsolateral prefrontal cortex (DLPFC), and the medial prefrontal cortex were identical to the earlier analysis in PSP. Motor cortex, temporal mesial, temporal lateral, parietal, anterior cingulate gyrus, and postcentral cortical target regions of the Hammers atlas[30] were introduced as additional target regions. The maximum distribution volume ratio (DVR) of bilateral regions was used for group comparisons with account for asymmetric tracer distribution in CBS. All images of clinically left-dominant CBS patients were flipped for image visualization. Voxels with a DVR ≥ mean value (MV) + 2 standard deviations (SDs) of the controls were defined as positive and the percentage of positivity was calculated in Aβ(+)CBS, Aβ(−)CBS, and typical AD. The comparison was performed qualitatively. To address potential differences in tracer affinity to 4R- and 3R/4R tau,[20] we generated binarized voxel-based maps of [18F]PI-2620 positivity for all patients and compared the percentage of voxel positivity between Aβ(+)CBS and Aβ(−)CBS. The 12 Aβ-positive patients with typical AD were processed the same way and compared with CBS patients.

Assessment of Aβ Status

[18F]Flutemetamol, or [18F]Florbetaben, PET in some controls, was primarily used to detect Aβ deposition, indicating underlying AD pathophysiology. Eighty-four percent of CBS patients (38 of 45) and 100% of control subjects underwent Aβ-PET imaging as described previously[31,32] (see details in theFile S1). CSF Aβ was assessed in 87% of patients (39 of 45) and in all patients without Aβ-PET. Threshold for Aβ ratio (Aβ [1–42]/Aβ [1–40]) was set to <5.5% according to standardized laboratory diagnostics at LMU.

Statistical Analyses

SPSS (V25; IBM, Ehningen, Germany) was used for statistical testing. Statistical significance was set at $P < 0.05$. Age, PSPRS, PSP-CDS, DATE, SEADL, verbal fluency test, disease duration, and MoCA were compared between the different study groups (Aβ[+]CBS, Aβ[−]CBS, controls) by a 1-way analysis of variance, whereas sex was subject to a chi-square test. [18F]PI-2620 DVRs of predefined target regions (maximum value of bilateral regions) were compared between the study groups by multivariate analysis of variance including age and sex as covariates as well as false discovery rate correction[33] for multiple brain regions. A region-based classification was performed by a semi-quantitative analysis, defining regional DV R ≥ MV + 2 SD of the controls as positive. One positive target

region classified the subject as positive (dichotomous) for the [^{18}F]PI-2620 scan.

Partial correlations (Pearson's coefficient of correlation [R]) were calculated for [^{18}F]PI-2620 DVR in predefined regions (maximum value of bilateral regions) with PSPRS, PSP-CDS, SEADL, DATE, disease duration, verbal fluency test, and MoCA, controlled for age and sex. The analysis was performed separately for Aβ (+)CBS and Aβ(−)CBS.

Asymmetry of [^{18}F]PI-2620 PET scans was judged visually and semiquantitatively. An expert reader rated the presence of asymmetric tracer distribution of the whole scan taking cortical and subcortical regions into account (none, left, right). The asymmetry index for [^{18}F]PI-2620-binding asymmetry was calculated using a subcortical volume of interest composed of the putamen and the globus pallidus because the topology of asymmetry in cortical regions was too heterogeneous for a standardized quantification. Clinical symptoms were graded for asymmetry as 0 (both sides equally affected), 1 (mild clinical asymmetry), 2 (moderate clinical asymmetry), or 3 (strong clinical asymmetry) for left and right hemispheres based on a movement disorder specialist's neurological examination and clinical score findings in the PSPRS and DATE. Agreement of visual [^{18}F]PI-2620-PET asymmetry and the presence of contralateral clinical symptom asymmetry (≥1, asymmetric) was assessed by Fleiss-Kappa. For semiquantitative analysis, Spearman's coefficient of correlation (r_s) was calculated between the asymmetry index of [^{18}F]PI-2620 PET and clinical asymmetry.

Results

Demographics and Amyloid Status

Performance of [^{18}F]PI-2620 PET occurred in 45 patients (71.5 ± 7.6 years) and 14 age-matched controls without clinical evidence of neurodegenerative diseases (67.4 ± 9.5 years). Detailed demographic and clinical data of the study sample are provided in Table 1. Single patient data are provided in File S1 (Table S2 in File S1).

As positive controls for the Aβ PET and CSF analyses, we used data from 12 patients with typical AD (8 women, 4 men; 67.0 ± 8.1 years; 6 with dementia, 6 with MCI), reported in detail elsewhere.[21] In all AD cases, the Aβ status was positive in both CSF and PET.

In the sample of the current study, all 14 controls were amyloid negative (Aβ[−]) in Aβ PET. In all 34 CBS patients with both Aβ PET and CSF available, the Aβ status was consistent for both biomarkers (8 Aβ[+]/26 Aβ[−]).

Twenty-four percent of the CBS cohort (11 of 45) were amyloid positive, indicating AD pathology with atypical, nonamnestic clinical manifestations. Seventy-

TABLE 1 *Demographics at group level*

Demographics	All CBS	Aβ(+) CBS	Aβ(−) CBS	CTRL
n	45	11	34	14
Sex	18 ♂/27 ♀	3 ♂/8 ♀	15 ♂/19 ♀	5 ♂/9 ♀
Age at examination (y)	71.5 ± 7.6	76.2 ± 4.6[b,c]	69.9 ± 7.7[c]	67.4 ± 9.5
Age at disease onset (y)	68.7 ± 7.7	73.5 ± 4.6[c]	67.1 ± 7.9 [c]	n.a.
Disease duration (mo)	32.7 ± 19.7	32.0 ± 20.1	32.8 ± 19.3	n.a.
PSPRS	25.7 ± 12.0	23.3 ± 5.6	26.5 ± 13.3	n.a.
PSP-CDS	2.1 ± 1.0	2.2 ± 1.0	1.9 ± 0.6	n.a.
SEADL	64.8 ± 17.8	66.7 ± 8.2	64.2 ± 19.8	n.a.
Verbal fluency test	1.7 ± 1.1	1.4 ± 1.1	1.8 ± 1.1	n.a.
MoCA	21.3 ± 6.1	16.9 ± 7.3[b,c]	22.6 ± 5.2[a,c]	28.8 ± 1.6
DATE	41.3 ± 13.2	32.6 ± 12.6[c]	43.9 ± 12.4[c]	n.a.
Aβ-positive PET ([^{18}F]flutemetamol or [^{18}F] florbetaben)	9/38	9/9	0/29	0/14
Aβ-positive CSF (Aβ ratio < 5.5%)	10/41	10/10	0/31	0/4
Diagnostic allocation		11 atypical AD with CBS	17 probable CBD-CBS, 17 possible CBD-CBS[2], 24 probable 4R tauopathy, 10 s.o. PSP-CBS[1]	n.a.

Data are presented as mean ± standard deviation, unless indicated otherwise. Demographics were statistically tested by ANOVA or chi-square test.
[a]$P < 0.05$; [b]$P < 0.01$ of group differences between study population and controls; [c]$P < 0.05$ of group differences between Aβ-positive and Aβ-negative CBS patients.

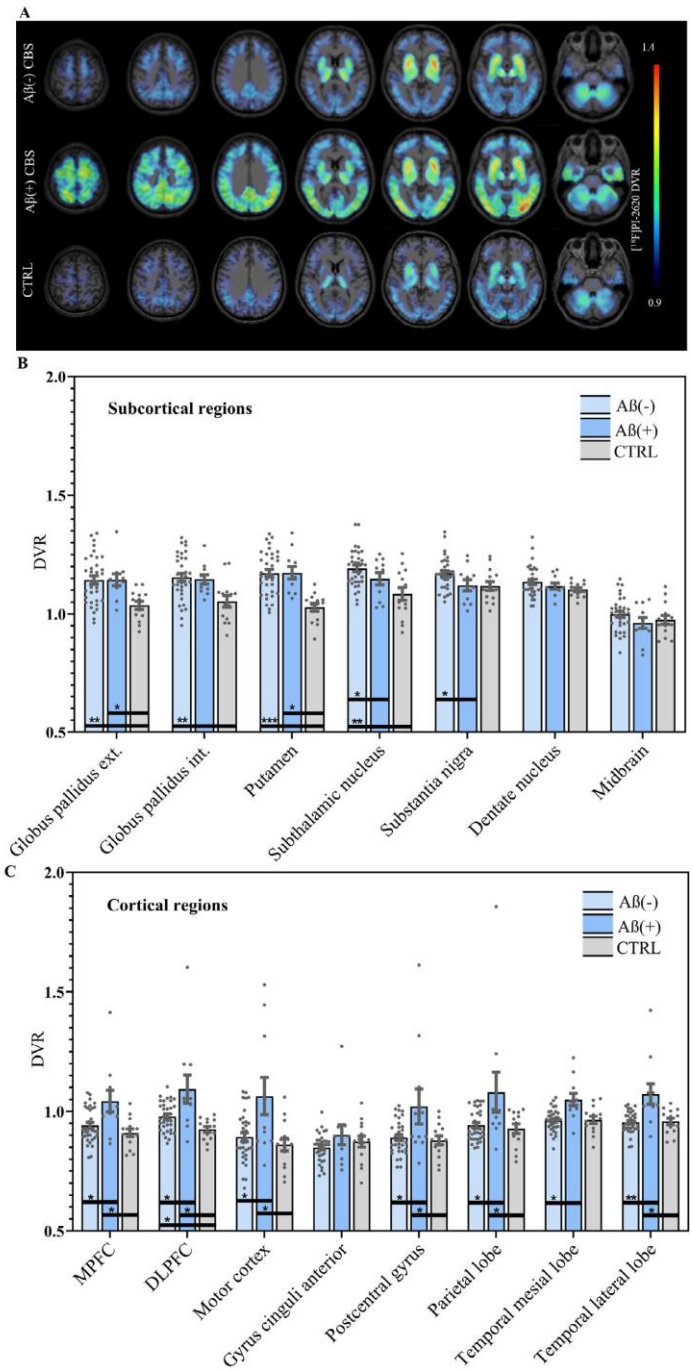

FIG. 1. Voxel-based differences in [^{18}F]PI-2620 binding in predefined tauopathy target regions. (**A**) Average [^{18}F]PI-2620 distribution volume ratio (DVR) binding maps presented as axial overlays on a standard MRI template for all study groups (Aβ[+]CBS, n = 11; Aβ[−]CBS, n = 34; and controls (CTRL), n = 14). Extracerebral voxels were masked. Images from patients with left-dominant symptoms were flipped. (**B**, **C**) [^{18}F]PI-2620 DVR comparison between Aβ(+) CBS, Aβ(−) CBS, and CTRL for 14 evaluated subcortical (**B**) and cortical (**C**) target regions. Statistics derive from multivariate analysis of variance including age and sex as covariates and false discovery rate correction for multiple brain regions. Error bars indicate standard error. *$P < 0.05$; **$P < 0.01$; ***$P < 0.001$ indicate significant [^{18}F]PI-2620-DVR group differences of Aβ(+)CBS and Aβ(−)CBS versus CTRL. [Color figure can be viewed at wileyonlinelibrary.com]

six percent (34 of 45) were amyloid negative (Aβ[−] CBS), of which 10 qualified for "suggestive of PSP with CBS phenotype" and 24 for "probable 4R tauopathy"[1]; 17 cases each fulfilled the diagnosis of CBS with "possible CBD" or "probable CBD," respectively.[2]

Age at examination of Aβ(+)CBS patients (76.2 ± 4.6 years) was significantly higher compared with both Aβ(−)CBS (69.9 ± 7.7 years, $P = 0.0156$) and controls (67.4 ± 9.5 years, $P = 0.0097$). The 2 groups did not significantly differ with regard to disease duration/severity, activities of daily living, and verbal fluency (Table 1).

MoCA was significantly reduced versus controls (28.8 ± 1.6) in both Aβ(+)CBS (16.9 ± 7.3, $P = 0.004$)

TABLE 2 *[^{18}F]PI-2620-PET results at group level*

[^{18}F]PI-2620 distribution volume ratio				Cohen's *d*	
Subcortical target regions	**Aβ(−)CBS, n = 34**	**Aβ(+)CBS, n = 11**	**CTRL, n = 14**	**Aβ(−) CBS/ CTRL**	**Aβ(+) CBS/ CTRL**
Globus pallidus externus	1.143 ± 0.104 (1.107–1.179)[b]	1.144 ± 0.083 (1.088–1.200)[a]	1.037 ± 0.063 (1.000–1.073)	1.242	1.453
Globus pallidus internus	1.154 ± 0.098 (1.120–1.189)[b]	1.146 ± 0.065 (1.102–1.189)	1.053 ± 0.089 (1.002–1.105)	1.082	1.190
Putamen	1.171 ± 0.094 (1.139–1.204)[c]	1.174 ± 0.088 (1.115–1.232)[a]	1.028 ± 0.061 (0.992–1.063)	1.813	1.926
Subthalamic nucleus	1.192 ± 0.079 (1.165–1.220)[b]	1.148 ± 0.085 (1.091–1.205)	1.085 ± 0.103 (1.025–1.144)	1.173	0.672
Substantia nigra	1.171 ± 0.067 (1.147–1.194)	1.121 ± 0.077 (1.069–1.172)	1.118 ± 0.070 (1.077–1.158)	0.769	0.037
Dentate nucleus	1.135 ± 0.065 (1.112–1.158)	1.117 ± 0.043 (1.088–1.146)	1.103 ± 0.031 (1.085–1.121)	0.630	0.385
Midbrain	0.999 ± 0.070 (0.975–1.024)	0.962 ± 0.078 (0.909–1.014)	0.975 ± 0.071 (0.935–1.016)	0.337	−0.184
Cortical target regions	**Aβ(−)CBS, n = 34**	**Aβ(+)CBS, n = 11**	**CTRL, n = 14**	**Aβ(−) CBS/ CTRL**	**Aβ(+) CBS/ CTRL**
MPFC	0.942 ± 0.073 (0.916–0.967)	1.043 ± 0.149 (0.943–1.143)[a]	0.910 ± 0.062 (0.874–0.947)	0.455	1.156
DLPFC	0.979 ± 0.061 (0.957–1.000)[a]	1.093 ± 0.195 (0.962–1.224)[a]	0.925 ± 0.045 (0.899–0.951)	1.000	1.186
Motor cortex	0.893 ± 0.105 (0.856–0.930)	1.064 ± 0.257 (0.891–1.237)[a]	0.861 ± 0.099 (0.804–0.919)	0.307	1.040
Anterior cingulate gyrus	0.849 ± 0.059 (0.828–0.870)	0.902 ± 0.138 (0.809–0.995)	0.874 ± 0.088 (0.823–0.925)	−0.332	0.243
Postcentral gyrus	0.891 ± 0.071 (0.866–0.916)	1.021 ± 0.244 (0.857–1.184)[a]	0.879 ± 0.071 (0.838–0.920)	0.173	0.788
Parietal lobe	0.942 ± 0.065 (0.919–0.965)	1.080 ± 0.277 (0.894–1.266)[a]	0.928 ± 0.073 (0.885–0.970)	0.207	0.753
Temporal mesial lobe	0.963 ± 0.047 (0.946–0.979)	1.049 ± 0.087 (0.991–1.107)	0.965 ± 0.057 (0.932–0.998)	−0.039	1.147
Temporal lateral lobe	0.955 ± 0.045 (0.939–0.970)	1.073 ± 0.142 (0.977–1.168)[a]	0.958 ± 0.051 (0.929–0.988)	−0.079	1.072

Values represent regional group means of [^{18}F]PI-2620 distribution volume ratios as determined by PET imaging, the standard error, and their 95% confidence interval in predefined subcortical and cortical brain areas and the effect size Cohen's *d*. Single subject values are illustrated in Figure 1. Significance levels are indicated by [a]$P < 0.05$, [b]$P < 0.01$, [c]$P < 0.001$. *P* values were derived from multivariate analysis of variance with age and sex as covariates and false discovery rate correction for multiple brain regions.

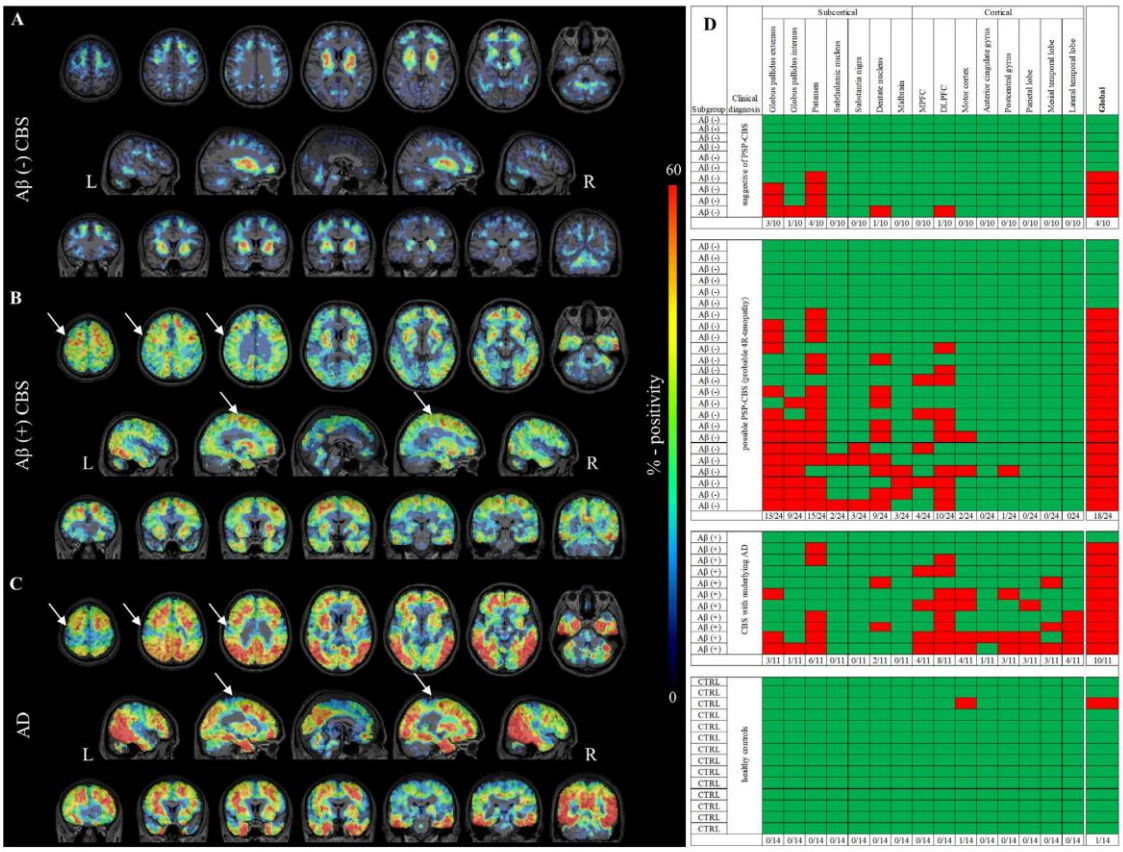

FIG. 2. Regional [18F]PI-2620 PET positivity. (**A**) Aβ(−)CBS, n = 34; (**B**) Aβ(+)CBS, n = 11; (**C**) typical AD, n = 12. (**A–C**) [18F]PI-2620 PET percentage positivity of single voxels was calculated in a 2-step approach. First, binarized maps of [18F]PI-2620 PET positivity were calculated for each patient against controls (MV + 2 SD control threshold). Second, the percentage positivity within the groups of Aβ(+)CBS, Aβ(−)CBS, and Aβ(+)-typical AD was calculated and illustrated. Arrows highlight the pre- and postcentral gyri that are spared from tracer deposition in Aβ(+) typical AD but rich in tracer deposition in Aβ(+)CBS. (**D**) For a multiregion classifier for diagnosis of CBS by [18F]PI-2620 PET, semiquantitative classification (red, positive; green, negative) of CBS target regions was performed by applying a threshold of mean + 2 standard deviations as obtained from the controls without objectified memory impairment and with intact motor function. One positive region defined the scan as global positive (Global). Aβ(−)CBS patients are arranged according to the MDS-PSP criteria.[1] [Color figure can be viewed at wileyonlinelibrary.com]

and Aβ(−)CBS (22.6 ± 5.2, $P = 0.0124$), with Aβ(+) CBS patients significantly more affected by cognitive impairment than Aβ(−)CBS patients ($P = 0.0126$).

The DATE yielded significantly lower scores (indicating more prominent apraxia) in Aβ(+)CBS patients (32.6 ± 12.6) compared with Aβ(−)CBS patients (43.9 ± 12.4, $P = 0.0294$).

Distribution of [18F]PI-2620 Binding

Predefined subcortical regions of interest had significantly elevated [18F]PI-2620 DVRs in both CBS groups versus controls, with the strongest differences in putamen (Fig. 1A,B; Table 2). Aβ(+)CBS displayed higher [18F]PI-2620 DVRs compared with controls in several cortical target regions (Fig. 1A,C; Table 2). Aβ(−)CBS patients showed higher [18F]PI-2620 DVRs compared with controls in the DLPFC (Fig. 1A,C; Table 2).

In both CBS groups, regional subcortical [18F]PI-2620 positivity (threshold > MV + 2 SD of controls) was of similar magnitude (Fig. 2A,B). Aβ(+)CBS patients yielded regional [18F]PI-2620 positivity compared with Aβ(−)CBS in cortical areas, most pronounced in the central region and prefrontal cortex (Fig. 2A,B). Only Aβ(+)CBS patients also showed regional [18F]PI-2620 positivity versus controls in pre- and postcentral gyri, which were spared in Aβ(+) typical AD patients with amnestic syndromes,[21] used as a positive control data set (Fig. 2B,C).

A multiregion classifier for [18F]PI-2620 using a DVR threshold (>MV + 2 SD of controls) was calculated to

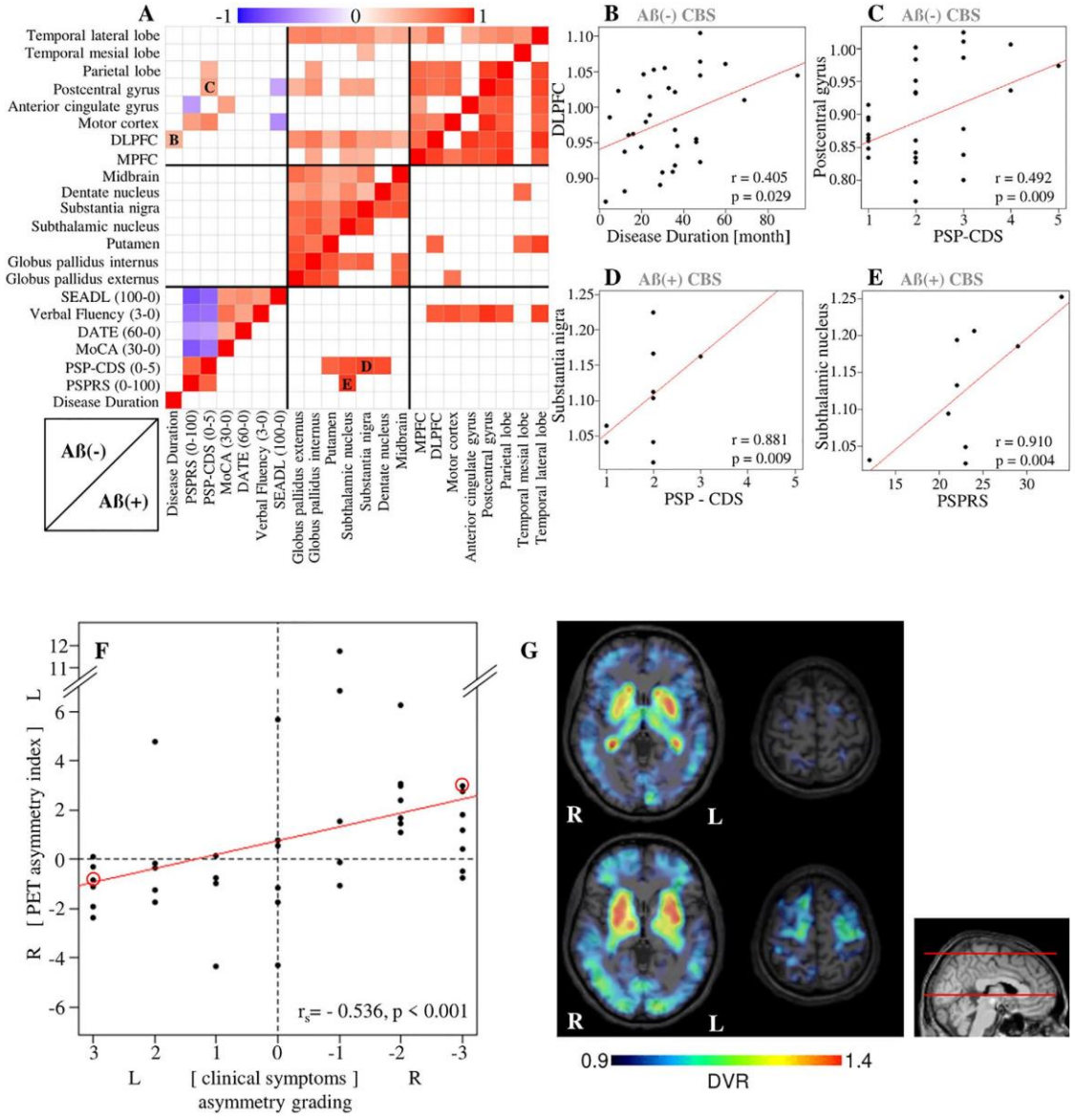

FIG. 3. Correlations between clinical symptoms and [^{18}F]PI-2620 PET in CBS. (**A**) Correlation matrix between [^{18}F]PI-2620 DVR in all evaluated target regions and clinical parameters. Color coding illustrates partial correlations (Pearson's coefficient of correlation, red, positive; purple, negative) with correction for age and sex. The analysis was performed separately for Aβ-positive and Aβ-negative CBS patients. Only associations with a significance of $P < 0.05$ are illustrated. (**B–E**) Key associations between parameters of disease duration/progression and [^{18}F]PI-2620-DVR data. R/*P* values derive from partial correlation, controlled for age and sex. (**F**) Asymmetric clinical presentation (asymmetry grading between left- and right-dominant symptoms) as a function of the [^{18}F]PI-2620 PET asymmetry index in n = 41 CBS patients. The degree of association was calculated by Spearman's correlation coefficient. (**G**) Exemplary subcortical [^{18}F]PI-2620-DVR binding in a clinically right-dominant patient (upper row) and a clinically left-dominant patient (lower row). [Color figure can be viewed at wileyonlinelibrary.com]

identify CBS patients based on PET data (Fig. 2D). This approach yielded a sensitivity of 71% for the total cohort (32 of 45), of 91% for Aβ(+)CBS, and of 65% for Aβ(−)CBS.

Cortical [^{18}F]PI-2620 binding in predefined target regions was positive in 47% of all patients (21 of 45), in 82% of Aβ(+)CBS patients (9 of 11), and in 35% of Aβ(−)CBS patients (12 of 34); see Figure 2D. The

DLPFC was the most frequently involved cortical target region compared with controls (Aβ(+)CBS, 73%; Aβ(−)CBS, 32%).

Associations of [18F]PI-2620 Binding with Clinical Symptoms

To assess the potential of [18F]PI-2620 as a biomarker of disease severity, a correlation analysis of [18F]PI-2620 DVR in predefined target regions and clinical parameters was performed.

Figure 3A shows a correlation matrix between all target regions and clinical parameters. In general, clinical scales correlated well with each other in Aβ(−)CBS, but less so in Aβ(+)CBS patients. Also [18F]PI-2620 DVRs in subcortical regions correlated well with each other in Aβ(−)CBS patients, but less so in Aβ(+)CBS patients. Inversely, [18F]PI-2620 DVRs in cortical regions correlated well with each other in Aβ(+)CBS patients, but less so in Aβ(−)CBS patients.

Key associations between [18F]PI-2620-DVR data and clinical parameters corrected for age, sex, and multiple comparisons are displayed in Figure 3B–E.

In Aβ(−)CBS, but not Aβ(+)CBS, disease duration was positively correlated with [18F]PI-2620 DVRs in the DLPFC ($R = 0.405$, $P = 0.029$; Fig. 3A,B). Also, PSP-CDS scores were positively correlated with [18F]PI-2620 DVRs in cortical regions (Fig. 3A), most pronounced in the postcentral gyrus ($R = 0.492$, $P = 0.009$; Fig. 3C) in Aβ(−)CBS, but not Aβ(+) CBS. In Aβ(−)CBS patients, [18F]PI-2620 DVR in subcortical target regions did not correlate significantly with clinical parameters.

In contrast, in Aβ(+)CBS patients, PSP-CDS scores were positively correlated with [18F]PI-2620 DVRs in subcortical regions (Fig. 3A), most pronounced in the substantia nigra ($R = 0.881$, $P = 0.009$; Fig. 3D). Also, PSPRS scores were positively correlated with [18F]PI-2620 DVR in the subthalamic nucleus ($R = 0.910$, $P = 0.004$; Fig. 3A,E) in Aβ(+)CBS, but not Aβ(−)CBS. Verbal fluency positively correlated with [18F]PI-2620 DVR in several cortical areas (Fig. 3A) only in Aβ(+) CBS patients. Tracer binding did not significantly correlate with MoCA, DATE, or SEADL.

With regard to asymmetry of phenotype manifestations, asymmetric presentation of subcortical and cortical symptoms coincided on the same side of the body in all patients (see File S1 for details). An observer-blinded visual read of the asymmetry of [18F]PI-2620 tracer uptake matched the contralateral clinical dominance in 75% of cases (see Table S3 in File S1). A semiquantitative analysis of asymmetry indicated that lateralization of the [18F]PI-2620 signal reflected asymmetry of clinical symptoms in CBS to the hemisphere contralateral of the clinical phenotype ($r_s = -0.536$, $P < 0.001$; Fig. 3F). Figure 3G shows an exemplary subcortical [18F]PI-2620-DVR binding in a clinically left-dominant patient and right-dominant patient.

Discussion

We present the first study applying the novel tau PET tracer [18F]PI-2620 in a cohort of CBS patients with underlying probable 3R/4R- or 4R tauopathy. Our data indicate elevated tracer retention in cortical and subcortical brain areas of Aβ(+)CBS and Aβ(−)CBS patients when compared with cognitively healthy controls without motor symptoms. Strongest binding differences between CBS patients and controls were seen in the putamen and in the globus pallidus. Cortical binding was higher and more frequent in Aβ(+)CBS compared with Aβ(−)CBS patients, with DLPFC being the most frequently positive cortical area in both subgroups. In additional, Aβ(+)CBS patients showed an elevated [18F]PI-2620 binding in pre- and postcentral gyri in contrast to amnestic AD patients. A positive [18F]PI-2620 PET was observed in 91% of Aβ(+)CBS patients and in 65% of all Aβ(−)CBS patients, which is in excellent agreement with prior clinicopathological data. Aβ status in amyloid PET and CSF was coherent in all CBS patients, with Aβ positivity in 24%. Asymmetry of [18F]PI-2620-PET binding corresponded to the contralateral dominance of the clinical phenotype.

The main question still remained: if the next-generation tau-PET ligands have the ability to capture 4R tau in vivo. Subcortical brain areas are subject to several relevant off-target sources such as neuromelanin, iron, or microhemorrhage,[34] but particularly cortical binding in 4R-tauopathy patients could substantiate the claim to image 4R tau in vivo. Our previous [18F]PI-2620 investigation revealed blockable tracer binding in cortical autoradiography of deceased PSP patients, but we were not able to show an elevated cortical signal of PSP patients against controls at the group level by PET in vivo.[21] In the current study, we found a significantly elevated binding in the DLPFC of Aβ(−)CBS patients compared with controls, which was still present after correction for multiple comparisons. Our observation fitted topologically to the cortical predilection sites of CBD, involving the motor cortices, which are also characterized by the strongest neuronal injury.[35] Thus, although we acknowledge missing autopsy validation in CBS patients, our data provide the first promising data suggesting in vivo 4R-tau detection in an Aβ(−)CBS cohort by a next-generation tau tracer with limited off-target binding.[20] As a potential caveat, we note that the tracer binding observed in our study could still derive from a neuropathological process very closely paralleling tau pathology. Claims of 4R-tau binding in vivo indeed need to be interpreted with caution because a quantitative correlation between

[^{18}F]AV-1451 PET and 4R-tau burden in autopsy has been reported[36] despite the low or absent autoradiography binding of this tracer.[34,37] Earlier studies with the 2-arylquinoline [^{18}F]THK5351 suggested to detect tau in CBS in vivo,[38] but the majority of the signal was afterward reported to depend on monoamine oxidase binding.[39] However, a very recent study of [^{18}F]PM-PBB3 also showed tracer binding to 4R tau in vitro and pathology controlled in vivo retention was observed in the motor cortex of few CBS patients.[40] There have been previous studies evaluating [^{18}F]AV-1451 PET in CBS, showing an increase in tracer uptake in the motor cortex and basal ganglia contralateral to the clinical phenotype,[41-43] but these studies investigated substantially smaller CBS cohorts and only 1 study compared 2 Aβ(+)CBS and 6 Aβ(−)CBS with each other.[43]

Together with our study, this suggests that PET imaging of tau pathology is potentially feasible in CBS with fluorinated next-generation tracers with less off-target binding. Barring head-to-head-comparison studies, it is not possible to ascertain which tau-PET tracer performs better than the other.

Importantly, the cortical [^{18}F]PI-2620 signal of Aβ(+) cases was stronger and more widespread compared with that of Aβ(−)CBS cases. This fits to the lower affinity of the compound reported for 4R-tau binding compared with 3R/4R tau,[20] which was also reflected by different kinetic profiles in vivo.[21] Thus, affinity differences need to be taken into account when comparing [^{18}F]PI-2620-PET data quantitatively. To circumvent this issue, we calculated the percentage of patient positivity per voxel in subgroups of Aβ(+)CBS and Aβ(−) CBS, which is less sensitive to differences in the binding magnitude. This approach showed that Aβ(+) and Aβ (−) cases had a similar frequency of [^{18}F]PI-2620 positivity in the basal ganglia but Aβ(+)CBS patients had more frequent [^{18}F]PI-2620-positive voxels in the cortex compared with Aβ(−)CBS patients. The putamen and the external part of the globus pallidus showed the highest discrimination rate in the whole CBS cohort against controls. Noteworthily, our data in PSP with Richardson syndrome patients indicated the best discrimination between patients and controls for the internal part of the globus pallidus and also had more frequent elevation in the subthalamic nucleus and the substantia nigra.[21] Thus, patterns of [^{18}F]PI-2620 binding differed in CBS compared with PSP, indicating a shift in [^{18}F]PI-2620 binding toward brain areas with higher brain function when compared with our clinical PSP series, composed predominantly of Richardson syndrome patients.

Interestingly, cognition was more impaired in Aβ(+) CBS than in Aβ(−)CBS patients, whereas motor symptoms did not differ between the 2 groups. This fits with the high frequency of [^{18}F]PI-2620 positivity in the supplemental motor areas of both groups, whereas parietotemporal areas were only affected in the Aβ(+) CBS group. In addition, we noted a correlation of the [^{18}F]PI-2620 DVRs in cortical regions in Aβ(+)CBS, whereas Aβ(−)CBS [^{18}F]PI-2620 DVRs in subcortical regions correlated with each other.

In contrast to our Aβ(+)CBS cohort, the pre- and postcentral gyri in amnestic AD patients are usually spared of tracer deposition,[21] which may serve as an important diagnostic clue for AD patients with different phenotypes.

Even though [^{18}F]PI-2620 binding was higher in cortical regions in patients with atypical AD with the CBS phenotype, there was no significant correlation between cognition and tracer retention. Relatively low correlations between [^{18}F]PI-2620 binding and the clinical phenotype (cognition, apraxia, verbal fluency) may stem from variable or nonlinear sensitivity of clinical rating scales for the assessment of CBS, especially for Aβ(+) patients. Surprisingly, different CBS-relevant clinical rating scales correlated weakly or not with each other in our cohort of Aβ(+)CBS patients, whereas the same scales correlated well with each other in the Aβ (−)CBS group.

Importantly, we found a positive association between disease duration and [^{18}F]PI-2620 binding in the DLPFC in Aβ(−)CBS, which indicates that neuropathology potentially increases during the disease course in this area. In previous studies, the relation of disease duration or disease severity and early tau-tracer binding has been shown to be inconsistent when 4R tauopathies were assessed.[14,15,44,45] A limitation of the correlation analysis between tracer uptake and disease duration may also be caused by a discrepancy between subjective symptom onset and clinical assessment of cognitive and motor dysfunction, as disease duration is defined as the time between subjective symptom onset and PET imaging. Also, it has to be taken into account that our analysis of comparisons between clinical data and [^{18}F]PI-2620 binding DVRs, was corrected for age and sex, but not for multiple comparisons. Nonetheless, the correlation matrix may already give an impression of potential correlations in larger cohorts.

Longitudinal studies will need to address if an increase over time can be monitored by [^{18}F]PI-2620 PET in CBS.

Amyloid PET and CSF assessments were used to detect the β-amyloid status and were fully matched in all patients, indicating for the first time in CBS patients that both methods serve as a reliable biomarker to predict AD pathology. Either examination may be used for clinical decision taking in CBS patients.

The observed proportion of 24% of the cohort being Aβ positive fits well with the expected distribution of AD neuropathology in CBS[3] and indicates a coherence of postmortem pathology and antemortem biomarker–based classification for Aβ(+)CBS. Proportions of cases

with negative Aβ PET and negative [18F]PI-2620 PET (35%, 12 of 34) are similar to non–4R tauopathy autopsy results of 31% in clinical CBS cases.[3] However, we note a limited sensitivity of the tracer, especially for diagnosis of suggestive of PSP-CBS.

Our more general rating of asymmetry of clinical symptoms corresponded very well with contralateral dominance of [18F]PI-2620 binding, suggesting that neuropathology is detected where it causes brain dysfunction.

Given the nature of a rare disease, the relatively small number of 45 CBS patients, of whom 11 patients were Aβ positive, needs to be considered as a limitation of our study. Furthermore, as all observed patients are still alive, so far there is no autopsy validation available of the studied clinically diagnosed cases. Taken together, longitudinal PET studies and autopsy validation are needed for further exploration of in vivo tau PET as a diagnostic and progression biomarker in CBS.[46] The current Aβ(+) and Aβ(−)CBS study population will be followed clinically and by serial tau PET to address these questions.

Conclusion

Our results show that [18F]PI-2620-PET imaging is a useful biomarker for evaluation of CBS, facilitating detection of heterogeneous neuropathology with differences in tracer binding between probable 3R/4R tauopathy Aβ(+)CBS and Aβ(−)CBS cases. [18F]PI-2620 is a sensitive marker to detect tau binding in Aβ(+)CBS with underlying AD pathology. Elevated cortical tracer binding in the DLPFC was found in both probable 3R/4R and Aβ(−)CBS cases. Hence, [18F]PI-2620 PET may serve as a molecular diagnostic marker, detecting tau pathology in various cortical and subcortical sites. Thus, the combination of [18F]PI-2620 with Aβ status (PET or CSF) in CBS may allow the identification of CBS patients for tau-targeting therapeutic trials.

Future work with autopsy validation and longitudinal imaging and clinical assessment in CBS patients will have to investigate sensitivity to change, that is, the usefulness of [18F]PI-2620 as a progression biomarker and as possible target-engagement marker for therapeutic studies. ■

Acknowledgments: We thank all our patients and their caregivers for making this work possible. Furthermore we thank the cyclotron and radiochemistry crews at DZNE Munich and Leipzig University as well as the PET imaging crew and the Clinical Trials Unit at DZNE Munich. Life Molecular Imaging (LMI) provided material support for the manufacturing of PI-2620 and was involved in the analysis and interpretation of the data. LMI provided financial support to separate studies from which data (5 controls from New Haven and 5 controls from Melbourne) are included in this analysis.

Appendix

German Imaging Initiative for Tauopathies (GII4T)

Sabrina Katzdobler, Catharina Prix, Jonathan Vöglein, Urban Fietzek, Sonja Schönecker, Georg Nübling.

References

1. Hoglinger GU, Respondek G, Stamelou M, et al. Clinical diagnosis of progressive supranuclear palsy: the Movement Disorder Society criteria. Mov Disord 2017;32(6):853–864.
2. Armstrong MJ, Litvan I, Lang AE, et al. Criteria for the diagnosis of corticobasal degeneration. Neurology 2013;80(5):496–503.
3. Ling H, O'sullivan SS, Holton JL, et al. Does corticobasal degeneration exist? A clinicopathological re-evaluation. Brain 2010;133(Pt 7): 2045–2057.
4. Rösler TW, Tayaranian Marvian A, Brendel M, et al. Four-repeat tauopathies. Prog Neurobiol 2019;180:101644.
5. Höglinger GU. Is it useful to classify progressive supranuclear palsy and corticobasal degeneration as different disorders? No. Mov Disord Clin Pract 2018;5(2):141–144.
6. Maltête D, Guyant-Maréchal L, Mihout B, Hannequin D. Movement disorders and Creutzfeldt-Jakob disease: a review. Parkinsonism Relat Disord 2006;12(2):65–71.
7. Cali CP, Patino M, Tai YK, et al. C9orf72 intermediate repeats are associated with corticobasal degeneration, increased C9orf72 expression and disruption of autophagy. Acta Neuropathol 2019; 138(5):795–811.
8. Litvan I, Agid Y, Goetz C, et al. Accuracy of the clinical diagnosis of corticobasal degeneration: a clinicopathologic study. Neurology 1997;48(1):119–125.
9. Jabbari E, Holland N, Chelban V, et al. Diagnosis across the spectrum of progressive supranuclear palsy and corticobasal syndrome. JAMA Neurol 2019;77(3):377–387.
10. McFarland NR. Diagnostic approach to atypical Parkinsonian syndromes. Continuum (Minneap Minn) 2016;22(4 Movement Disorders):1117–1142.
11. McKhann GM, Knopman DS, Chertkow H, et al. The diagnosis of dementia due to Alzheimer's disease: recommendations from the National Institute on Aging-Alzheimer's Association workgroups on diagnostic guidelines for Alzheimer's disease. Alzheimers Dement 2011;7(3):263–269.
12. Jack CR Jr, Bennett DA, Blennow K, et al. NIA-AA Research Framework: toward a biological definition of Alzheimer's disease. Alzheimers Dement 2018;14(4):535–562.
13. Barthélemy NR, Li Y, Joseph-Mathurin N, et al. A soluble phosphorylated tau signature links tau, amyloid and the evolution of stages of dominantly inherited Alzheimer's disease. Nat Med 2020;26:398–407.
14. Brendel M, Schönecker S, Höglinger G, et al. [(18)F]-THK5351 PET correlates with topology and symptom severity in progressive supranuclear palsy. Front Aging Neurosci 2017;9:440.
15. Schonecker S, Brendel M, Palleis C, et al. PET imaging of astrogliosis and tau facilitates diagnosis of Parkinsonian syndromes. Front Aging Neurosci 2019;11:249.
16. Saint-Aubert L, Lemoine L, Chiotis K, Leuzy A, Rodriguez-Vieitez E, Nordberg A. Tau PET imaging: present and future directions. Mol Neurodegener 2017;12(1):19.
17. Lemoine L, Leuzy A, Chiotis K, Rodriguez-Vieitez E, Nordberg A. Tau positron emission tomography imaging in tauopathies: the added hurdle of off-target binding. Alzheimers Dement (Amst) 2018;10:232–236.
18. Chiotis K, Stenkrona P, Almkvist O, et al. Dual tracer tau PET imaging reveals different molecular targets for (11)C-THK5351 and

(11)C-PBB3 in the Alzheimer brain. Eur J Nucl Med Mol Imaging 2018;45(9):1605–1617.

19. Wren MC, Lashley T, Årstad E, Sander K. Large inter- and intra-case variability of first generation tau PET ligand binding in neurodegenerative dementias. Acta Neuropathol Commun 2018;6(1):34.
20. Kroth H, Oden F, Molette J, et al. Discovery and preclinical characterization of [(18)F]PI-2620, a next-generation tau PET tracer for the assessment of tau pathology in Alzheimer's disease and other tauopathies. Eur J Nucl Med Mol Imaging 2019;46(10):2178–2189.
21. Brendel M, Barthel H, van Eimeren T, et al. Assessment of 18F-PI-2620 as a biomarker in progressive supranuclear palsy. JAMA Neurol 2020;77:1408–1419.
22. Golbe LI, Ohman-Strickland PA. A clinical rating scale for progressive supranuclear palsy. Brain 2007;130(Pt 6):1552–1565.
23. Piot I, Schweyer K, Respondek G, et al. The progressive supranuclear palsy clinical deficits scale. Mov Disord 2020;35(4):650–661.
24. Schwab R, England A. Projection technique for evaluating surgery in Parkinson's disease. In: Gillingham FJ, IML D, eds. Third Symposium on Parkinson's Disease. Edinburgh, UK: E&S Livingston; 1969:152–157.
25. Nasreddine ZS, Phillips NA, Bédirian V, et al. The Montreal Cognitive Assessment, MoCA: a brief screening tool for mild cognitive impairment. J Am Geriatr Soc 2005;53(4):695–699.
26. Johnen A, Frommeyer J, Modes F, Wiendl H, Duning T, Lohmann H. Dementia Apraxia Test (DATE): a brief tool to differentiate behavioral variant frontotemporal dementia from Alzheimer's dementia based on apraxia profiles. J Alzheimers Dis 2016;49(3):593–605.
27. Dubois B, Slachevsky A, Litvan I, Pillon B. The FAB: a Frontal Assessment Battery at bedside. Neurology 2000;55(11):1621–1626.
28. Respondek G, Grimm MJ, Piot I, et al. Validation of the movement disorder society criteria for the diagnosis of 4-repeat tauopathies. Mov Disord 2020;35(1):171–176.
29. Grimm MJ, Respondek G, Stamelou M, et al. Clinical conditions "suggestive of progressive supranuclear palsy"-diagnostic performance. Mov Disord 2020;35:2301–2313.
30. Hammers A, Allom R, Koepp MJ, et al. Three-dimensional maximum probability atlas of the human brain, with particular reference to the temporal lobe. Hum Brain Mapp 2003;19(4):224–247.
31. Brendel M, Schnabel J, Schonecker S, et al. Additive value of amyloid-PET in routine cases of clinical dementia work-up after FDG-PET. Eur J Nucl Med Mol Imaging 2017;44(13):2239–2248.
32. Wollenweber FA, Darr S, Muller C, et al. Prevalence of amyloid positron emission tomographic positivity in poststroke mild cognitive impairment. Stroke 2016;47(10):2645–2648.
33. Benjamini Y, Hochberg Y. Controlling the false discovery rate: a practical and powerful approach to multiple testing. J R Stat Soc B Methodol 1995;57(1):289–300.
34. Aguero C, Dhaynaut M, Normandin MD, et al. Autoradiography validation of novel tau PET tracer [F-18]-MK-6240 on human post-mortem brain tissue. Acta Neuropathol Commun 2019;7(1):37.
35. Beyer L, Meyer-Wilmes J, Schonecker S, et al. Clinical routine FDG-PET imaging of suspected progressive supranuclear palsy and corticobasal degeneration: a gatekeeper for subsequent tau-PET imaging? Front Neurol 2018;9:483.
36. Josephs KA, Whitwell JL, Tacik P, et al. [18F]AV-1451 tau-PET uptake does correlate with quantitatively measured 4R-tau burden in autopsy-confirmed corticobasal degeneration. Acta Neuropathol 2016;132(6):931–933.
37. Lowe VJ, Curran G, Fang P, et al. An autoradiographic evaluation of AV-1451 Tau PET in dementia. Acta Neuropathol Commun 2016;4(1):58.
38. Kikuchi A, Okamura N, Hasegawa T, et al. In vivo visualization of tau deposits in corticobasal syndrome by 18F-THK5351 PET. Neurology 2016;87(22):2309–2316.
39. Ng KP, Pascoal TA, Mathotaarachchi S, et al. Monoamine oxidase B inhibitor, selegiline, reduces (18)F-THK5351 uptake in the human brain. Alzheimers Res Ther 2017;9(1):25.
40. Tagai K, Ono M, Kubota M, et al. High-contrast in-vivo imaging of tau pathologies in Alzheimer's and non-Alzheimer's disease tauopathies. Neuron 2021;109(1):42–58.e8.
41. Niccolini F, Wilson H, Hirschbichler S, et al. Disease-related patterns of in vivo pathology in Corticobasal syndrome. Eur J Nucl Med Mol Imaging 2018;45(13):2413–2425.
42. Tsai RM, Bejanin A, Lesman-Segev O, et al. (18)F-flortaucipir (AV-1451) tau PET in frontotemporal dementia syndromes. Alzheimers Res Ther 2019;11(1):13.
43. Smith R, Schöll M, Widner H, et al. In vivo retention of (18)F-AV-1451 in corticobasal syndrome. Neurology 2017;89(8):845–853.
44. Whitwell JL, Lowe VJ, Tosakulwong N, et al. [(18) F]AV-1451 tau positron emission tomography in progressive supranuclear palsy. Mov Disord 2017;32(1):124–133.
45. Schonhaut DR, McMillan CT, Spina S, et al. (18) F-flortaucipir tau positron emission tomography distinguishes established progressive supranuclear palsy from controls and Parkinson disease: a multicenter study. Ann Neurol 2017;82(4):622–634.
46. van Eimeren T, Antonini A, Berg D, et al. Neuroimaging biomarkers for clinical trials in atypical parkinsonian disorders: Proposal for a Neuroimaging Biomarker Utility System. Alzheimers Dement (Amst) 2019;11:301–309.

Supporting Data

Additional Supporting Information may be found in the online version of this article at the publisher's web-site.

SGML and CITI Use Only
DO NOT PRINT

Author Roles

1. Research project: A. Conception: C.P., M.B., A.F., P.B., R.P., C.H., J.L., and G.U.H.; B. Organization: C.P., M.B., A.F., A.S., P.B., R.P., C.H., J.L., and G.U.H.; C. Execution: M.B, A.F., L.B., A.N., M.K., and G.B. performed human PET scans and their analysis. E.W., C.P., K.B., A.D., B-S.R., J.H., M.H., R.P, J.L., the German Imaging Initiative for Tauopathies (GII4T), and G.H. recruited patients, examined patients and controls. A.St., A.D., T.v.E., V.L.V., A.S., H.B., M.P., and O.S. produced the tracer.

2. Statistical analysis: A. Design C.P., E.W., K.B., A.D., B-S.R., R.P, J.L., and G.U.H. designed analysis of clinical data; B. Execution, A.F., E.W., C.P., K.B., A.D., B-S.R., R.P, J.L,. and G.U.H. analyzed clinical data. A.F., M.B., L.B., M.K., G.B., A.N., and P.B. interpreted human PET data. C. Review and critique: all authors.

3. Manuscript preparation: A. Writing of the first draft: C.P., M.B., J.L., and G.U.H.; B. Review and critique: all authors.